



The University of Edinburgh

School of Engineering

Academic Year 2019-2020

**Experimental and numerical study on the effect of horizontal openings  
within informal settlement dwellings**

Karim Omar Mohamed

Promoter(s): Dr David Rush

Mr Mohamed Beshir

Master thesis submitted in the Erasmus+ Study Programme

International Master of Science in Fire Safety Engineering

**School of Engineering – Incident Management**



**DISCLAIMER**

This thesis is submitted in partial fulfilment of the requirements for the degree of *The International Master of Science in Fire Safety Engineering (IMFSE)*. This thesis has never been submitted for any degree or examination to any other University/programme. The author(s) declare(s) that this thesis is original work except where stated. This declaration constitutes an assertion that full and accurate references and citations have been included for all material, directly included and indirectly contributing to the thesis. The author(s) gives (give) permission to make this master thesis available for consultation and to copy parts of this master thesis for personal use. In the case of any other use, the limitations of the copyright have to be respected, in particular with regard to the obligation to state expressly the source when quoting results from this master thesis. The thesis supervisor must be informed when data or results are used.

Read and Approved

Karim Omar

Word Count: 16946

## Abstract (English)

An experimental investigation supported by numerical analysis was carried out to study the effect of horizontal ceiling openings in an informal settlement dwelling in reducing fire spread between dwellings. FDS was later used to analyze these experimental data.

The experimental part included a quarter scale ISO-9705 compartment of dimensions 0.6x0.9x0.6 m (Length×Width×Height) with a vertical door opening of dimensions 0.2 x 0.5m (W ×H) and variable areas of horizontal openings. The study investigated different shapes of horizontal openings, the first one being four-square corner openings with dimensions of 0.025x0.025, 0.05x0.05, 0.1x0.1, 0.15x0.15 and 0.2x0.2 m while the second shape was one rectangular central opening with dimensions of 0.6x0.02, 0.6x0.07, 0.6x0.15 and 0.6x0.27 m. The compartment had a thermally-thin steel sheet boundary materials, while polypropylene was used as a fuel source with a fuel load of 80 MJ/m<sup>2</sup>.

The study showed that the horizontal opening size had an insignificant effect on the gas layer temperatures with a horizontal opening size of 0.04 m<sup>2</sup> or less. Beyond that size there was a considerable reduction in temperatures of about 40% with the 0.16 m<sup>2</sup> ceiling opening leading to no flashover. The radiative heat flux to the surrounding decreased significantly by about 50% with the increase of the size of the horizontal opening until 0.16 m<sup>2</sup>. With a horizontal opening area of 0.04 m<sup>2</sup> or more the time to flashover increased and the neutral plane almost vanished, in addition to the vanishing of the ventilation pulsation phenomenon (Oscillating flames) that occurred with 0.01 m<sup>2</sup> or less of horizontal openings.

The validation process indicated the ability of FDS to model these under-ventilated dwellings with horizontal opening sizes of 0.04 m<sup>2</sup> or less with high accuracy except for the ventilation pulsation phenomenon (oscillating flames) which struggled to model. However, with a horizontal opening size of 0.09 m<sup>2</sup> or more indicating over-ventilated compartments, FDS failed to capture the flow fields through the openings, the heat balance within the compartment and the combustion efficiency which could require using finer meshes and test its accuracy.

## Abstract (Arabic)

### المخلص

أوضحت الدراسة تحليلاً تجريبياً وعددياً لتأثير إضافة فتحات السقف الأفقية في مسكن غير رسمي (ISD). ثم ، تم إنشاء عملية التحقق من صحة موثوقية FDS مع نمذجة حرائق المستوطنات غير الرسمية.

تضمن الجزء التجريبي حجرة ربع ISO-9705 بأبعاد 0.6 م × 0.9 م × 0.6 م (الطول × العرض × الارتفاع) مع فتحة باب رأسية بأبعاد 0.2 م × 0.5 م (عرض × ارتفاع) ومساحات متغيرة من الفتحات الأفقية. بحثت الدراسة في الأشكال المختلفة للفتحات الأفقية ، أولها فتحات الزاوية الأربعة بأبعاد 2.5 2.5 ، x5 5 ، x10 10 ، x15 15 و x20 20 سم 2 ، بينما كان الشكل الثاني عبارة عن فتحة مركزية مستطيلة واحدة بأبعاد 2.5 60 ، x7 60 ، x15 60 و x27 60 سم 2. تحتوي المقصورة على مواد حدود صفائح فولاذية رقيقة حرارياً ، في حين تم استخدام البولي بروبيلين كمصدر وقود مع حمولة وقود 80 ميغا جول / م<sup>2</sup>.

أوضحت الدراسة أن حجم الفتح الأفقي كان له تأثير ضئيل على درجات حرارة طبقة الغاز ما لم يزداد حجم الفتحة بشكل كبير وهذا سيؤدي إلى انخفاض كبير في درجات الحرارة مما أدى في بعض الأحيان إلى عدم القدرة على الوصول إلى معايير الوميض. من ناحية أخرى ، انخفض تدفق الحرارة الإشعاعية إلى المناطق المحيطة بشكل ملحوظ بحوالي 50٪ مع زيادة حجم الفتحة الأفقية. وقد وجد أيضاً أن موقع المحور المحايد عند الفتحة العمودية يزداد مع زيادة حجم فتحات السقف ، ومع ذلك ، عندما زادت التهوية الأفقية بما يتجاوز حجم معين ، اختفى المحور المحايد مما يشير إلى تدفق مهيم للهواء عبر الباب فوق تدفق الدخان. أخيراً ، انخفض وقت اللعان في البداية مع فتحة سقف أكبر ، ومع ذلك ، عندما تم الوصول إلى قيمة عتبة معينة ، بدأ وقت اللعان في الزيادة مرة أخرى.

تم استخدام Fire Dynamics Simulator (FDS) لتطوير نماذج لتقليد التجارب المعملية. أشارت عملية التحقق من قدرة FDS على نمذجة مساكن ناقصة التهوية بدقة عالية ؛ ومع ذلك ، كافحت FDS لالتقاط ديناميكيات النار عندما أصبحت المقصورة مفرطة التهوية بسبب فتحات السقف الأكبر.

## Acknowledgement

I can't believe my IMFSE journey is getting to an end after an amazing two-year experience. I had a lot of ups, but my biggest down was losing my father midway. That's why I am grateful to all the support I got from the IMFSE family which pulled me through these unimaginably tough times.

Big thanks to Prof. David Rush for accepting my thesis proposal to conduct my thesis in Edinburgh under his supervision. Massive thanks to the one and only Mohamed Beshir, who helped me in every step of the way, from the master application until submitting this great thesis which would not be a success without his help and assistance. He kept pushing me to do great work and I am so grateful and happy to know someone like him.

Big thanks to the IMFSE board for choosing me to be a part of such a program and grant me a scholarship I never dreamed to have. Big thanks to Prof. Bart Merci, Prof. Grunde Jomaas and Lies for their non-stop help with our frequent questions and problems.

Special thanks to Adina and Sandesh, I remember Sandesh treated me with a very nice lunch couple of days after landing in Edinburgh (Btw this was the only time he did that, the rest were all my treats. I think he was fooling me into being his friend and he was successful I guess). Adina did not need to do much effort for me to love being her friend and build a very solid friendship that would last forever. The experience would not be complete without everyone being great and helpful throughout the way. Shoutout to the Edinburgh first semester team (Dan, Kevin, Rey, Adina, Sandesh, Danni), without forgetting Tanja and Ewana for being kind and amazing friends and for everyone else that made this journey special.

I would never have made it so far without my family, I wish my father was here so I celebrate the end of this journey with him, and I hope I can always make him proud. This master is my gift to him for making me be the person I am today. If I needed to thank my mom, I would not find enough words to describe my love and gratitude for her in addition to my brother who has been and will always stand by my side and to whom I always turn to and learn from. Family will always come first no matter what.

'Family always comes first'

# Table of Contents

<b>Abstract (English)</b> .....	<b>iii</b>
<b>Abstract (Arabic)</b> .....	<b>iv</b>
<b>Acknowledgement</b> .....	<b>v</b>
<b>Table of Contents</b> .....	<b>vi</b>
<b>Appendix</b> .....	<b>ix</b>
<b>List of figures</b> .....	<b>x</b>
<b>1. Introduction</b> .....	<b>1</b>
1.1 Informal Settlements background .....	1
1.2 Previous Work .....	3
1.3 Scope of the Study (Approach).....	6
<b>2. Methodology</b> .....	<b>7</b>
2.1 Experimental Setup .....	7
2.1.1 Locations and calibration of measurement instrumentation.....	10
2.2 Experimental Results .....	13
2.2.1 Repeatability of experimental work.....	13
2.2.1.1 Closed Ceiling Experiments.....	14
2.2.1.2 Corner/Central openings.....	15
2.2.2 Hot gas layer temperature .....	17
2.2.3 Incident heat flux to the surrounding .....	19
2.2.3.1 Effect of opening size .....	21
2.2.3.2 Effect of the opening characteristics .....	25
2.2.3.3 Effect of the TSC distance.....	26
2.2.3.4 Effect of the TSC location (side / back/door) .....	28
2.2.4 Inflow/Outflow from the compartment openings.....	29
2.2.5 Gas products species .....	33
2.2.6 Time to Flashover (Using Top TC in all corners) .....	34
<b>3. Validation of experimental data</b> .....	<b>36</b>
3.1 Numerical set-up & simulation parameters .....	36
3.2 Validation Process .....	37
3.2.1 Closed_2 Case.....	39
3.2.1.1 Combustion Efficiency .....	39
3.2.2 0.025x0.025 m square Corner Openings .....	40
3.2.2.1 Heat Balance .....	40

3.2.2.2	Mass Balance.....	42
3.2.2.3	External Flaming.....	43
3.2.3	0.05x0.05 m square Corner Openings .....	44
3.2.3.1	Heat Balance .....	44
3.2.3.2	Mass Balance.....	45
3.2.3.3	External Flaming.....	46
3.2.4	0.1x0.1 m square Corner Openings .....	47
3.2.4.1	Heat Balance .....	47
3.2.4.2	Mass Balance.....	49
3.2.4.3	External Flaming.....	50
3.2.5	0.6x0.07 m Central Opening.....	51
3.2.5.1	Combustion Efficiency .....	51
3.2.5.2	Heat Balance .....	51
3.2.5.3	Mass Balance.....	52
3.2.5.4	External Flaming.....	53
3.2.6	0.15 x0.15 m square Corner Openings .....	54
3.2.6.1	Heat Balance .....	54
3.2.6.2	Mass Balance.....	56
3.2.6.3	External Flaming.....	57
3.2.7	0.6x0.15 m Central Opening.....	58
3.2.7.1	Combustion Efficiency .....	58
3.2.7.2	Heat Balance .....	59
3.2.7.3	Mass Balance.....	60
3.2.7.4	External Flaming.....	61
3.2.8	0.2x0.2 m square corner openings .....	62
3.2.8.1	Combustion Efficiency .....	62
3.2.8.2	Heat Balance .....	63
3.2.8.3	Mass Balance.....	64
3.2.8.4	External Flaming.....	65
3.2.9	0.6x0.27 m Central Opening.....	66
3.2.9.1	Combustion Efficiency .....	66
3.2.9.2	Heat balance .....	66
3.2.9.3	Mass balance .....	67
3.2.9.4	External flaming .....	67

<b>4.</b>	<b>Uncertainty and impact of the shutdown .....</b>	<b>68</b>
4.1	Experimental Setup .....	68
4.2	FDS .....	69
<b>5.</b>	<b>Conclusion .....</b>	<b>70</b>
5.1	Future Work .....	72
<b>6.</b>	<b>References .....</b>	<b>73</b>
	<b>Appendix.....</b>	<b>76</b>



## Appendix

<b>A.</b>	<b>Small Scale Model</b> .....	<b>76</b>
	A.1.1 Peak HRR Values for all the cases .....	76
	A.1.2 HRR Data .....	77
	A.2. TC Trees Results .....	78
	A.2.1 Closed Ceiling Repeated Tests .....	78
	A.2.2 Central Slot Opening Covered with Polycarbonate .....	78
	A.3. Heat Flux Gauges .....	79
	A.3.1 Corner Openings .....	79
	A.3.2 Openings without Polycarbonate 30 cm from the door .....	80
	A.3.3 Openings without Polycarbonate 15 cm from the side .....	81
<b>B.</b>	<b>Validation</b> .....	<b>82</b>
	B.1. 60 cm by 27 cm Central Opening Without Polycarbonate Cover .....	82
	B.1.1 Combustion Efficiency .....	82
	B.1.2 Heat Balance .....	82
	B.1.3 Mass Balance .....	83
	B.1.4 External Flaming .....	84
	B.2. FDS Code .....	85

## List of figures

FIGURE 1: CAPE TOWN INFORMAL SETTLEMENTS [5] .....	1
FIGURE 2: THE CONFLAGRATION OF (A) IMIZAMU YETHU (B) MASIPHUMELELE [9] .....	3
FIGURE 3: WELL-VENTILATED COMPARTMENT FIRE DEVELOPMENT (LEFT) AND THE EFFECT OF ENCLOSURES ON THE FIRE DEVELOPMENT (RIGHT) [11] .....	4
FIGURE 4: QUARTER SCALE ISO-9705 COMPARTMENT (OPEN CEILING FOR DEMONSTRATION) [18] .....	7
FIGURE 5: QUARTER ISO-9705 EXPERIMENTAL COMPARTMENT WITH FOUR 0.025X0.025 M CORNER OPENINGS (A) AND A 0.6X0.27 M CENTRAL OPENING (B) .....	8
FIGURE 6: MEASUREMENTS LOCATIONS (NOT TO SCALE) .....	10
FIGURE 7: HRR FOR REPEATED CLOSED CEILING EXPERIMENTS .....	14
FIGURE 8: REPEATED TESTS FOR 0.2X0.2 M CORNER (A) AND 0.6X0.27 M CENTRAL OPENINGS (B) .....	15
FIGURE 9: TOP TCS IN THE RIGHT FRONT AND BACK FOR BOTH CORNER AND CENTRAL CEILING OPENINGS .....	17
FIGURE 10: OPENINGS SIZE EFFECT ON THE INCIDENT HEAT FLUX TO THE SURROUNDING .....	21
FIGURE 11: SCREENSHOTS FOR THE EXTERNAL FLAMING FOR THE CORNER OPENING TESTS (DURING THE STEADY STATE) .....	22
FIGURE 12: SCREENSHOTS FOR THE EXTERNAL FLAMING FOR THE CENTRAL OPENING TESTS (DURNING THE STEADY STATE) .....	22
FIGURE 13: HOT SPOT ON THE COMPARTMENT WALLS FOR THE CLOSED CEILING CASE .....	23
FIGURE 14: EFFECT OF THE OPENING SHAPE ON THE INCIDENT HEAT FLUX .....	25
FIGURE 15: TSC DISTANCE EFFECT ON INCIDENT HEAT FLUX FROM THE DOOR .....	27
FIGURE 16: SIDE TSC LIMITATIONS WITH CORNER OPENINGS EXPERIMENTS .....	28
FIGURE 17: TSC LOCATION EFFECT ON INCIDENT HEAT FLUX FROM THE COMPARTMENT .....	28
FIGURE 18: BACK GAS ANALYZER DATA AIMING AT EXPLAINING THE OSCILLATING FLAMES .....	30
FIGURE 19: OSCILLATING FLAMES IN THE 0.05X0.05 M CORNER OPENING CASE .....	30
FIGURE 20: FLOW PROFILE ACROSS THE COMPARTMENT DOOR .....	31
FIGURE 21: FLOW VELOCITY IN/OUT OF THE DOOR FOR 0.04 M <sup>2</sup> HORIZONTAL AREA AT (A) 0.4 M, (B) 0.25 M AND (C) 0.1 M FROM THE FLOOR .....	32
FIGURE 22: BACK GAS ANALYZER DATA .....	33
FIGURE 23: GEOMETRY OF THE NUMERICAL SET UP FOR THE CORNER CEILING OPENINGS (LEFT) AND THE CENTRAL CEILING OPENING (RIGHT) AS SHOWN IN SMOKEVIEW .....	36
FIGURE 24: THE VALIDATION PROCESS .....	38
FIGURE 25: VALIDATION OF THE COMBUSTION EFFICIENCY FOR THE CLOSED_2 CASE FOR (A) CO <sub>2</sub> (B) O <sub>2</sub> .....	40
FIGURE 26: VALIDATION OF THE HEAT BALANCE FOR THE 2.5_OPEN CASE .....	40
FIGURE 27: VALIDATION OF THE MASS BALANCE FOR THE 2.5_OPEN CASE .....	42
FIGURE 28: VALIDATION OF THE EXTERNAL FLAMING FOR THE 2.5_OPEN CASE .....	43
FIGURE 29: VALIDATION OF THE HEAT BALANCE OF THE 5_OPEN CASE .....	44
FIGURE 30: VALIDATION OF THE MASS BALANCE OF THE 5_OPEN CASE .....	45
FIGURE 31: VALIDATION OF THE EXTERNAL FLAMING FOR THE 5_OPEN CASE .....	46
FIGURE 32: VALIDATION OF THE HEAT BALANCE FOR THE 10_OPEN CASE .....	48
FIGURE 33: VALIDATION OF MASS BALANCE FOR THE 10_OPEN CASE .....	49
FIGURE 34: VALIDATION OF THE EXTERNAL FLAMING OF THE 10_OPEN CASE .....	50
FIGURE 35: VALIDATION OF THE COMBUSTION EFFICIENCY FOR THE 60X7_OPEN CASE FOR (A) O <sub>2</sub> (B) CO <sub>2</sub> .....	51
FIGURE 36: VALIDATION OF THE HEAT BALANCE FOR THE 60X7_OPEN CASE .....	52
FIGURE 37: VALIDATION OF THE MASS BALANCE FOR THE 60X7_OPEN CASE .....	53
FIGURE 38: VALIDATION OF THE EXTERNAL FLAMING FOR THE 60X7_OPEN CASE .....	54
FIGURE 39: VALIDATION OF THE HEAT BALANCE FOR THE 15_OPEN CASE .....	56
FIGURE 40: VALIDATION OF THE MASS BALANCE OF THE 15_OPEN CASE .....	57

FIGURE 41: VALIDATION OF THE EXTERNAL FLAMING 0.3 M FROM THE DOOR FOR THE 15_OPEN CASE.....	58
FIGURE 42: VALIDATION OF THE COMBUSTION EFFICIENCY FOR THE 60X15_OPEN CASE FOR (A) O <sub>2</sub> AND (B)CO <sub>2</sub> .....	59
FIGURE 43: VALIDATION OF THE HEAT BALANCE FOR THE 60X15_OPEN CASE .....	60
FIGURE 44: VALIDATION OF THE MASS BALANCE FOR THE 60X15_OPEN CASE .....	61
FIGURE 45: VALIDATION OF THE EXTERNAL FLAMING FOR THE 60X15_OPEN CASE .....	62
FIGURE 46: VALIDATION OF THE COMBUSTION EFFICIENCY FOR THE 20_OPEN_1 CASE FOR (A) O <sub>2</sub> AND (B) CO <sub>2</sub> .....	63
FIGURE 47: VALIDATION OF THE HEAT BALANCE FOR THE 20_OPEN_1 CASE .....	64
FIGURE 48: VALIDATION OF THE MASS BALANCE FOR THE 20_OPEN_1 CASE .....	65
FIGURE 49: VALIDATION OF THE EXTERNAL FLAMING AT 0.3 M FROM THE DOOR FOR THE 20_OPEN_1 CASE.....	66
FIGURE 50: VALIDATION OF FLOW VELOCITY LEAVING THE CEILING OPENING FOR 60X27_OPEN_1 CASE .....	67
FIGURE 51: HRR FOR CORNER OPENINGS WITHOUT POLYCARBONATE .....	77
FIGURE 52: HRR FOR CENTRAL OPENINGS WITHOUT POLYCARBONATE.....	77
FIGURE 53: TC COMPARISON BETWEEN THE FIRST (LEFT) AND SECOND (RIGHT) CLOSED CEILING TEST .....	78
FIGURE 54: TOP TC IN RIGHT BACK (LEFT) AND FRONT (RIGHT) CENTRAL WITH POLYCARBONATE.....	78
FIGURE 55: HEAT FLUX SENSOR (LEFT) VS. TSC (RIGHT) AT 60 CM FROM DOOR FOR CORNER OPENINGS WITHOUT POLYCARBONATE .....	79
FIGURE 56: HEAT FLUX SENSOR (LEFT) VS. TSC (RIGHT) 15 CM FROM SIDE WALL FOR CORNER OPENINGS WITHOUT POLYCARBONATE .....	79
FIGURE 57: CLOSED CEILING VS. OPEN CORNER OPENINGS VS. OPEN CENTRAL OPENING (HEAT FLUX 30 CM FROM THE DOOR)).....	80
FIGURE 58: CLOSED CEILING VS. OPEN CORNER OPENINGS VS. OPEN CENTRAL OPENING (HEAT FLUX 15 CM FROM THE SIDE).....	81
FIGURE 59: VALIDATION OF THE COMBUSTION EFFICIENCY FOR THE 60X27_OPEN_1 CASE .....	82
FIGURE 60: VALIDATION OF THE HEAT BALANCE FOR THE 60X27_OPEN_1 CASE .....	83
FIGURE 61: VALIDATION OF THE MASS BALANCE FOR THE 60X27_OPEN_1 CASE .....	84
FIGURE 62: VALIDATION OF THE EXTERNAL FLAMING FOR THE 27_OPEN_1 CASE .....	84

# 1. Introduction

## 1.1 Informal Settlements background

Urban growth is one of the most concerning global phenomena, which posed immense burdens on the infrastructure and essential services provided to the people[1]. This phenomenon is mainly found in developing countries where statistics showed a population growth by about 70 million people yearly[2]. As a result to the unprecedented spike in world's population, informal settlements ,as shown in Figure 1, started appearing due to the lack of affordable urban housing , climate change, wars or conflicts. The latest statistics showed that more than one billion people live in informal settlements around the globe [3], this number was reached due to the addition of about 213 million informal settlement residents to the world population since 1990 which meant that about 25% of the world's urban population are residing in informal settlements[4].

The term 'informal' was used to describe these dwelling owing to the absence of any formal guidelines, standards or permissions from the government, The only way for people to avoid being homeless was to build their own homes from any available materials (e.g. steel sheets and timber).



Figure 1: Cape Town informal settlements [5]

These settlements are highly vulnerable to the risk of fires due to the very close proximity between each dwelling, in addition to the use of flammable materials inside the dwellings, for instance, using kerosene stoves for cooking, furniture, curtains or clothing. As a result of that, over 95% of the deaths caused by fires took place within low and middle-income countries which contain the majority of these informal settlements[6].

Many fires have occurred over the past few years, with an increase in the number and intensity of fires resulting in substantial financial and humanitarian losses. Thousands of families were left homeless after their homes were destroyed. Table 1 shortlisted some of the modern history of fires in IS based on the consequential impact on the number of destroyed homes and displaced people[3].

**Table 1: Modern history of IS Fires worldwide [3] [7]**

<b>Date</b>	<b>Fire Incident</b>	<b>Country</b>	<b>Destroyed Homes</b>	<b>Displaced People (Fatalities)</b>
March 2013	Kayamandi, Cape town	South Africa	1357	4500 (2)
November 2015	Masiphumelele, cape town	South Africa	1000	4000 (2)
March 2017	Imizamu Yethu, Cape town	South Africa	2194	10,000 (4)
January 2018	Cebu	Philippines	326	3570
January 2018	Kijiji, Lang'ata, Nairobi	Kenya		6000
February 2018	Sawang Calero	Philippines	145	1500
March 2018	Mirpur, Dhaka	Bangladesh	1000	4484
April 2018	Rohini, Delhi	India	500	1000
July 2018	Jolo, Sulu Province/Lambayog	Philippines	3000 /5000	
October 2018	Khayelitsha, Cape Town	South Africa	1000	4000(1)
December 2018	Alexandra, Johannesburg	South Africa	500	2000
December 2018	Manaus, Amazonas state	Brazil	600	2000

IRIS-Fire is an international and interdisciplinary research project aiming to improve the resilience of informal settlements during fire incidents. The project is mainly focusing on South Africa as studies showed that approximately one-third of its population resided in IS. Cape Town, which is known as ‘the fire capital of South Africa’ had a jump in the number of informal dwellings from 28,000 in 1993 to 220,000 in 2011 [8]. Between 2003-2016, the Fire Protection Association of Southern Africa ‘FPASA’ published data showing that the number of fires increased by about 1.7% with a jump in the number of fatalities by about 5-10% annually. This data was later proven to be an underestimation of the real number of fatalities as only the people found dead in the fire location were counted while the remaining injury-related deaths occurring in hospitals were neglected. Surveys demonstrated that the number of fire incidents almost doubled from 150 in 2009 to more than 320 in 2015 with one-third of these fires spreading beyond the original fire dwelling which is indicative of the significance of fire spread in these communities. Fire spread in informal settlements is the center of this study and the heart of most IS fire-related research, as it poses the biggest risk on these communities as seen in Imizamo Yethu and

Masiphumelele conflagrations illustrated below in **Error! Reference source not found.a** and 2b indicating how catastrophic fire spread can be if not controlled[3].



**Figure 2: The conflagration of (a) Imizamu Yethu (b) Masiphumelele [9]**

Despite the occurrence of such blazes, most of the fire research community was focused on finding intervention solutions like the application of intumescent paint on the outer dwelling walls, using new building materials, adding sprinkler systems or attaching smoke detectors to quickly detect the fires and suppress them. However, due to the socio-economic aspects of these communities like theft, unawareness, rejection of such solutions due to beliefs or cost-related problems, therefore, such solutions were not realistic and it was essential to focus more on the technical aspects of fires by checking gas temperatures, heat fluxes, spreading mechanisms, smoke and fire dynamics to understand the nature of fire in IS. Therefore, this study will aim to understand the impact of the addition of horizontal ceiling openings and how it changes the fire dynamics and fire spread probability within dwellings[10].

## 1.2 Previous Work

Seminal contributions were made within the IRIS-Fire project in the field of improving the resilience of informal settlements and finding novel ways to control the fire spread between dwellings. It was proved via experimental work that the fire spread may occur either due to direct flame impingement through openings in the dwelling where the fire starts or via the high intensity of radiative energy enough to cause spontaneous ignition to other materials in some cases. So, in order to develop new ways to improve these dwellings response to fires, we need to understand the fire dynamics of a typical compartment fire and how flashover can be defined in such an enclosure which is displayed in Figure 3. The enclosure characteristics may not be related to the fire initiation, but the growth and progression of the fire are profoundly affected by the compartment size, the opening sizes and the boundary ‘wall’ materials. If the enclosure has enough fuel and ventilation, then the fire will develop until everything is burning inside the compartment, this is known as ‘flashover’. When a fuel source starts burning in a compartment, it

releases smoke and pyrolysis gases that get trapped below the ceiling to form a smoke layer. This stage is called the 'pre-flashover stage', Then the smoke layer thickness and temperature will increase until the radiation intensity to the floor, and the remaining fuel is enough for spontaneous ignition. This stage is called the 'Post-flashover stage' or 'fully developed stage' which is shown in Figure 3 below.[11].

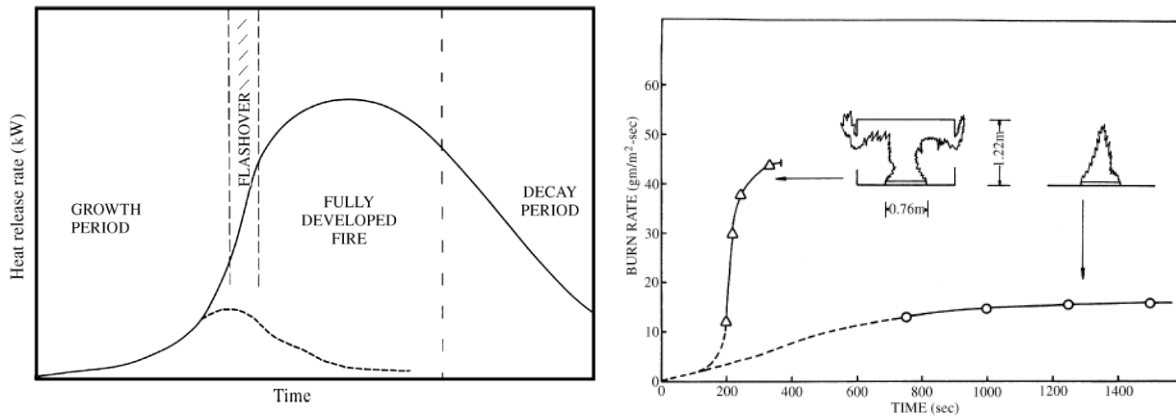


**Figure 3: Well-ventilated compartment fire development (Left) and the effect of enclosures on the fire development (Right) [11]**

Flashover is a qualitative transitional phenomenon which does not have a precise value or state; researchers developed different criteria for flashover, The common theme of flashover includes rapid-fire growth happening in a short time which in return result in engulfing the whole enclosure with flames [12]. The earliest attempt to define flashover was conducted by Waterman (1968) [13] when he characterized flashover occurrence with an incident heat flux of  $20 \text{ kW/m}^2$  on the floor and a minimum heat of burning of  $40 \text{ g/s}$ [14]. Hagglund et al. [15] also found that flashover occurred when the ceiling temperature reached  $600 \text{ }^\circ\text{C}$  with flames emerging from enclosure openings. Nevertheless, the flashover criteria method used in this report was the McCaffrey et al. (MQH) [16] flashover criteria which specified the flashover criteria to be when the gas layer temperature reaches  $525 \text{ }^\circ\text{C}$ . MQH then ended up with an empirical equation defining the onset HRR needed to reach flashover after they analyzed many experiments with different fuel and enclosure characteristics to come up with such criteria The IRIS-Fire team conducted many bench scale, small scale and large scale experimental work and linked the founding to the work done via the Geographic Information System (GIS). A recent study by Wang et al. [17] investigated a fire occurred in Masiphumelele, South Africa, in 2015. The study estimated a critical distance of 3.5m, which, when exceeded, there was no fire spread between dwellings. This estimated distance was estimated theoretically then confirmed by aerial photography of the fire scene. Nevertheless, this was not the sole effort to try and investigate fire spread between informal settlement dwellings, as many attempts varied between experimental testing (Full-scale & Small-scale), numerical modelling, or both.

Koker et al. [6] conducted a full-scale experimental testing recently with a 20 large-scale mock settlement dwelling with the very close proximity of 1-2 m between each dwelling, to replicate the large-scale urban conflagration. The study investigated the influence of wind on fire spread between

dwellings; the results showed that even with a mild wind speed of 15-25 km/h, the entire mock caught fire within the first 5 minutes after the fire started. Also, a flashover occurred very quickly in each dwelling, with internal temperatures exceeding 1000 °C.

Beshir et al. [18] developed a recent study that is related to the current work. which was the first step in a series of small-scale experiments to investigate the mechanism of heat transfer and fire dynamics within these informal settlement dwellings. This study used a small-scale ISO-9705[19] compartment to develop a semi-empirical model to estimate the HRR needed for flashover using corrugated steel sheeting as thermally thin boundary walls to replicate the wall materials of the informal settlement dwellings in Cape Town, South Africa. The fuel used in this study was Polypropylene with 200 ml of heptane as an accelerant and the flashover was found to be reached with at least 32 MJ/m<sup>2</sup>. The flashover criteria used in this study was the MQH method which specified the occurrence of flashover whenever all top thermocouples reached 525 °C. This quarter scale ISO-9705 compartment is the same room used in the current study with some modifications to the ceiling, which will be discussed later in this report. The test was repeated few time and repeatability was ensured.

In addition to the empirical co-relation to estimate the HRR needed for flashover, the paper also presented a validated Computational Fluid Dynamics (CFD) model via the Fire Dynamics Simulator (FDS) for these under ventilated compartment fire. The results showed an acceptable replication of the experimental measurements like HRR, gas layer temperature, incident heat fluxes to the surrounding and the flow velocity through the compartment door. Finally, a semi-empirical correlation is devised for the HRR required for flashover in compartments with thermally thin boundaries and ultra-fast fire. The resulting correlation is:

$$\theta_{rad} = 10^{7.542} (\varepsilon \sigma A_T A_W H_W^{\frac{1}{2}})^{-0.117} \quad (1)$$

$$\dot{Q}_{FO} = 10^{19.606} \theta_{rad}^{-2.099} \quad (2)$$

The  $\theta_{rad}$  is defined as  $(T_B^2 + T_S^2)(T_B + T_S)$  with  $T_S$  being the surrounding temperature and  $T_B$  as the boundary wall temperature. The equation also includes the wall emissivity  $\varepsilon$ ,  $A_W H_W^{\frac{1}{2}}$  as the ventilation factor and  $A_T$  as the total area. The future work aims at the inclusion of the horizontal ventilation factor within this equation as most research work focused on vertical ventilation opening, hence a factor representing the presence of horizontal ventilation is required.

It is apparent in light of the previous studies, that the main focus was on ventilation factors associated with vertical openings like doors and windows, yet, several questions regarding the effect of horizontal openings remained to be addressed in detail. Therefore, a study by Beshir et al.[20] proposed a computational study on the effect of horizontal openings on fire dynamics within informal settlement dwellings. The model was developed using FDS, with the fire compartment being an ISO-9705 room with boundary walls made of corrugated steel sheets



The study showed that for high fuel loads when the horizontal opening area increased, the time to reach flashover slightly increased since the amount of smoke leaving the opening was negligible compared to the produced gases. On the other hand, for lower fuel loads, the increase in horizontal opening size resulted in a more significant increase in the time to flashover. This could be explained through the mass balance within the compartment, as the mass flow rate of gases escaping from the openings could be comparable to that produced by the fire resulting in a more sensitive change in temperatures.

At the same time, the incident heat flux to the surrounding was analyzed, and it concluded that any increase in the size of the horizontal openings would decrease the heat flux to the surrounding regardless of the fuel load used. On the contrary, as the size of horizontal openings increased, the visible flame length ejecting from the window decreased by about 6% for small horizontal openings compared to about 28% on average for larger horizontal openings.

A study by Qiang et al. [21].investigated the change in the gas layer temperature with the increase in the size of horizontal openings. The study found out that the ceiling opening size had an insignificant effect on the rise of the gas layer temperature opposing to the fire size which had a more significant effect

With all efforts to investigate the impact of adding a ceiling opening to an ISD, there were still some points overlooked. That is why this study would give a general overview of the influence of adding these openings, in addition to making sure whether FDS could be a reliable tool to model such fire or not.

### **1.3 Scope of the Study (Approach)**

In short, this report will focus on two main points, the influence of the HZ openings on the fire dynamics within an ISD. The reliability of the Computational Fluid Dynamics (CFD) code, namely Fire Dynamics Simulator (FDS) to model compartments with unique conditions beyond flashover. Therefore, a quarter-scale ISO-7905 compartment made of corrugated steel sheets with different combinations of ceiling openings is tested under the lab hood. This will be achieved by observing the changes in gas layer temperatures, radiative heat flux to the surrounding, gas products species and in/outflow velocities from the vertical and horizontal openings based on the measurement instrumentations positioned inside and outside the compartment. Following the analysis of experimental data, numerical models are developed on Fire Dynamics Simulator (FDS) for the same room. Finally, these numerical data are compared to the experimental ones to decide if these models were to be validated against the small-scale testing or not.

In order to achieve these goals, the following objectives need to be completed:

- Conducting three main sets of small-scale experiments, i.e. (1) a closed ceiling compartment, (2) square corner openings in the compartment ceiling and (3) rectangular central ceiling opening. Ten experiments were completed within the scope of this point.

- Checking the repeatability of each set of experiments by conducting each of the following tests more than once: closed ceiling, 0.2x0.2 m open corner openings and 0.6x0.27 m open central opening. Four experiments were repeated, leading to a total of fourteen small-scale experiments through the whole study.
- Ten numerical models will be developed on FDS to simulate the closed ceiling case and all the different sizes of the corner and central ceiling openings and then compared with experimental data.

## 2. Methodology

### 2.1 Experimental Setup

Fourteen small-scale ISD experiments are carried out in the fire lab of the University of Edinburgh under the big hood. The experimental set-up is illustrated by dividing each component to the factors influencing fire development in the enclosure, as discussed below:

**The geometry of enclosure:** This experimental design illustrated in Figure 4 is employed to replicate a small-scale model of ISDs similar to the ones in South Africa. This quarter scale ISO-9705 compartment was constructed of corrugated steel sheets, with dimensions of 0.9x0.6x0.6 m (Length × width × height). The compartment was seated under a large-scale calorimetry hood that utilizes a suction fan to extract the gases produced from the fire in the small-scale room to calculate HRR in each case using the oxygen consumption method along with the formulations derived by Janssens[22]. A small room would lead to higher temperatures, faster smoke filling and more heat transfer feedback from the gas layer to the fuel, causing faster fire growth. So, in other words, it would give the expected results at a faster pace.[23]

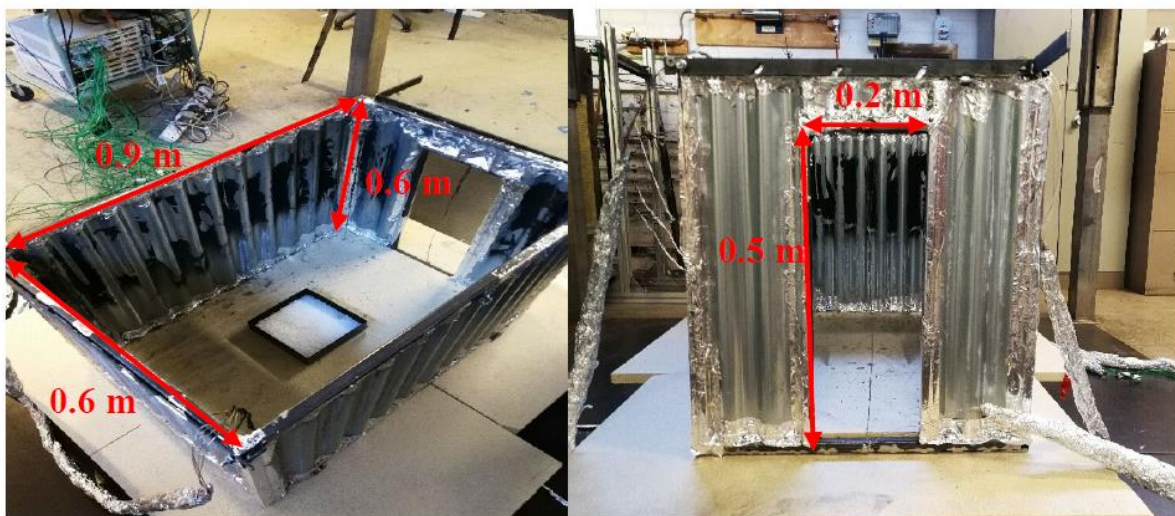
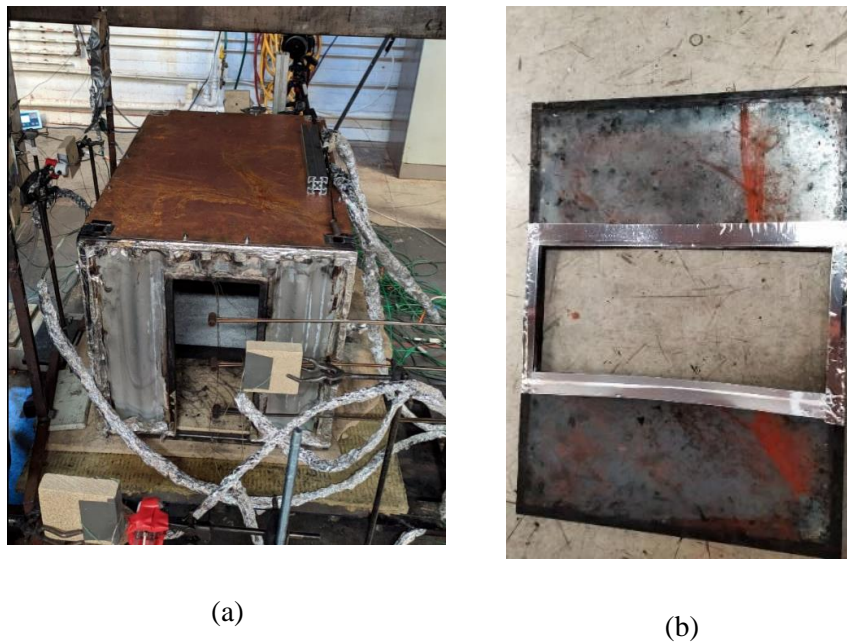


Figure 4: Quarter scale ISO-9705 compartment (open ceiling for demonstration) [18]

**The size and locations of compartment openings:** The size, shape and position of enclosure openings would be highly influential to the fire development in an enclosure. The small-scale compartment had mm or m width door carved on the short wall of the compartment. The sizes and locations of the ceiling horizontal openings would be varied for each test. Two ceiling opening shapes would be checked with one being four square corner openings while the other shape would be a central rectangular opening. The corner openings areas were altered by the following sizes: 0.025x0.025, 0.05x0.05, 0.1x0.1, 0.15x0.15 and 0.2x0.2 m. Whereas the central opening had the following sizes: 0.6x0.02, 0.6x0.07, 0.6\*0.15 and 0.6x0.27 m. The areas of the central openings were chosen to be equivalent to the total areas of the four corner openings. The 0.6x0.02, 0.6x0.07, 0.6\*0.15 and 0.6x0.27 m central openings would be equivalent to total area of the four corners for the 0.05x0.05, 0.1x0.1, 0.15x0.15 and 0.2x0.2 m corner openings respectively. The different opening shapes were manufactured, as illustrated in Figure 5 below.



**Figure 5: Quarter ISO-9705 experimental compartment with four 0.025x0.025 m corner openings (a) and a 0.6x0.27 m Central opening (b)**

No central opening was chosen as an equivalent to mm or m corner openings because it would require a tiny central opening which seemed unpractical. The criteria behind choosing corner vs central openings were to investigate different smoke movement patterns, ventilation conditions, smoke layer thickness, external flaming, thermal feedback from smoke layer, heat balance and mass balance within the enclosure and investigate whether these parameter change or not with different ventilation sizes.

**Table 2: Horizontal Openings Characteristics**

<b>Total Horizontal Openings area (m<sup>2</sup>)</b>	<b>Equivalent four-Corner Openings (m<sup>2</sup>)</b>	<b>Equivalent central Opening (m<sup>2</sup>)</b>	<b>Percentage of the total ceiling area (%)</b>
<b>0.0025</b>	(0.025 × 0.025) × 4	Too small	0.4%
<b>0.01</b>	(0.05 × 0.05) × 4	0.6 × 0.02	2%
<b>0.04</b>	(0.1 × 0.10) × 4	0.6 × 0.07	7.4%
<b>0.09</b>	(0.15 × 0.15) × 4	0.6 × 0.15	16%
<b>0.16</b>	(0.2 × 0.2) × 4	0.60 × 0.27	29.6%

**Ignition source:** 200 ml of Heptane was used as an accelerant for the fuel burning, and hence it would be considered the ignition source. In order to start the burning of Heptane, a blowtorch pilot flame would be utilized to start the ignition in all experiments. The location of pilot flame was of great importance, and the blowtorch flame was pointed at the center of the fuel tray to try to get the same fire pattern in every experiment concerning fire initiation and hence the same fire growth within the tray to have reliable, comparable data.

**The type, amount, position and surface area of the fuel package:** The type and amount of the fuel package would be considered a critical factor that would affect the fire behavior in a compartment. 1000 gm of polypropylene (PP), equivalent to a fuel load of 80 MJ/m<sup>2</sup>, was chosen as the fuel package for our experiment. The 80 MJ/m<sup>2</sup> fuel load was chosen in the experiment based on the previous observations by Beshir et al. [18] which found out that using any fuel load below this value would result in two HRR peak with the one resulting from the accelerant heptane burning to be higher than the flashover peak. The fuel used was chosen to be Polypropylene (PP) which is a type of plastics that would be found in many of today's equipment and gadgets without forgetting its ability to burn very well. Also, it has been exploited as a fuel package in many experiments, and that would make it easier to compare the results with other studies. 200 ml of heptane were added to the PP tray to accelerate the burning rate for the incipient stage of the fire. It was taken into consideration to try to spill the heptane with the same pattern in every experiment. This fuel package was positioned in a 0.4x0.4 m steel tray located at the centre of the compartment, as shown in Figure 6.

**Boundary wall material:** The walls were made of corrugated steel sheets with a thickness of 0.5 mm which is considered a thermally thin material with an estimated Biot number of less than 0.1 at which the temperature gradient can be neglected [11]. The type of wall material could profoundly affect the gas layer temperature, in the case of the steel sheets, it would not retain the energy within the

compartment leading to lower heat transfer feedback from the smoke layer and more energy out to the surrounding which then would lead to fire spreading.

### 2.1.1 Locations and calibration of measurement instrumentation

Several measuring devices were positioned inside and outside the compartment to incorporate all the changes that may occur as a result of adding horizontal openings to an ISD. All the instrumentations would be listed and explained in detail below. The measurement devices utilized in the experiments were as follows:

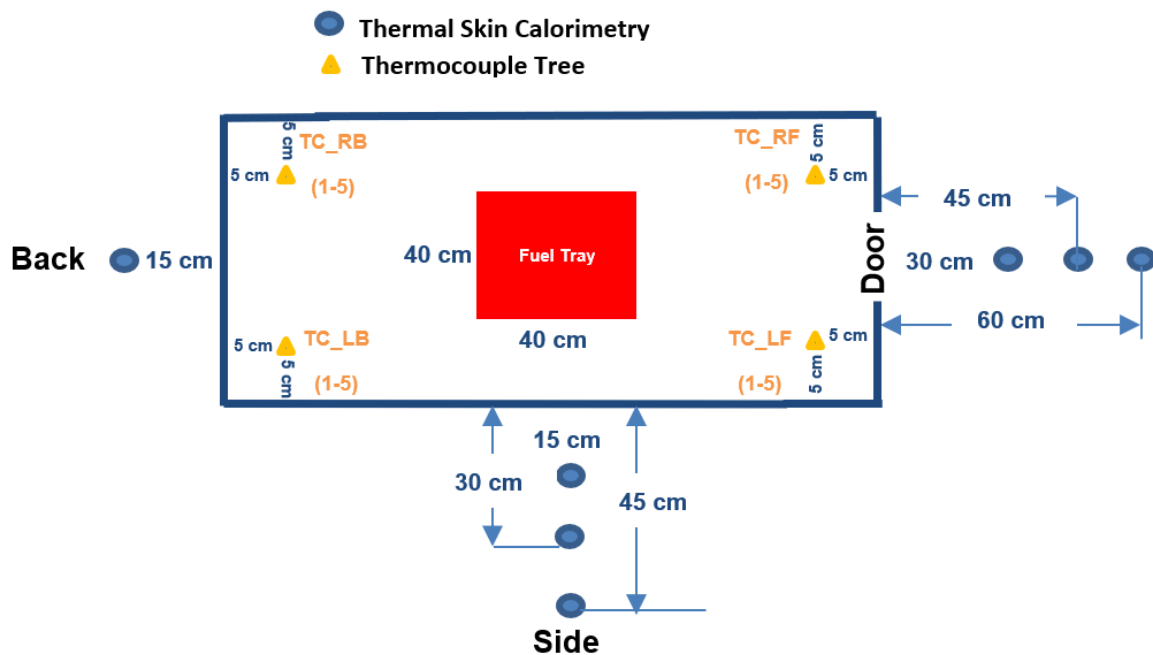


Figure 6: Measurements locations (Not to scale)

**HRR (Using Oxygen Consumption OC)** The small-scale compartment was positioned under a large-scale hood that has a suction fan extracting all the gas products resulting from the fire testing in order to calculate the HRR. The large-scale calorimetry hood uses the Oxygen Consumption (OC) principle plus the measured gas volume fraction besides the flow velocity of the exhaust gases. The HRR was measured based on the formulations derived by Janssens [22] which has an estimated error of  $\pm 10\%$  for the complete combustion, which then increases in case of incomplete combustion or more production of soot and carbon monoxide.

**K type thermocouples (TCs):** As shown in Figure 6, four TC trees were installed at each corner of the room to record the inside temperatures at different heights for the hot gas and cold air layer. The thermocouples are of 1.5 mm type K with five thermocouples at each tree distanced from each other by 0.1 m. The top and bottom ones were located at 0.1 m away from the ceiling and the floor respectively, with each tree fixed at 0.05 m away from the walls.

**Thin skin Calorimeters (TSCs):** the TSCs were incorporated in the study to record the incident heat flux radiating from the compartment at all directions. The TSCs were mounted outside the compartment with their orientation parallel to the room walls. A TSC consists of a small metallic thermally-thin disc fixed to a thick insulator body (vermiculate board) to make sure that the disc temperature was uniform across the whole disc which can be measured using a TC attached to the backside of the disc. The TSC is used to measure the irradiance of the incident heat flux by resolving the energy balance of the disc using equation 3 by incorporating the disc and TC temperatures in addition to the heat losses in conduction, convection and radiation from the side, back and edges of the metallic disc. The equation is as follows:

$$q_{inc}''(T_{disc}) = \frac{1}{\alpha_{disc} - (1-C)} \left[ \gamma \cdot \frac{m_{disc}}{S_{disc}} \cdot C_p \cdot \frac{dT_{disc}}{dt} + \epsilon_{TSC} \cdot \sigma \cdot T_{disc}^4 + h_c \cdot (T_{disc} - T_{\infty}) \right] \quad (3)$$

Where  $\alpha_{disc}$  is the absorptivity of the disc, C refers to the TSC factor, while  $\gamma$ ,  $\frac{m_{disc}}{S_{disc}}$ ,  $C_p$  and  $\frac{dT_{disc}}{dt}$  are the transient compensation, areal density, specific heat capacity of the change in temperature with time for the disc representing conduction heat transfer in the disc body.  $(\epsilon_{TSC} \cdot \sigma \cdot T_{disc}^4)$  represents the radiation losses with  $\epsilon$  as emissivity,  $\sigma$  as Stephan-Boltzmann constant and  $T_{disc}$  being the disc measured temperature. Finally, the convective heat losses are represented by  $h_c$  as the convective heat transfer coefficient with  $T_{\infty}$  being the ambient temperature.

There was a total of thirteen TSCs, three were mounted at distances of 0.3, 0.45 and 0.6 m from the top of the door, One TSC was placed at 0.15 m from the backside, and three were placed at 0.15, 0.3 and 0.45 m from the top middle side of the left wall. Two other vertical sets of three TSCs each were mounted 0.15 m from the front and back corners of the left sidewall.

**Bi-directional flow probes:** They were added to measure the flow velocity through the door and horizontal openings, in addition to estimating the position of the neutral axis which is known to be an imaginary axis at which the flow velocity is equal to zero and it marks as a line separating the cold air and hot gas layers.

Three flow probes were mounted in front of the door at vertical positions of 0.1, 0.25 and 0.4 m from the floor. Two more flow probes were accounted for to measure the flow velocities leaving from the ceiling openings. For the corner ceiling openings, one flow probe would measure the flow velocity of the smoke leaving the front opening while the other would measure the flow escaping from the back one. On the other hand, In the case of the central slot opening, flow velocities would be measured at the middle and side of the central opening. A thermocouple would be attached to each flow probe to help calculate different flow rates at different temperatures. These probes give voltage signals, and therefore these voltages need to be converted to pascals. The conversion ratio for the used probes was 2.5 Pa/voltage. Then this pressure difference needs to be converted into flow velocities. In order to convert the pressure measurement into a flow velocity, equation 4 was needed:

$$V (\text{Flow velocity}) = C \sqrt{\frac{2 \cdot \Delta P \cdot K}{\rho_{\text{gas}}}} \quad (4)$$

Where,  $K=0.88$  (Pitot constant average value) and  $C=$  probe constant which is a function of Reynolds number and the gas density as shown in equation 5

$$\rho_{\text{gas}} = \frac{353}{(T_g + 273)} \quad (5)$$

The  $T_{\text{gas}}$  was measured through the thermocouples attached to the flow probes.

**Water-cooled heat flux sensors:** 2 water-cooled heat flux sensors were also accounted for to measure the heat fluxes radiating from the door and side of the compartment with higher accuracy. One was placed at 0.6 m from the top of the door while the other was mounted at 0.15 m from the middle of the sidewall. Each heat flux gauge was positioned side by side with a TSC to be a method of calibrating the TSCs and make sure that they were giving the right measurements. The heat flux sensors give a voltage output, and in order to convert it to the incident heat flux, equation 6 is required:

$$\phi \left( \frac{\text{W}}{\text{m}^2} \right) = \frac{V (\text{Volts})}{S \left( \frac{\text{Volts}}{\frac{\text{W}}{\text{m}^2}} \right)} \quad (6)$$

Where (V) represents the differential voltage signal of the heat flux gauges divided by the sensitivity of the gauge (S).













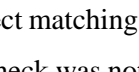
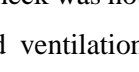
**Gas Analyzer:** Two gas analyzers were added at the second set of tests for the closed ceiling and central opening cases. The first gas analyzer had its probe fixed at the top left corner of the backside of the compartment through a hole made specifically to fit the probe at that position. The second probe was positioned close to the top door flow probe for the closed ceiling cases, but for the central opening cases, the probe was moved to the top of the compartment to analyze the smoke leaving through the ceiling. The analyzers would measure the percentage concentrations of  $\text{O}_2$ ,  $\text{CO}_2$  and  $\text{CO}$ , in addition, the particle count of the hydrocarbon products in ppm. It is noteworthy that one of the main objectives of adding the gas analyzers was to help with the validation process later in this study.

However, it was worth noting that not all the equipment were present from the beginning of the testing as one thermal skin calorimeter was positioned later at 0.45 m from the door in addition to the two gas analyzer that had its probe positioned at the top TC in the left-back corner whereas the second probe was fixated at the top of the door capturing the smoke leaving through there.

## 2.2 Experimental Results

Before starting with the analysis of the experimental results, it was necessary to list all the tests that would be analyzed within the scope of this report. Each test had a particular name and color to be used within the remaining part of the report.

**Table 3: Experimental Matrix**

Test Number	Test name	Opening size (m)	Number of openings	Opening Location	Legend Colour <sup>1</sup>
1	Closed_1	N/A	N/A	N/A	
2	Closed_2				
3	2.5_open	0.025x0.025	4	Corner	
4	5_open	0.05x0.05			
5	10_open	0.1x0.1			
6	15_open	0.15x0.15			
7	20_open_1	0.2x0.2			
8	20_open_2				
9	20_open_3				
10	60X2_open	0.6x0.02	1	Central	
11	60X7_open	0.6x0.07			
12	60X15_open	0.6x0.15			
13	60X27_open_1	0.6x0.27			
14	60X27_open_2				

<sup>1</sup> The matching colours are for the cases with equivalent total areas

### 2.2.1 Repeatability of experimental work

In traditional small-scale testing, repeating the experiment twice or more may not give perfect matching, but it would give similar patterns with very negligible margin of delay. Nevertheless, this check was not investigated before for cases with different shapes and distributions of horizontal and ventilation openings. To investigate the repeatability, the traditional closed ceiling test was repeated twice, similar to the 0.6x0.27 m central opening case while the 0.2x0.2 m corner case was replicated three times to help answer any questions regarding the impact of four different openings making it very hard to replicate.



### 2.2.1.1 Closed Ceiling Experiments

Table 4: Comparison of Closed Ceiling Repeated Tests

Case Name	Average Temperatures for top TCs over the steady-state period				The area under the heat flux curve (Total Radiative Energy)		HRR (When all Top TC reached 525 °C) (KW)
	TC_RB (°C)	TC_LB (°C)	TC_RF (°C)	TC_LF (°C)	TSC_DOO R_0.3m (KJ/m <sup>2</sup> )	TSC_SIDE _0.15m (KJ/m <sup>2</sup> )	
Closed_1	517	480	536	512	3554	2493	87
Closed_2	511 (-1%)*	462 (-4%)	535 (-0.1%)	511 (-0.1%)	3711 (4%)	1955 (-22%)	66 (-24%)

\*Closed\_2 case is compared to the closed\_1 case

As depicted in Figure 7, there was a great extent of accuracy in the duplicated tests as the two curves followed the same trend indicating the same fire dynamics with some delay and a small difference in the peak HRR of about 10 kW. The first test had a peak HRR of 121 kW compared to 113 kW in the repeated test. However, an instantaneous peak HRR value would not be representative when comparing two experiments. Therefore Table 4 was added to show to what extent were the two tests duplicated over the steady-state period to have an averaged value better than an instantaneous one.

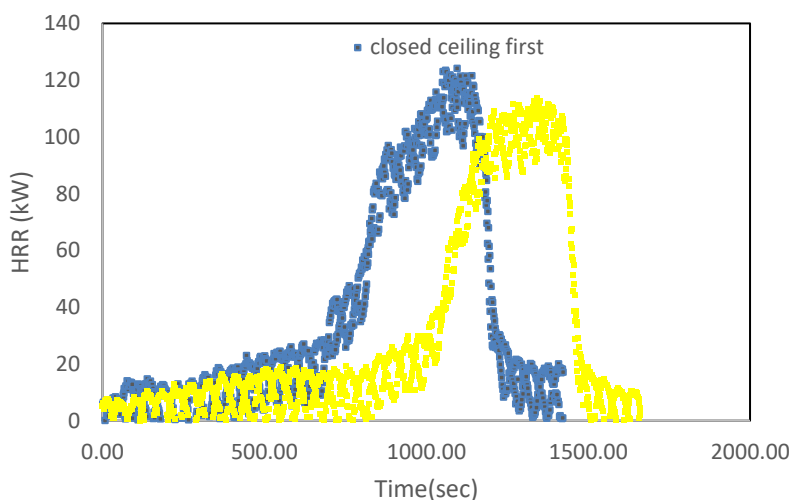


Figure 7: HRR For Repeated Closed Ceiling Experiments

The first comparison was established by calculating the average temperatures for the hot gas layer over the steady-state period in addition to the total radiative energy calculated by integrating the instantaneous incident heat fluxes over the same steady period to get the total radiative energy generated to the

surrounding (area under the curve). Table 4 demonstrated that the average temperatures for the top TCs were matching very well with a maximum margin of  $\pm 4\%$  in one corner, the same observation was noticed for the total radiative energy at 0.3 m from the door with a small alteration of  $\pm 4\%$  also. On the other hand, there were higher variations of about  $\pm 23\%$  for the radiative energy generated from the side and the HRR value at which all the top TCs reach flashover criteria.

Besides, less leakage led to quickly form the hot gas layer increasing the heat transfer feedback to the floor resulting in a lower HRR value of 66 kW required for flashover in the repeated test compared to 87 kW for the first closed ceiling experiment. Another observation was the time delay between the two curves, which reached an approximate value of 400 seconds. The explanation would require visual observations throughout the whole experimental study which showed that even with meticulous considerations to fuel amount, location, accelerant amount, location and the piloted flame location, the way the flames would spread across the tray burning the heptane then spreading to the PP would vary in some experiments. It was apparent that any judgement or human error would lead to some time delay in the incipient phase, but this would not affect the growth or flashover phase, as observed in the HRR curves.

### 2.2.1.2 Corner/Central openings

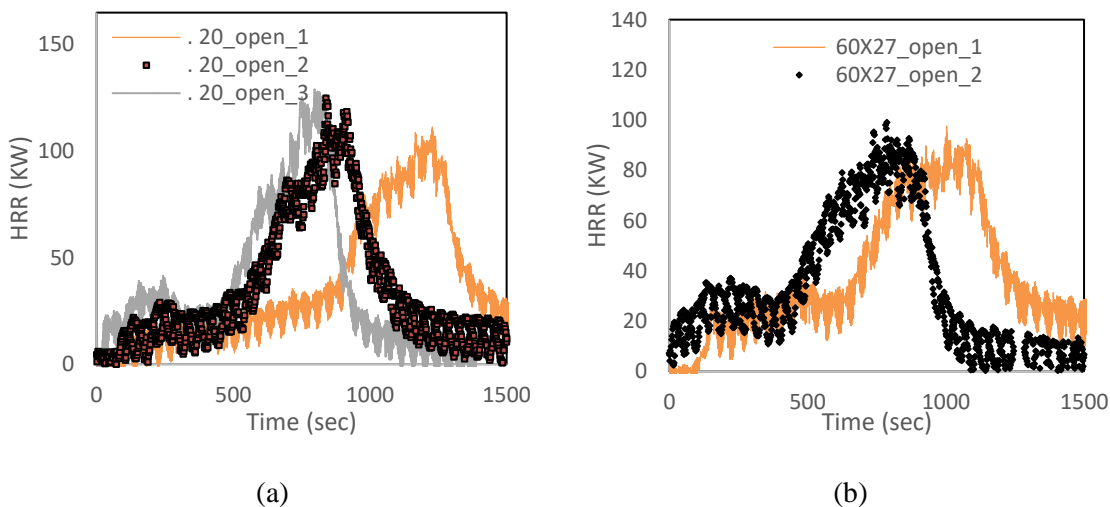


**Figure 8: Repeated Tests for 0.2x0.2 m Corner (a) and 0.6x0.27 m Central Openings (b)**

Based on Figure 8a and 8b, there were similar trends in the HRR curves for the repeated tests for the 0.2x0.2 m corner openings and the 0.6x0.27 m. However, Figure 8 revealed some apparent differences within the corner openings cases than the central opening one, especially in the heat flux, radiated from the sidewall. As a result of this, further analysis of the different smoke movements for the corner openings case is required as it seems that having four different openings will lead to different smoke movement every time. It was demonstrated in that the peak HRR for the three cases ranged between 111 kW- 129 kW showing a difference of 15% which could be considered as an acceptable margin.

**Table 5: Average steady-state Temperatures and Radiative energy for Corner/Central Ceiling Openings Repeated Tests**

Case Name	Average Temperatures for top TCs over the steady-state period				The area under the heat flux curve (Total Radiative Energy)	
	TC_RB (°C)	TC_LB (°C)	TC_RF (°C)	TC_LF (°C)	TSC_DOOR_0.3 (kJ/m <sup>2</sup> )	TSC_SIDE_0.15 (kJ/m <sup>2</sup> )
<b>Corner Openings</b>						
20_open_1	313	302	328	313	1478	935
20_open_2 <sup>1</sup>	324 (4%)	304 (0.1%)	318 (-3%)	305 (-3%)	1572 (6%)	1161 (24%)
20_open_3 <sup>1</sup>	360 (15%)	336 (11%)	351 (7%)	343 (10%)	1466 (-1%)	1215 (30%)
<b>Central Openings</b>						
60x27_open_1	294	291	274	275	1587	1170
60x27_open_2 <sup>2</sup>	331 (13%)	320 (10%)	286 (4%)	290 (5%)	1526 (-4%)	1160(-1%)

<sup>1</sup> The cases were compared to the 20\_open\_1 case

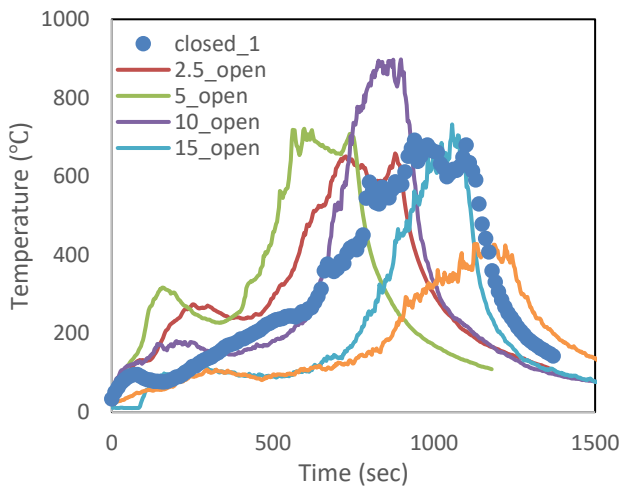
<sup>2</sup> This case was compared to the 60\*27\_open\_1 case

Another good fit was seen in Table 5 for the average temperatures of the top TC especially between the first two tests with a margin of  $\pm 3\%$  whereas the third test showed higher margins of about 15% and 10% for the back and front TCs respectively. Besides, the most significant margin appeared in the radiative heat flux from the sidewall, with approximately 30% difference between the first and third test. The higher margins in the temperatures and radiative energy from the side could be discussed by looking at the ceiling design with four corner openings. In order to get the same data when duplicating the experiment, everything must act similar, starting from the smoke production, smoke movement, mass flow from each opening and door. These parameters were rarely expected to duplicate in the corner ceiling openings because the presence of four openings would lead to different patterns of smoke movement and ventilation conditions for each test. One corner would have more burning in one experiment leading to more flames from the corner which would be captured by the TSC located at 0.15 m from the centre of the sidewall. The fire location would play a crucial role with such a horizontal opening type, and it was believed that if the fire were located at one of the corners, it would generate better fit for the temperatures and radiative energy from the side as the smoke movement would be directed by the sidewalls and the ceiling corner opening, leading to similar behaviour.

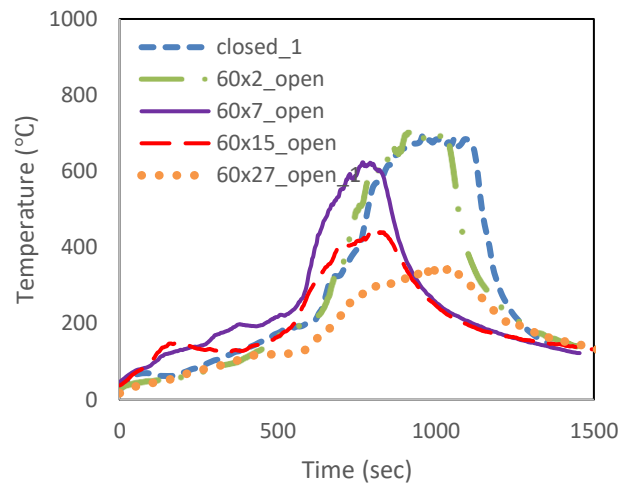
The relation between the fire vs opening location could be emphasized by looking at the central opening repeated tests which illustrated a very close matching in all the data, starting from the peak HRR which ranged between 97-99 kW for both as shown in Figure 8b. Then moving to the calculated average

temperatures and the radiative energy to the surrounding, which displayed a  $\pm 5\%$  margin of difference between the two tests. This almost matching fit would be the result of the fire location being in the centre of the compartment with the horizontal opening being right above it which limited the direction of the hot produced gases and in return would help replicate the experiment while having almost the same curve or the same fire dynamics.

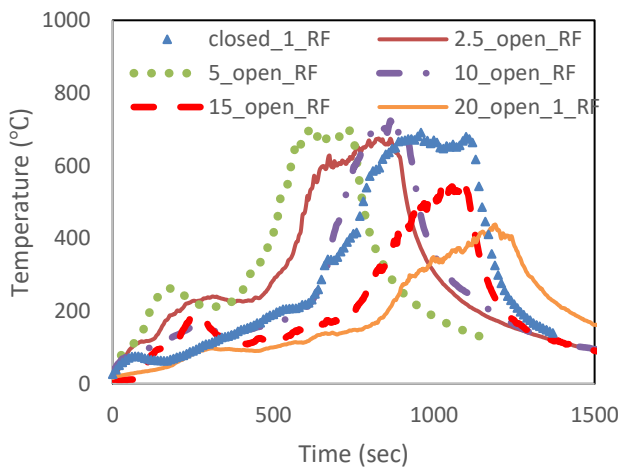
### 2.2.2 Hot gas layer temperature



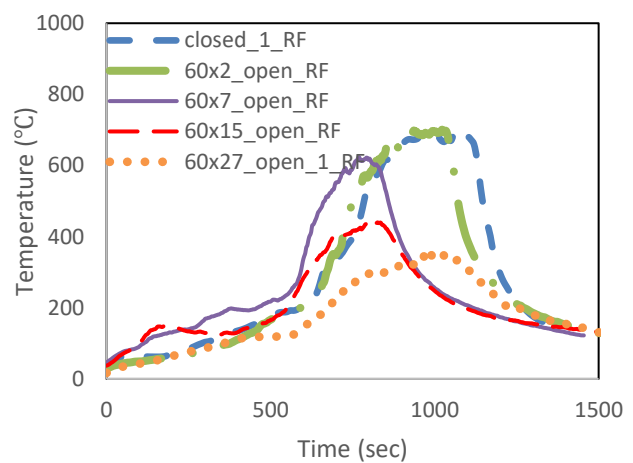
(a) Right back for corner opening cases



(b) Right back for central opening cases



(c) Right front opening cases



(d) Right front for ceiling opening cases

**Figure 9: Top TCs in the right front and back for both corner and central ceiling openings**

Analysing the influence of the horizontal ceiling openings on the temperature profile would be demonstrated qualitatively by visually analysing the curve trends for each opening size as seen in Figure 9, and quantitatively by looking at the average values of the top TCs in each corner as displayed in Table 6. By resolving the curves' patterns in Figure 9, it was observed that the relation between the

temperature and horizontal opening size and type was not linear, therefore, the analysis would be divided based on the temperature profile at the backside of the compartment then the front side.

**TC\_LB/TC\_RB\_Corner:** The results showed in Figure 9a and 9b that the smoke layer temperature would be slightly affected by the increase in ceiling openings size, but the point that stood out in our study was the higher peak appearing for the 10\_open corner openings case. This difference from the prior study would be due to the different TC tree location for both studies, as in our study the TC tree was positioned under each corner opening opposed to the previous study which had the TC trees away from the ceiling openings. Besides, during the experiments there was consistent flame appearing starting to impinge from the ceiling opening when its area exceeded the 0.01 m<sup>2</sup> with the 5\_open case indicating more burning happening at that location causing temperatures to increase and flames to appear from the ceiling openings. Another justification could be that when the ceiling ventilation increased, this led to the neutral axis height to increase more from the floor and this meant more air in that could tilt and push the flame backwards which would explain why the spike in the back temperatures occurred. When the ceiling opening size exceeded 0.04 m<sup>2</sup> (10\_open corner case), the peak started decreasing until reaching its lowest value at 0.16 m<sup>2</sup> corner opening size with the 20\_open case. So, it can be concluded that the 0.04 m<sup>2</sup> corner opening area could be considered a threshold value after which the change in temperature would decrease significantly. As shown in Table 6, the 10\_open case showed an increase in the top back TC temperature by 27% compared to a decrease of about 19% for 15\_open case (0.09m<sup>2</sup> opening size) Visually, the 15\_open and 20\_open cases had negligible door flames indicating that they failed to achieve flashover which reflected on the temperatures.

**The top TC in the backside of the compartment for central opening cases:** The central opening case followed a similar yet insignificant increase-then-decrease trend similar to the corner openings case. However, despite showing a maximum peak temperature at the 60x7\_open case (0.04 m<sup>2</sup>), it showed lower average values than the 60x2\_open case (0.01 m<sup>2</sup>). This meant that the threshold value for the central openings was the 0.01 m<sup>2</sup> after which the smoke layer temperatures started decreasing significantly until failing to reach flashover for the 60x15\_open and 60x27\_open cases.. The fire location just below the opening in addition to the bigger area for a single central opening compared to an equivalent four-opening area would have a bigger effect regarding the smoke layer building up. It was also demonstrated in the Figure 9a and 9b that the temperatures were higher for the corner cases in comparison to the central cases, and this would also be explained with the TC trees' locations to the opening type. The corner openings trees would capture the external ceiling flames, which was not the case in the central openings and therefore the temperatures were smaller.

**The top TCs in front side of the compartment for corner/central opening cases:** The front side gave the exact conclusion that was suggested by Qiang et al. [21] as it showed very slight changes in temperatures with the increase of the ceiling openings area, excluding the biggest two openings which failed to achieve the flashover criteria and hence showed much lower temperatures. In the front side, it

was obvious that temperatures would be represented through the external door flaming and the addition of more air to the fire would lead to more burning and hence higher temperatures. This was noticed for the 5\_open and 60x2\_open cases, as they represented the higher values in the front side but with a minimal margin that would not be considered. The less external flaming, the less burning at the top front TCs and as a result, lower temperatures for bigger opening sizes.

**Table 6: Average Temperatures over a steady period for Top Thermocouples for each case**

Case Name	Top TC in the left-back tree (°C)	Top TC in the right-back tree (°C)	Top TC in the left front tree (°C)	Top TC in the right front tree (°C)
<b>Closed_1</b>	517	480	536	512
<b>Corner Openings</b>				
<b>2.5_open</b>	487 (-6%)	516 (8 %)	501 (-7%)	522 (2%)
<b>5_open</b>	571 (10%)	585 (22%)	556 (4%)	564 (10%)
<b>10_open</b>	658 (27%)	627 (31%)	559 (4%)	538 (5%)
<b>15_open</b>	420 (-19%)	437 (-9%)	384 (-28%)	403 (-21%)
<b>20_open_1</b>	313 (-40%)	302 (-37%)	328 (-39%)	313 (-39%)
<b>Central Openings</b>				
<b>60x2_open</b>	529 (2%)	539 (12%)	535 (-0.1%)	537 (5%)
<b>60x7_open</b>	518 (0.2%)	503 (5%)	455 (-15%)	445 (-13%)
<b>60x15_open</b>	378 (-27%)	369 (-23%)	339 (-37%)	326 (-36%)
<b>60x27_open_1</b>	294 (-43%)	291 (-39%)	274 (-49%)	275 (-46%)

### 2.2.3 Incident heat flux to the surrounding

The focal point of this study was to find novel solutions to limit the fire spread between ISDs, which could either occur through direct flame impingement or radiation and incident heat flux to the surrounding to start spontaneous ignition of other materials and in return spreading the fire. The analysis would be extended to four main points regarding the incident heat flux, naming: 1) Effect of opening size, 2) Effect of the opening shape, 3) Effect of the TSC distance 4) Effect of the TSC location

(side/back). Table 7 demonstrates the total radiative energy to the surroundings, which was calculated by estimating the area under each curve over a steady-state duration. Besides, all the cases were compared to the closed ceiling case (closed\_1) to observe the percentage reduction or increase in the incident heat flux to the door, side or back with the steady-state durations chosen based on the HRR curves that can be found in the appendix.

**Table 7: Radiative Heat Energy from the compartment to the surroundings**

Case Name	Steady State Duration (sec)	The area under the curve (Total Radiative Energy) (kJ/m <sup>2</sup> )		
		0.3 m from the door	0.15 m from the sidewall	0.15 m from the back
<b>Closed_1</b>	567	3554	2493	2166
<b>Corner Openings</b>				
<b>2.5_open</b>	490 (-14%)*	2603 (-27%)	1542 (-38%)	1823 (-16%)
<b>5_open</b>	392 (-31%)	2856 (-20%)	1404 (-44%)	1827 (-16%)
<b>10_open</b>	351 (-38%)	2473 (-30%)	1366 (-45%)	2835 (31%)
<b>15_open</b>	486 (-14%)	1897 (-47%)	1218 (-51%)	2700 (25%)
<b>20_open_1</b>	527 (-7%)	1478 (-58%)	935 (-62%)	1064 (-51%)
<b>Central Openings</b>				
<b>60x2_open</b>	510 (-10%)	2669 (-25%)	1932 (-23%)	2002 (-8%)
<b>60x7_open</b>	370 (-35%)	1248 (-65%)	1475 (-41%)	1510 (-30%)
<b>60x15_open</b>	486 (-14%)	1162 (-67%)	1133 (-55%)	1195 (-45%)
<b>60x27_open_1</b>	637 (12%)	1587 (-55%)	1170 (-53%)	1085 (-50%)
*All the cases are compared with reference to the closed_1 case				

### 2.2.3.1 Effect of opening size

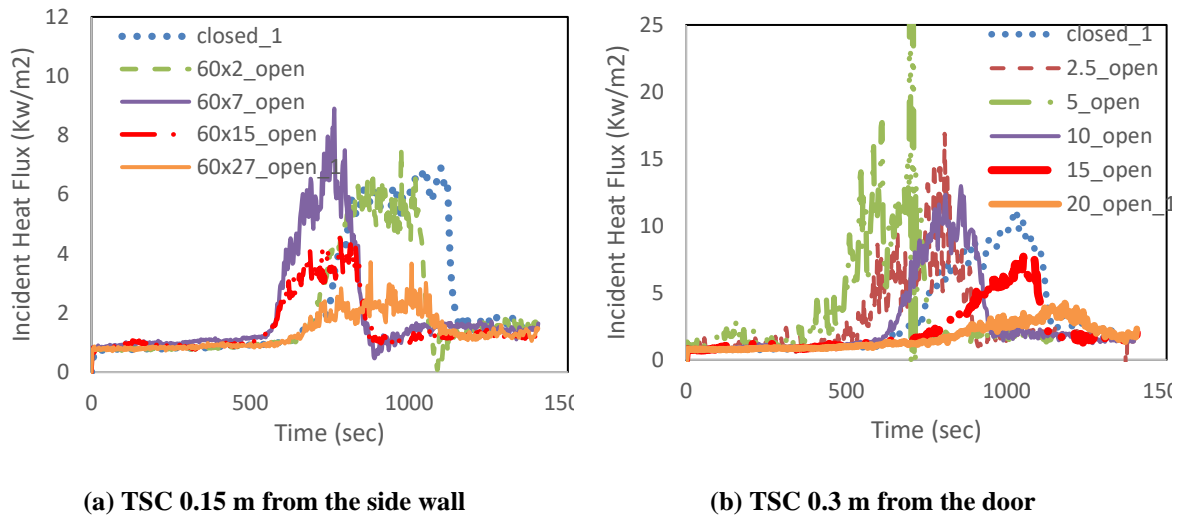


**Figure 10: Openings size effect on the incident heat flux to the surrounding**

Figure 10a and 10b showed that the incident heat fluxes from both the side wall and the door were almost similar for the closed ceiling and the horizontal openings up to 0.04 m<sup>2</sup> total area (10\_open/60x7\_open). However, the total radiative energy decreased dramatically up to 60% as seen in Table 7 when the horizontal openings' sizes increased up to 0.16 m<sup>2</sup>. Based on the visual observations displayed in Figure 11 and Figure 12, the external door flaming size for each case. It was speculated while observing the experiments that the incident heat flux from the side would exceed the closed ceiling case due to the presence of ceiling flames, however, It turns out that the closed\_1 case had the maximum values of radiative energy to the door and side wall. The answer to that point would be the thermally-thin wall. With no ceiling opening present, all the heat was trapped inside and the only heat transfer mechanisms available were exiting through the door as a flame and transferring the heat through the sidewall which was observed visually with the presence of hot spots on the compartment walls as displayed in Figure 13.

Qualitatively speaking the presence of horizontal ventilation would be a compromise tool between the door, side. As the heat balance would be directed to the ceiling openings rather than radiating through the thermally-thin wall or the main compartment door. Based on the heat balance rule, with more flames and hot smoke vented through the ceiling, less heat would transfer to the sidewall or the door and would prove the impact of horizontal ventilation of the reduction of radiative heat flux to the surrounding.



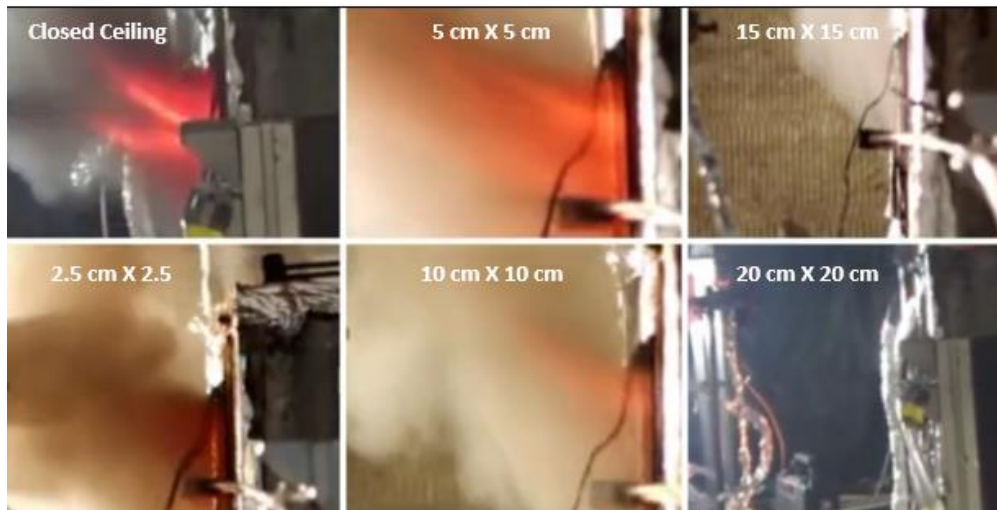


**Figure 11: Screenshots for the external flaming for the corner opening tests (during the steady state)**



**Figure 12: Screenshots for the external flaming for the central opening tests (during the steady state)**

It was observed from Table 7 that the steady-state duration was the longest for the closed ceiling case when compared to the remaining cases, and that would explain clearly why its total radiative energy was higher than the rest.

It was speculated while observing the experiments that the incident heat flux from the side would exceed the closed ceiling case due to the presence of ceiling flames, however, It turns out that the closed\_1 case had the maximum values of radiative energy to the door and side wall. The answer to that point would be the thermally-thin wall. With no ceiling opening present, all the heat was trapped inside and the only heat transfer mechanisms available were exiting through the door as a flame and transferring the heat through the sidewall which was observed visually with the presence of hot spots on the compartment walls as displayed in Figure 13.



**Figure 13: Hot spot on the compartment walls for the closed ceiling case**

It is interesting to note that the hot spots also appeared for the 2.5\_open, 5\_open, 60x2\_open and 60x7\_open cases, but for shorter times, which could be explained by looking at the heat balance for each case. For the closed ceiling case, as there were no horizontal openings, then the smoke layer would build up faster, resulting in re-radiation from the ceiling to the floor. In thermally thick compartments, most of the heat losses are through the external plume, however, in the thermally thin compartment the heat could transfer by conduction through the wall materials then radiates to the outside. When horizontal openings were added, a percentage of the heat will be lost through horizontal opening, leading to a reduction in the heat flux from the door and the sidewall (less glowing of the hot spot). Besides, the reason for the shorter peak steady-state duration, especially for the 2.5\_open, 5\_open and 60x2\_open, could be related to the burning rate. The closed\_1 case, was severely under ventilated with not enough oxygen available which led to slower burning rate. With the addition of horizontal openings, a stream of air and oxygen entered the room increasing the combustion efficiency, burning rate and in return decrease the steady-state period. For the cases with horizontal opening sizes beyond  $0.04 \text{ m}^2$  the compartment became an over-ventilated leading to a reduction in all the thermal characteristics of the compartment.

The main reason for analyzing the total radiative energy in Table 7 was to test it against the critical heat fluxes of materials found in informal settlements based on the study done by Wang et al.[24], where a database of the burning characteristics of the materials existing in IS was gathered through lab experiments with some of these materials listed below in Table 8. Based on the measured data in our study, some materials were chosen from the burning materials database, which was expected to start igniting even with the small-scale compartment. This requires further analysis, especially for the remaining materials, which can start burning with a scaled-up dwelling. It can be concluded from Table 8 that some materials will mostly burn because of their ability to ignite spontaneously when exposed to a very insignificant amount of radiative energy, naming : rubber, some types of plastic, newspapers, some types of foam, bedding and most types of clothing. Nevertheless, some other materials would need

much higher critical radiative energy for them to start igniting on their own, for instance, the cardboard and vinyl would require an approximate amount of energy of about 3311 and 2724 kJ/m<sup>2</sup> respectively. The addition of horizontal ceiling openings would matter with such materials, based on the calculated data stated in Table 7, it seemed that most of the corner openings cases would cause the spontaneous ignition of these materials compared to the central opening cases. Again, this was a very small analysis of this point as it needs further analysis, but at least it showed that the presence of horizontal openings could make an impact of reducing the amount of radiative energy to the surrounding and in return would help prevent fire spread considerably.

**Table 8: Burning characteristics of materials found in informal settlements [24]**

<b>Material Number</b>	<b>Material Name</b>	<b>Average Ignition Time (sec)</b>	<b>Critical Incident Heat flux (kW/m<sup>2</sup>)</b>	<b>Critical radiative energy kJ/m<sup>2</sup></b>
7	Rubber (Clear Plastic)	42	10-11	462
8	Plastic and rubber (shade netting)	68	9-10	680
9	Cardboard	301	10-11	3311
14	Newspaper	7	20	140
15	Light Yellow Foam	54	8-9	486
19	Bedding (Colourful blanket)	71	8-9	639
23	Green Carpet	485	7-8	3880
24	Vinyl	227	11-12	2724
29	Clothing (Blue T-shirt)	18	14-15	270
31	Clothing (Grey trousers)	15	11-12	180
32	Clothing (Women leggings)	12	12-13	156

### 2.2.3.2 Effect of the opening characteristics

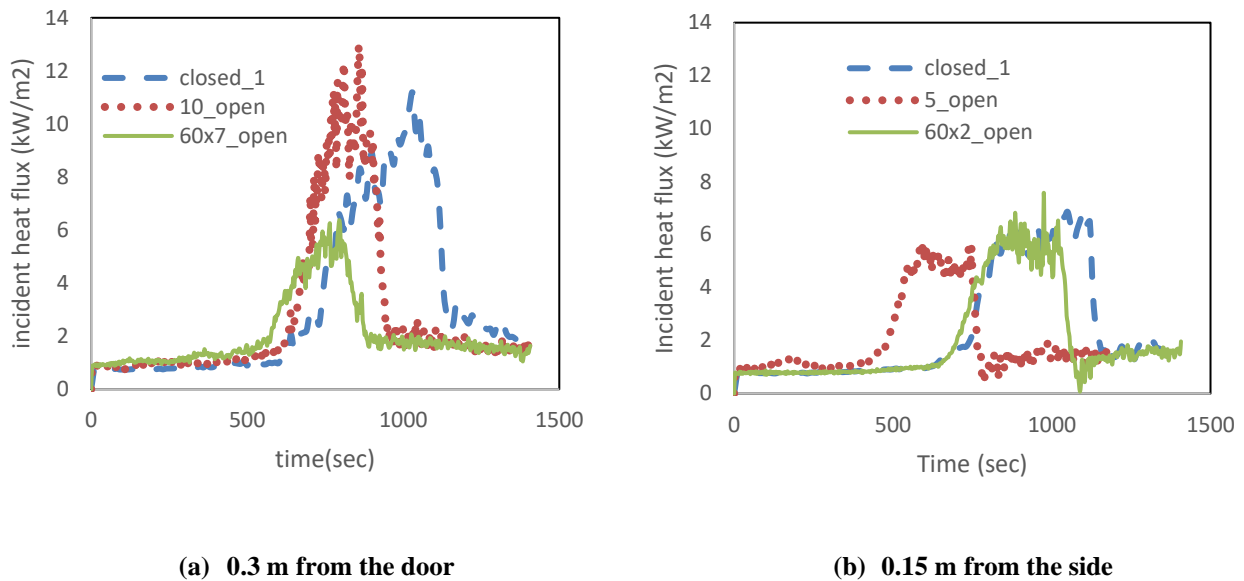


**Figure 14: Effect of the opening shape on the incident heat flux**

After understanding the effect of increasing the area of the horizontal opening, it was the turn to keep the area constant while checking the impact of the opening shape on the radiative heat flux to the surrounding. It was crucial to know how the distribution of these openings across the compartment ceiling would affect the fire development within the dwelling. Based on Table 9, there were different patterns taking place for each horizontal opening area; hence, the analysis would investigate each area on its own.

**0.01 m<sup>2</sup>:** There was an apparent trend in the resulting data from the door and side from Figure 14b and Table 9 where the corner cases were dominant over the central opening cases from the door side. Starting with by the door side where there was a small difference between the two types of openings, this could be justified by looking at the experimental screenshots in Figure 11 and Figure 12 where there was a continuous visible external door flame, yet the flame was more significant for the 5\_open case compared to the 60x2\_open case despite having a similar horizontal opening area of 0.01m<sup>2</sup>. The reason for that would be related to heat and mass balance of the compartment for each opening's type. The 5\_open corner case had no visible flames from the horizontal openings indicating less mass and heat leaving from the ceiling whereas the 60x2\_open central case had a steady high flame visible from the ceiling opening indicating more mass and heat loss to the outside and therefore would lead to lower heat and mass burned at the door. This external ceiling flame for the 60x2\_open case would justify the higher radiative energy measured by the side TSC compared to the equivalent corner case which did not have visible external ceiling flames.

**0.04 m<sup>2</sup>/0.09m<sup>2</sup>:** The same justification could be used on the 0.04 and 0.09 m<sup>2</sup> cases based on Figure 14a and Table 9. Any increase in the area of the horizontal opening would be divided over four corner

openings, and on the contrary, this would all go to one central opening making it more prominent and more influential on the hot gas layer thickness, heat and mass losses. With the smoke layer not building up as fast as the corner case, this meant less heat transfer feedback to the floor which in return resulted in less heat transfer through the thermally thin wall which explained the lower radiative energy from the side and back. Besides, external corner openings flaming started appeared clearly for these areas, which led to a significant increase in the backside radiative energy for the corner case compared to the central opening case.

**0.16 m<sup>2</sup>:** At last, this opening size was too large for flashover to happen, resulting in almost no external flaming at all from the door in either opening's types, which proved why their radiative energy was low and almost equal across all surroundings.

**Table 9: Effect of Horizontal Opening characteristics on radiative energy to the surrounding**

Total Horizontal Openings area (m <sup>2</sup> )	Radiative Energy from the door (kJ/m <sup>2</sup> )		Radiative Energy from the side (kJ/m <sup>2</sup> )		Radiative Energy from the back (kJ/m <sup>2</sup> )	
	Corner	Central	Corner	Central	Corner	Central
<b>0.01 (5_open/60x2_open)</b>	2856	2669	1404	1932	1827	2002
<b>0.04 (10_open/60x7_open)</b>	2473	1248	1366	1254	2835	1510
<b>0.09 (15_open/60x15_open)</b>	1897	1162	1218	1133	2700	1195
<b>0.16 (20_open/60x27_open)</b>	1478	1587	935	1170	1064	1085

### 2.2.3.3 Effect of the TSC distance

As shown in Figure 19, the incident heat flux value was non-linearly inversely proportional to the distance from the compartment. The closest TSC captured the highest incident heat flux from the compartment with a significant margin of difference with the one that was only 0.15 m away from it. The further the TSC was, the less the margin of difference between the TSCs measurements would be.

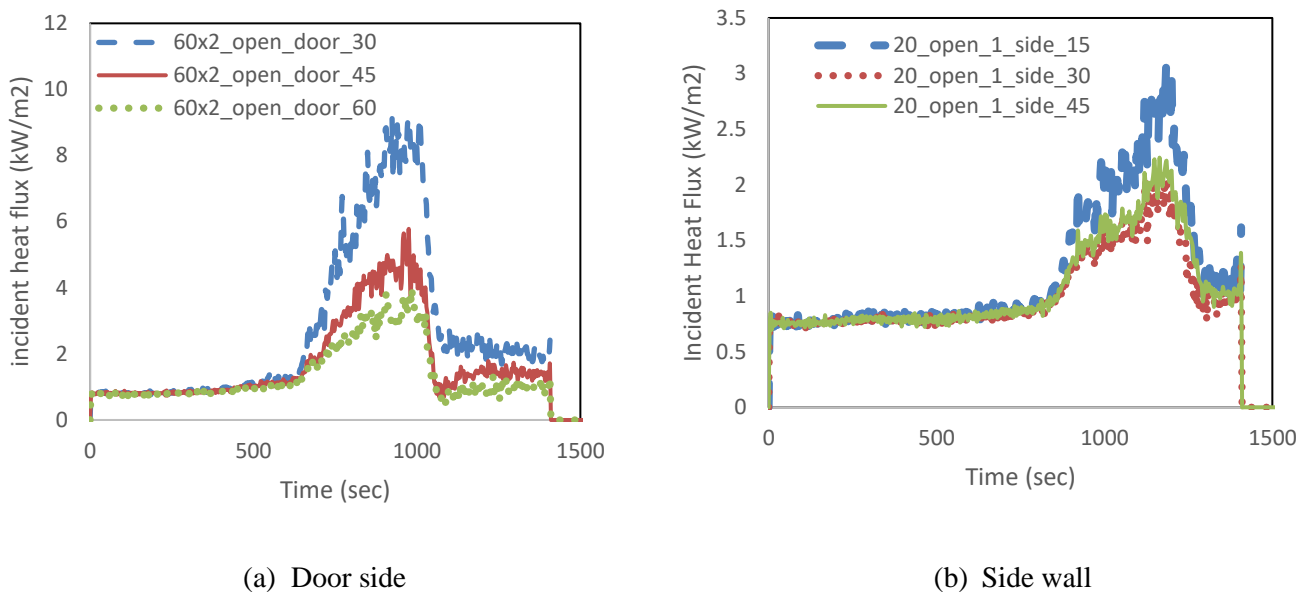


**Figure 15: TSC distance effect on incident heat flux from the door**

A limitation to the use of TSCs to capture the incident heat flux from the side in the corner openings experiment could be seen in the right chart of Figure 15 as the TSC located at 0.45 m from the centre of the wall captured more incident heat flux than the one location at 0.3 m from the wall. During the experimental set-up, in order to position the TSC disk directly facing the sidewall, it needed to be shifted a couple of centimeters aside to capture all the radiation without any blockage from the TSC positioned in front of it. This limitation would appear primarily with the corner ceiling openings as illustrated in Figure 16, because the distances between the corner and the central wall TSCs were diagonal, that is why any horizontal shifting of the TSCs in the back would make it closer to the corner than the one in front of it. On the other hand, the central openings had most of their radiative energy from the centre of the wall, and therefore small horizontal shifts would not make a significant effect as the distance between the disk, and the wall would be straight. This should be put into consideration in future experiments, especially with small distances in small scale tests. This might not be a problem in large scale as the TSC would capture the total radiative energy generated from the compartment walls or visible flames.

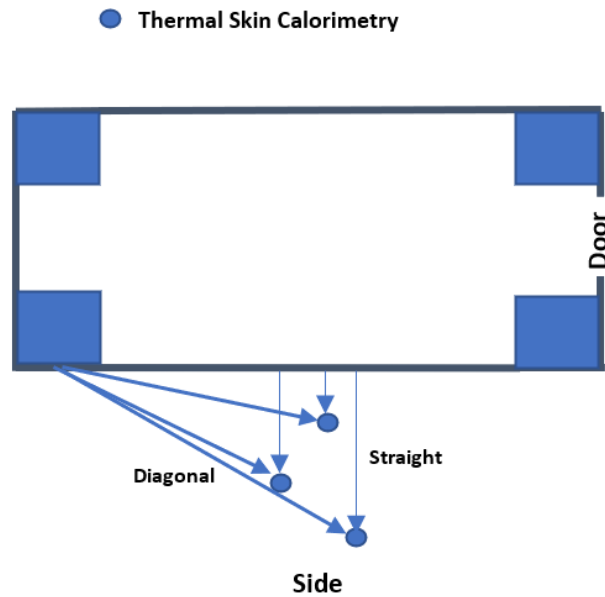
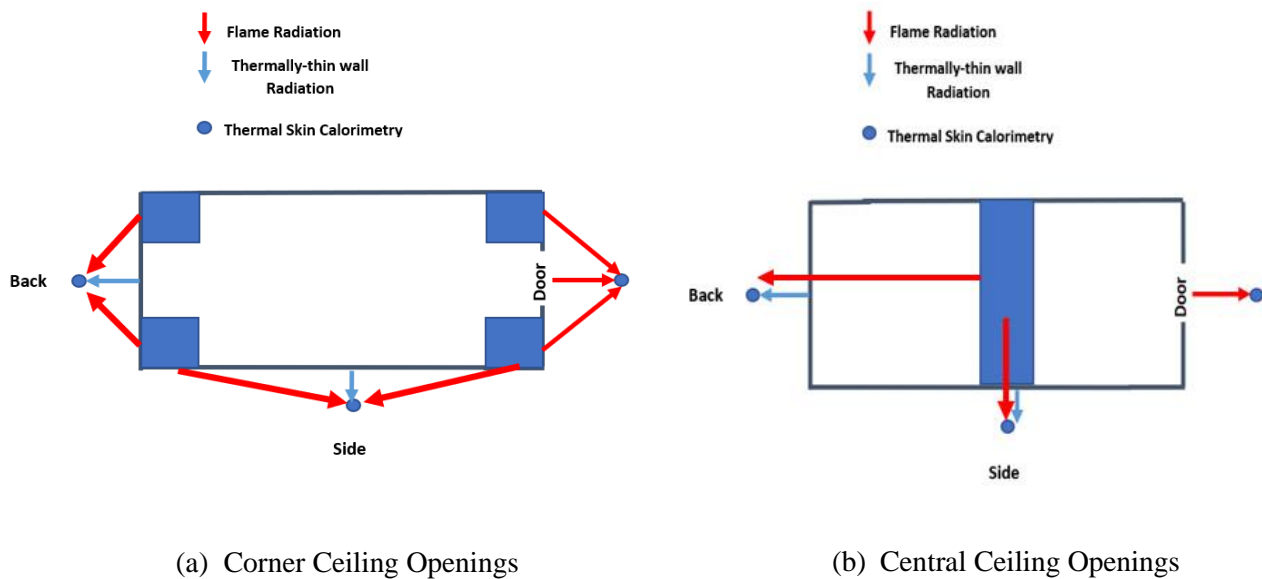


Figure 16: Side TSC limitations with corner openings experiments

### 2.2.3.4 Effect of the TSC location (side / back/door)



(a) Corner Ceiling Openings

(b) Central Ceiling Openings

Figure 17: TSC location effect on incident heat flux from the compartment

As seen in Figure 17a and 17b, the incident heat flux picked up by the TSC could come from two sources, the first one would be directly from the flames, while the second source would be the heat transfer through the thermally-thin boundary walls. There was no direct relation between the TSC location, and the magnitude of the radiative energy captured by it. It could be considered a function between the opening size, type and location. The analysis would require Figure 17 and Table 9 to understand why each location would have a different incident heat flux. Starting from the closed ceiling case, where the primary source of radiative energy was the consistent external flame from the door touching the TSC in

front of the door making it capture the maximum incident heat flux of all the surrounding sides. On the other hand, the side and back would pick up their measured radiative heat flux through the heat transferred through the thermally-thin wall causing both TSCs to measure an almost equal radiative energy with a small margin of difference arising from any extra leakage occurring at one side more than the other. Now, moving to the 2.5\_open, 5\_open and 60x2\_open cases where there was a significant visible flame extending from the top of the door leading to higher radiative energy from the door than the side and back. The lack of externally visible flame from the 2.5\_open and 5\_open corner openings resulted in most the measured radiation coming from the boundary walls. The 60x2\_open case had visible continuous flames from the central opening radiating to the side, on the other hand, due to the opening there was much less heat transfer from the boundary wall compared to the backside leading to equalizing the radiative energy at the two sides

A different pattern was observed in the 10\_open and 15\_open cases, as more flames were observed extending from the back openings compared to the door and front ceiling openings leading to higher measured radiative energy from the back compared to the other sides. The 20\_open and 60x27\_open cases had lower internal temperatures and no external flaming either from the door or the ceiling openings leading to a balance between the heat flux towards the different sides with no side being dominant over the others. Finally, cases like the 2.5\_open and 5\_open had only external flames from the door with no flames appearing from the ceiling openings, that is why the heat flux from the door for these cases is dominant over the remaining locations.

## **2.2.4 Inflow/Outflow from the compartment openings**

One primary phenomenon that was observed during specific experiments was the ‘Oscillating’ or ‘Ghosting’ flames. The oscillating phenomenon could be seen in Figure 19 when the flame started to decrease until it almost disappeared inside the compartment, and then it started to return to its original size. While the ghosting term meant that the flame would seem like leaving the fuel surface and start appearing in other places within the compartment or outside it. In [18], the flame oscillation cycle was found to differ with the opening size and type. One cycle in the 60x2\_open case ranged between 60 and 80 seconds, compared to (10-15) and (5-10) seconds for the 5\_open corner and closed\_1. This phenomenon occurs when a compartment becomes air-starved with not enough oxygen to sustain burning above the flame source. Therefore the flames started moving across the compartment to areas until it stabilizes in areas where there is enough oxygen and mostly these locations are the compartment air inlets, and this would be explained through the back gas analyzer data for the closed\_2 and 60x2\_open cases as illustrated in Figure 18 [25]. The reason for this phenomenon happening within these specific cases could be explained that for the closed ceiling case, the only source of oxygen was through the bottom side of the door, on the other hand, the presence of horizontal openings would add another source of air to the oxygen-starved locations. The rate of added oxygen would depend on the ventilation size, the bigger the opening size the more oxygen would be added to increase the oscillation



cycle as observed and explained above. The reason the 60x2 central opening case had the most extended cycle was due to the type, size and location of the opening with respect to the fire location. The dimensions of the central opening would allow for more air changes from the opening sides, allowing for more frequent oscillations. However, it is worth noting that there is the limit for ventilation openings size, as a more significant size means more air in the compartment and more air would make it over-ventilated, and therefore no oxygen starvation would exist inside the compartment.

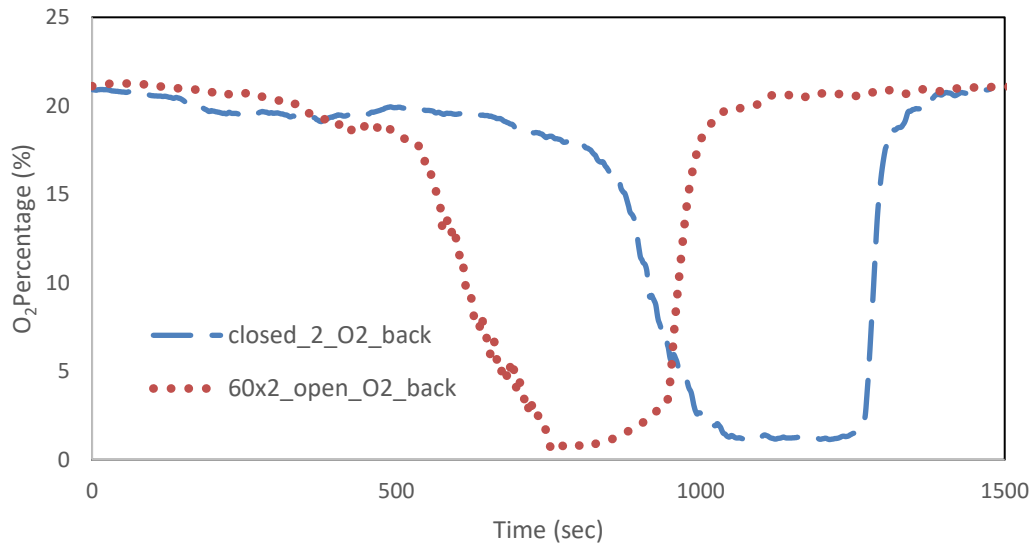


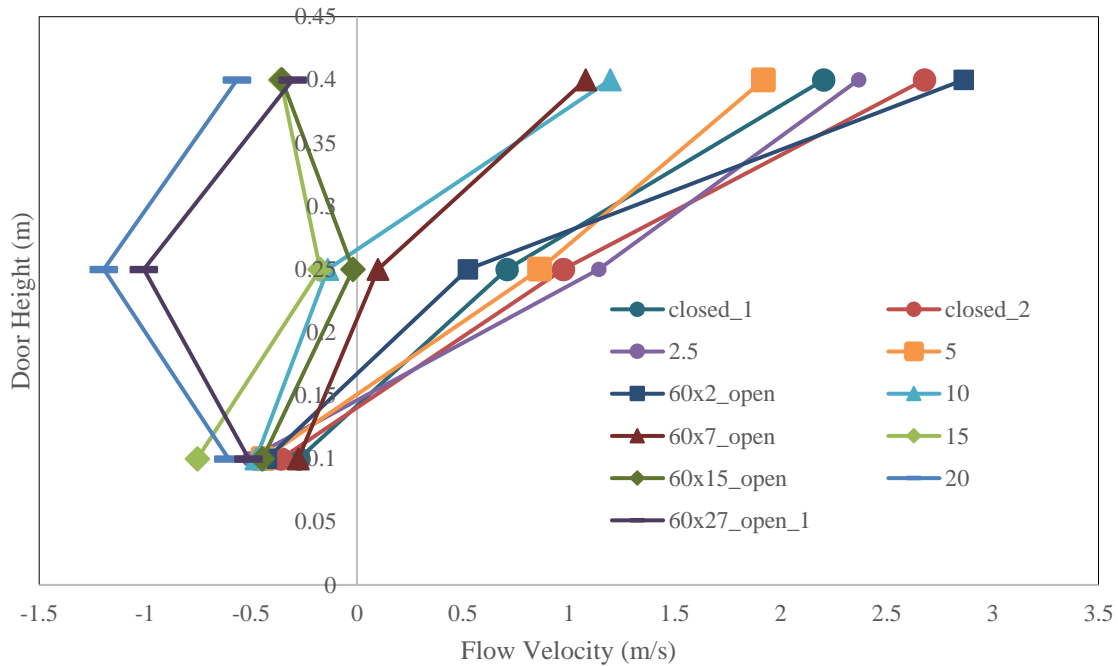
**Figure 18: Back gas analyzer data aiming at explaining the oscillating flames**



**Figure 19: Oscillating Flames in the 0.05x0.05 m corner opening case**

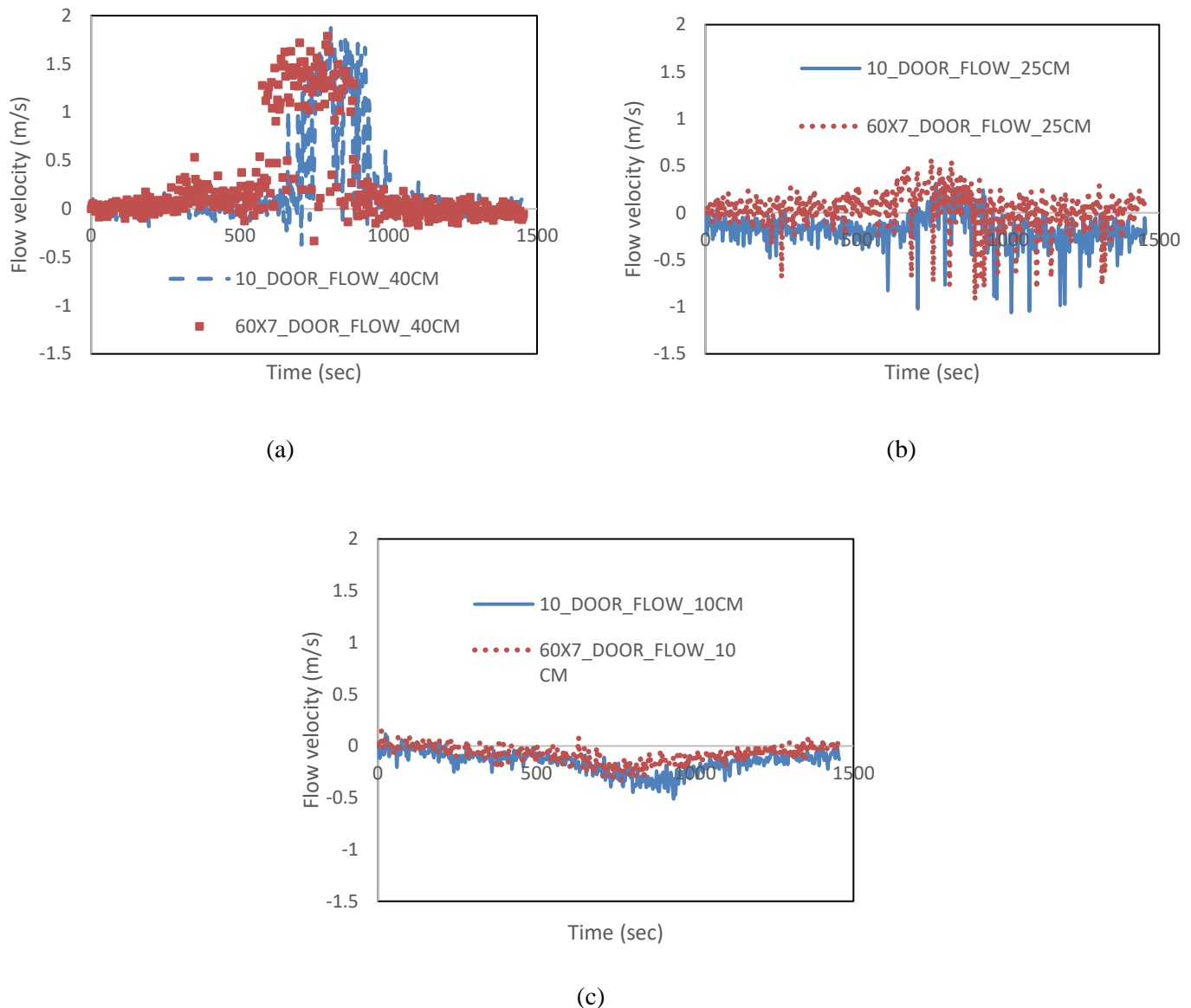
These oscillations led to fluctuations within the flow probe output signal Making it harder to define a neutral axis location. Therefore, even though the flow profiles will be analyzed briefly in this study, it still requires further analysis.

Figure 20 below demonstrated the flow profiles as a relation between the flow velocities across each of the door flow probes with their height from the floor.



**Figure 20: Flow Profile across the compartment door**

Figure 20 illustrated that the neutral axis location was found to be located at around 0.12 m from the floor for the closed\_1 and closed\_2 cases. When the horizontal opening size became 0.01 m<sup>2</sup> in total (5\_open/60x2\_open) the position barely reached 0.15 m. On the other hand, when the area was quadrupled (10\_open/60x7\_open), the axis height increased to approximately 0.25 m which was the central flow probe location, and this was confirmed by looking at Figure 21b.

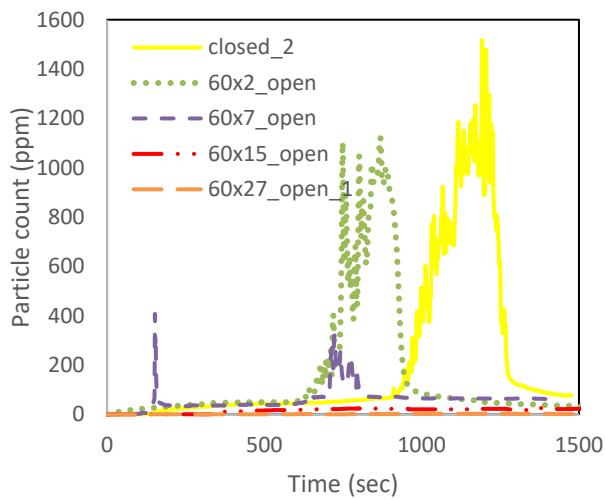


**Figure 21: Flow velocity in/out of the door for 0.04 m<sup>2</sup> horizontal area at (a) 0.4 m, (b) 0.25 m and (c) 0.1 m from the floor**

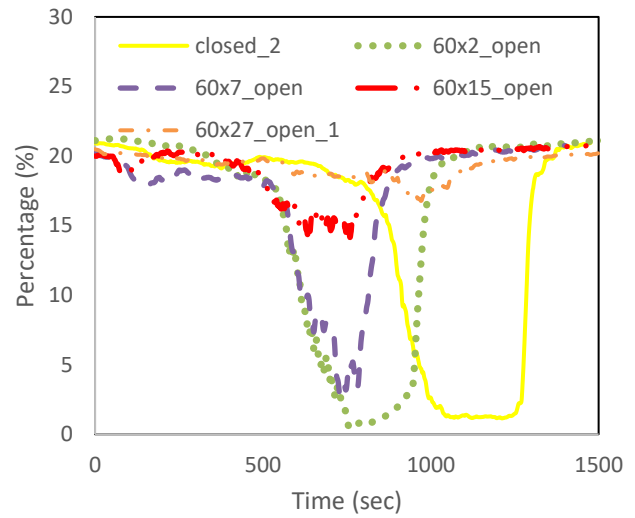
Figure 21a, 21b and 21c indicated that the flow velocities at the door match to an accurate extent for the corner and central ceiling openings for the same area size even though the horizontal area distribution was different. For the 0.09 m<sup>2</sup>, it was clear from Figure 20 besides the visual observations presented in Figure 11 and Figure 12 that the neutral axis was not there anymore as the smoke was mostly leaving through the ceiling allowing mostly air to enter through the door with weak hot gas outflow from the top flow probe. For the biggest ceiling opening area, it could be assumed that no smoke was leaving through the door and therefore the flow profile looked like a regular flow through a pipe where it would be maximum flow at the centre with minimal velocities neat the ends. Finally, It is believed that this flow probe/neutral axis point needs further investigating as it needs to be checked separately, not within many topics.

### 2.2.5 Gas products species

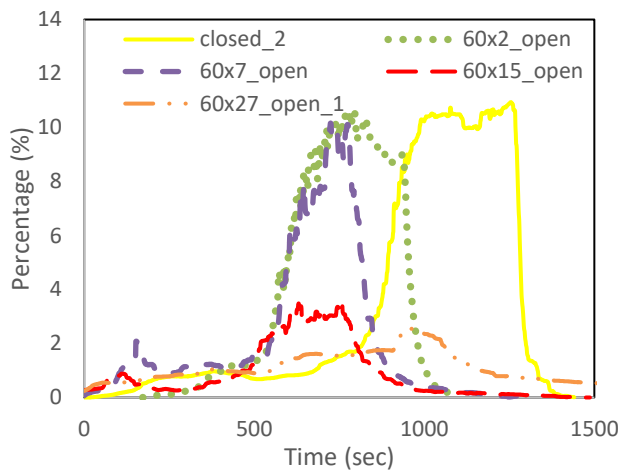
The two gas analyzers were added to the measurement equipment only for the second closed ceiling experiment and the central opening cases. These were incorporated in the resulting data for two reasons, the first one was to analyze the gas products and find out the particle count for the hydrocarbon particles in addition to the concentrations of O<sub>2</sub>, CO<sub>2</sub> and CO. The second reason for integrating the gas analyzers in the experimental set-up was to assist in the validation process of the FDS numerical data with the experimental results.



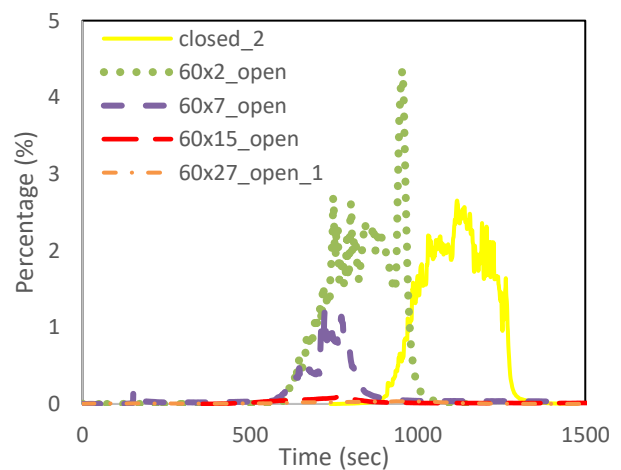
(a) HC Particle count (ppm)



(b) O<sub>2</sub> Percentage (%)



(c) CO<sub>2</sub> Percentage (%)



(d) CO Percentage (%)

Figure 22: Back gas analyzer data

The combustion efficiency could be the main parameter that would be identified qualitatively and quantitatively using the output data from the gas analysers as it would reveal whether the combustion complete or not. It would also give an indication of the availability of air and whether the air-fuel mixture inside the compartment was lean or rich and hence the compartment being over-ventilated or under-ventilated respectively. This last point would be compelling, especially while investigating the impact the horizontal openings had on the combustion efficiency. It should be noted that only the back gas analyser data would be illustrated in this report for the sake of investigating all the gas products coming from the fuel-burning while the front-located gas analyser's data would be listed in the appendix. It is noteworthy to break down the analysis of the gas products species into oxygen and other gas products.

**Oxygen (O<sub>2</sub>):** The curve demonstrated Figure 22b exhibited an oxygen starvation zone at the top left corner of the compartment revealing the presence of a thick hot gas layer even with an area of about 0.04 m<sup>2</sup> of ceiling openings. For the other cases where the horizontal opening area was larger than 0.04 m<sup>2</sup>, the oxygen concentration had a minimum value of approximately 15% for the 60x15\_open case showcasing that presence of excess oxygen throughout the whole compartment and the existence of a mixture of hot gas layer and cold air. The 60x27\_open case revealed that there was no hot gas layer formed with the oxygen concentration being about 20%.

**Gas products (HC, CO, CO<sub>2</sub>):** The concentrations of these gas product species could pinpoint the changes in combustion efficiency for each test. It could be concluded from Figure 22a, 22b and 22c that the closed\_1 case had the worst combustion efficiency meaning incomplete combustion due to the lack of oxygen (under-ventilation or rich mixture) followed by the 60x2\_open and 60x7\_open cases. With more oxygen available starting from the 60x15\_open case, the compartment tended to be over-ventilated, which meant the decrease in the particle count of any HC and the CO concentration to an almost zero percent. It should be emphasized that the decrease in the CO<sub>2</sub> concentration was due to the excess O<sub>2</sub> appearing in the gas products as pure oxygen not reacting with any carbon atoms.

## 2.2.6 Time to Flashover (Using Top TC in all corners)

Table 10: Time to Reach Flashover (525°C) for all the cases

Case Name	Time for all the top TCs to reach 525 °C				HRR (When Top TCs reach 525 °C) (KW)
	TC_RB (Sec)	TC_LB (Sec)	TC_RF (Sec)	TC_LF (Sec)	
<b>Closed Ceiling Cases</b>					
Closed_1	787	860	785	810	61
<b>Corner Openings</b>					
2.5_open	648 (-18%) *	597 (-31%)	614 (-22%)	597 (-26%)	97 (59%)
5_open	519 (-34%)	507 (-41%)	526 (-33%)	527 (-35%)	55 (-10%)

<b>10_open</b>	693 (-12%)	720 (-16%)	728 (-7%)	747 (-7%)	93 (52%)
<b>15_open</b>	937 (19%)	925 (8%)	1020 (-30%)	975 (20%)	137 (125%)
<b>20_open_1</b>	did not reach	did not reach	did not reach	did not reach	did not reach
<b>Central Openings</b>					
<b>60x2_open</b>	772 (-2%)	761(-12%)	773 (-2%)	765 (-5%)	83 (36%)
<b>60x7_open</b>	625 (-21%)	627 (-27%)	684 (-13%)	708 (-13%)	40 (-34%)
<b>60x15_open</b>	did not reach	did not reach	did not reach	did not reach	did not reach
<b>60x27_open</b>	did not reach	did not reach	did not reach	did not reach	did not reach

\*All the cases are compared with the closed\_1 case

In line with the study conducted by Beshir et al.[20], this section would investigate the effect of horizontal openings presence on time taken to reach flashover. It was expected that the current study would tie well with the previous one, but at first the data looked quite different from the study conducted by Beshir et al.[20], which was misleading at first. Before analyzing this section, it was essential to emphasize that the time to reach flashover would require a separate study where its primary focus would be flashover time.

The following trend was inferred based on Table 10 where the time for each top corner TC to reach 525°C (flashover criteria) would decrease with the increase in the area of the horizontal openings until reaching the 0.04 m<sup>2</sup> ceiling opening area where the trend was reversed, and the rest matched with the literature. The justification for the decrease in the time to flashover at first would be due to the fact that for the 0.0025 and 0.01 m<sup>2</sup> ceiling openings, extra air enters the compartment but due to the small openings size, the compartment is still under ventilated. When the threshold value for the area of the horizontal openings was exceeded, excess oxygen entered the compartment leading to overventilation of the compartment resulting in a decrease in the internal temperatures of the compartment. This led to less heat transfer feedback from the hot gas layer and also less burning rate. As a result, the time to reach flashover exceeded that for the closed\_1 case. It should also be underlined that for this study, the 20\_open\_1, 60x15\_open and 60x27\_open cases did not reach flashover criteria.

Therefore, at this stage of understanding, it was believed that neither this study nor the previous one could be considered mistaken yet it could be concluded that increasing the horizontal openings beyond a specific limit would lead to an increase in the time to reach flashover, and hence a separate study must be conducted specifically for flashover time relation with horizontal openings

### 3. Validation of experimental data

The software used for the numerical modelling in this study was Fire Dynamics Simulator (FDS). FDS is free online software that was developed by the National Institute of Standards and Technology (NIST). FDS is considered as a Computational Fluid Dynamics (CFD) model that can be utilized to solve a series of Navier-Stokes equations (NSE) for low speed buoyancy-driven fire flows with more focus on transporting smoke, and heat resulting from these fire flows. FDS is always accompanied by another software called Smokeview (SMV), which is a visualization tool for displaying the models developed in FDS. The models employed by FDS to solve a set of NSE are hydrodynamic turbulence model, combustion model and radiation model. The turbulence model simulates the small scale turbulences by a form of a Large Eddy Simulation (LES) which is the default operating mode in FDS. [26]

FDS (version 6.7.1) was used to model the fire development in a small-scale experiment where it will be assessed by validating its output data with the experimental data mentioned in the previous section. It would inspect temperatures inside and outside the compartment, radiative heat flux to the dwelling surrounding, flow velocities through vertical and horizontal openings and external flaming. In total, ten models were developed by FDS, and they were discussed further below.

#### 3.1 Numerical set-up & simulation parameters

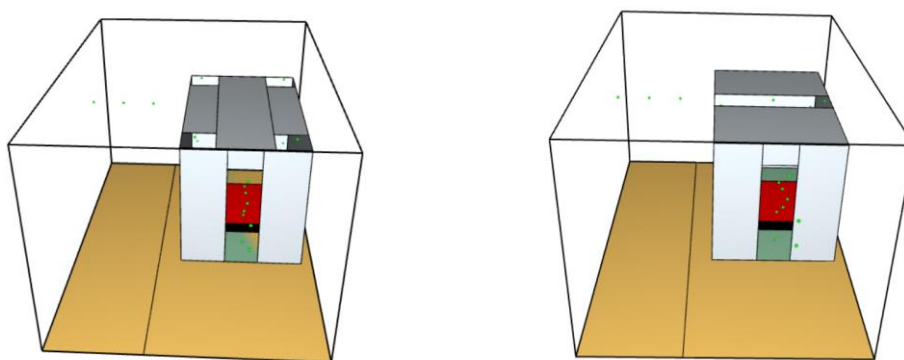


**Figure 23: Geometry of the numerical set up for the corner ceiling openings (left) and the central ceiling opening (right) as shown in Smokeview**

The geometry of the FDS model shown in Figure 23 resembles the small-scale model reported above. The same instrumentations used in the small-scale experiment were added to the model, where k-type thermocouples were used to measure temperatures, heat flux measuring devices were used to measure the radiative heat flux to the surrounding, a gas species analyzer was added at the same location as the top TC in the left-back corner, and flow velocity measuring devices were added at the door and the ceiling openings. The fuel tray was added as a surface at the centre of the compartment floor with the same dimensions and material (steel) as the real experiment. The ‘Simple Pyrolysis Model’ was used to model the fire and the fire curve was added as a ramped input using the Heat Release Rate Per Unit Area

(HRRPUA) data that was measured using an oxygen consumption method incorporated from the hood at the fire lab.

The original model was developed and validated by Beshir et al.[18] where a sensitivity analysis was conducted, and it was decided to use a 0.05 m cell size as it was found to be numerically efficient cell size. However, as this study had horizontal ceiling openings, the cell size was adjusted for each case to accommodate the opening sizes, as shown in Table 11. It is noteworthy to mention that no extra modelling was allowed and so no mesh sensitivity was conducted for the horizontal opening models in addition to no sensitivity analysis to check the effect of the fire location

**Table 11: Chosen cell size for each case**

Model Name	Cell Size
Closed_2	0.05x0.05x0.05 m
2.5_open	0.025x0.025x0.025
5_open	0.05x0.05x0.05 m
10_open	0.05x0.05x0.05 m
15_open	0.05x0.05x0.05 m
20_open_1	0.05x0.05x0.05 m
60x7_open	0.025x0.025x0.025
60x15_open	0.05x0.05x0.05 m
60x27_open_1	0.05x0.05x0.05 m

The fuel used was specified as polypropylene with the heat of combustion being 43.3 MJ/kg, soot yield value of 0.058, CO yield of 0.024 and a radiative fraction of 0.37. The ambient temperature in the model was adjusted to be 10°C to resemble the ambient conditions in the fire lab. The wall material was set to be carbon steel with a density of 7850 kg/m<sup>3</sup>, an emissivity of 0.6, a specific heat of 0.6 kJ/kg.K and a conductivity of 48 W/m.K. Besides, the floor insulation material had the following heat transfer properties: a density of 208 kg/m<sup>3</sup>, an emissivity of 1, a specific heat of 0.8 kJ/kg.K and conductivity of 0.1 W/m.K. [27]

## 3.2 Validation Process

As presented in Figure 24, there are many speculations when it comes to FDS's ability to model under-ventilated and over-ventilated fires especially with the addition of horizontal ceiling opening adding more turbulence in the shape of external flow of hot gases and also flames. However, the extent to which FDS could be a reliable source to model ISD fire was still unknown. Therefore, this study held a validation process to test the reliability of FDS appropriately modelling the complex turbulent



combustion in ISD, putting in mind all the limitations associated with the combustion and turbulence models within FDS. The validation procedures would require four checks, combustion efficiency check, heat balance check, mass balance check and finally external flaming check.

**Combustion Efficiency:** This would indicate that the ability of FDS to mimic the combustion within the model by showing accurate values for CO<sub>2</sub> and O<sub>2</sub> concentrations indicating whether the compartment was under-ventilated (rich mixture) or over-ventilated (lean mixture).

**Heat Balance:** By comparing the temperature of the gas layer at the top of each corner through thermocouples located at similar positions as the lab experiment. This would be a demonstration that combustion could be modelled accurately, especially near the openings where there could be an inflow/outflow of either smoke or air. Besides, the incident heat flux radiating from the sidewall would be compared between the heat flux devices in the model and the TSCs used in the experiments.

**Mass balance:** The mass balance would be checked by correlating the flow velocities measured by the flow probes in the lab test with the flow velocity measurements incorporated in FDS. Which would also prove the capturing of most eddies and turbulent flows, especially with the presence of oscillating flames in the experimental observations.

**External Flaming:** The data measured from the ‘radiative heat flux gas’ device in FDS would be compared to the TSC calculated incident heat fluxes at 0.3 m from the door. Also, there would be a visual check of the Smokeview output file compared with screenshots from the experiments to investigate if the visual representation would resemble the actual one.

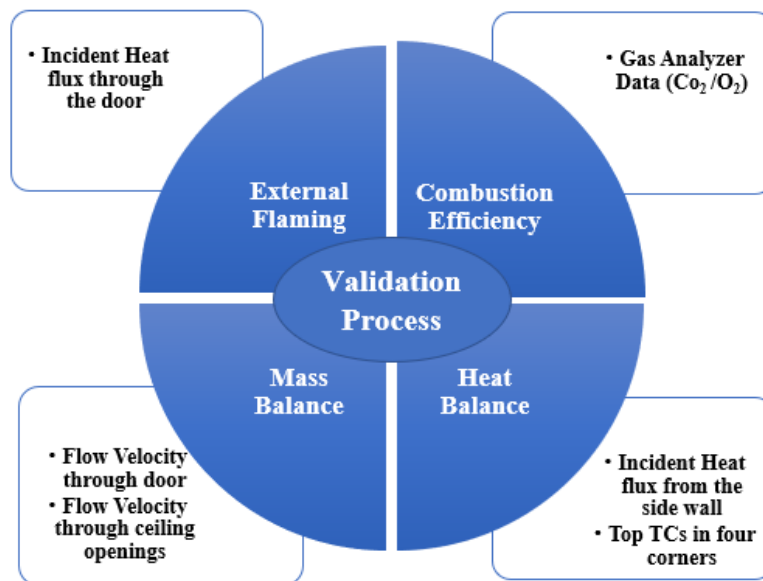


Figure 24: The Validation Process

In order to perform the validation process accurately based on average not instantaneous values, Table 12 will be used extensively to compare the experimental and numerical data especially with the radiative heat flux to the surrounding. It will give a good indication of FDS's ability to accurately model each case as it shows averaged values over steady-state.

**Table 12: Radiative Energy Comparison between Experimental and Numerical Data**

Case Name	(Radiative Energy at 0.3 m from the door) (kJ/m <sup>2</sup> )		(Radiative Energy at 0.15 m from the side) (kJ/sec)	
	Experiment	Numerical <sup>1</sup>	Experiment	Numerical <sup>1</sup>
<b>Corner Openings</b>				
<b>2.5_open</b>	2603	2301(-11%)	1542	1747(13%)
<b>5_open</b>	2856	2517(-12%)	1404	1437(2%)
<b>10_open</b>	2473	1640(-34%)	1366	1725(26%)
<b>15_open</b>	1897	1021(-46%)	1218	1180(-3%)
<b>20_open_1</b>	1478	1048(-29%)	935	891(5%)
<b>Central Openings</b>				
<b>60x7_open</b>	1248	1575(26%)	1475	2347(59%)
<b>60x15_open</b>	1162	1067(-8%)	1133	1675 (48%)
<b>60x27_open</b>	1587	1289(-19%)	1170	994(-15%)

<sup>1</sup> Each numerical case was compared with its equivalent experimental one.

### 3.2.1 Closed\_2 Case

#### 3.2.1.1 Combustion Efficiency

This case was validated by Beshir et al.[18], however, the gas analyzer data was not provided in the previous study, therefore, it will be presented as shown in Figure 25a and 25b. Figure 25a illustrated the accurate modelling of FDS with respect to the oxygen concentration in the gas layer, there were some slight differences but the model showed the under ventilated conditions within the compartment which was a clear representation of the realistic case. Same goes for Figure 25a, which indicated an accurate estimation of the carbon dioxide concentrations in the gas products indicating a rich mixture. Carbon monoxide data was not discussed within this report.

The figures prove that FDS's simple combustion model managed to capture the accurate combustion efficiency and assure that this case is validated completely.

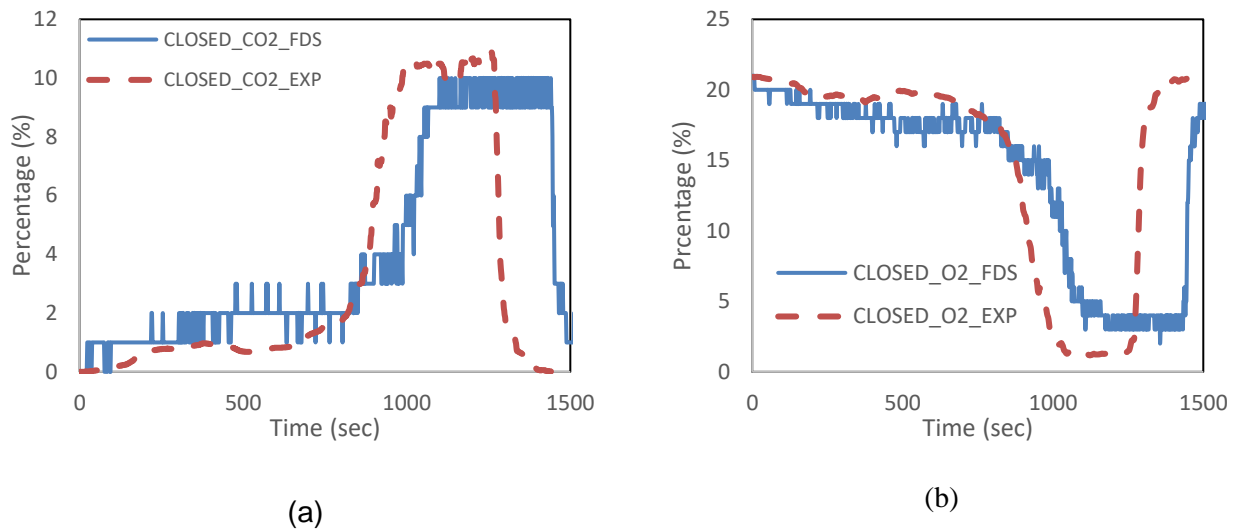


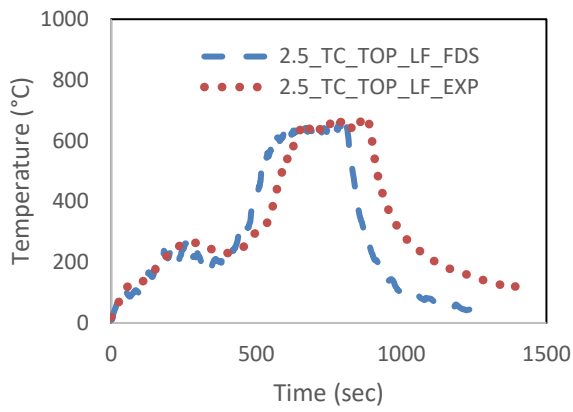
**Figure 25: Validation of the combustion efficiency for the closed\_2 case for (a) CO2 (b) O2**

### 3.2.2 0.025x0.025 m square Corner Openings

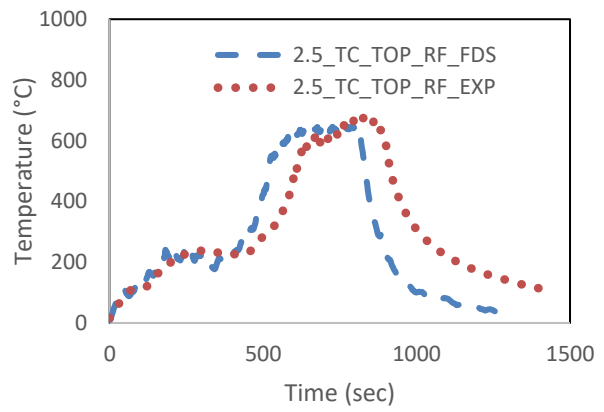
#### 3.2.2.1 Heat Balance

Figure 26a and 26b that the temperature of the hot gas layer (top TC) was accurately modelled by FDS to match the experimental data with more accuracy for the front tree than the back side however the margin is acceptable for the validation process. An explanation for the slight overestimation of FDS with the back side temperatures, as seen in Figure 26c and 26d, could be due to the presence of external flames from the ceiling openings which leads to more burning on the back side. This would require a slice file in FDS which was not available so further analysis is required as a future work.

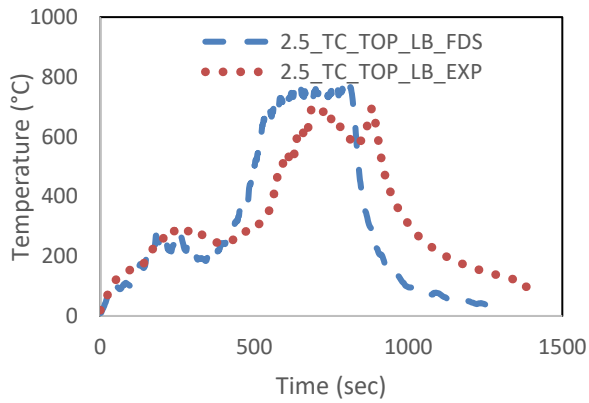
However, regardless of that minor margin of difference in the lower layer, it is fair to say that FDS successfully managed to mimic the real experiment and it was apparent now that a finer mesh had an impact on the accuracy of the numerical results. Moving to the incident heat flux at 0.15 m from the side, where it seemed that FDS showed a higher peak of the incident heat flux but for a shorter period. After measuring the radiative energy at 0.15 m from the side, the result showed about 13% increase in the numerical data value compared to the experiment. An explanation of this increase could be justified based on the Smokeview screenshot in Figure 28 below, where flames were extending from the ceiling openings which did not occur during the real test. These flames were mostly the reason for that high radiative energy.



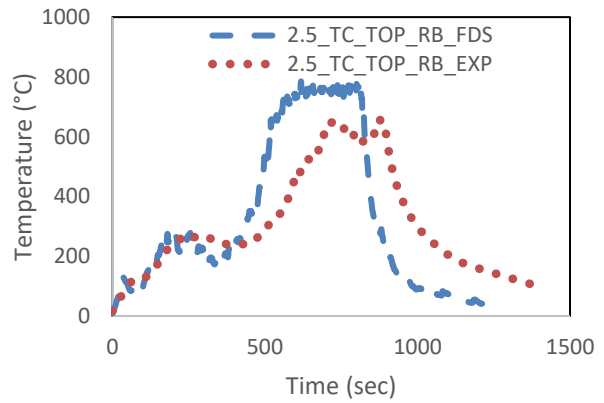
(a) TC Left Front corner



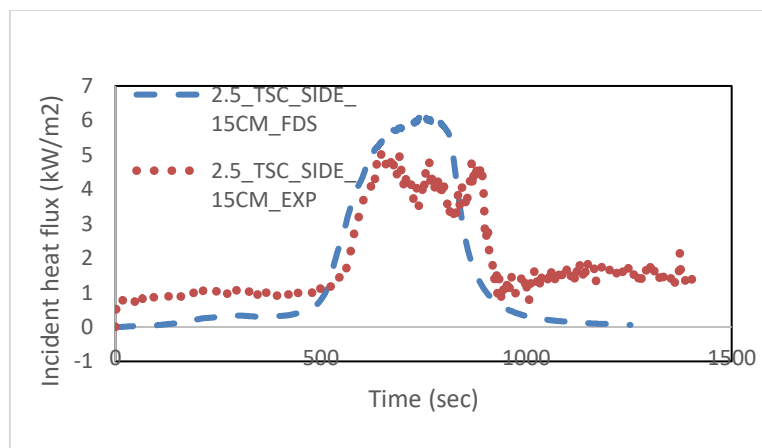
(b) TC Right Front corner



(c) TC Left Back corner



(d) TC Right Back corner

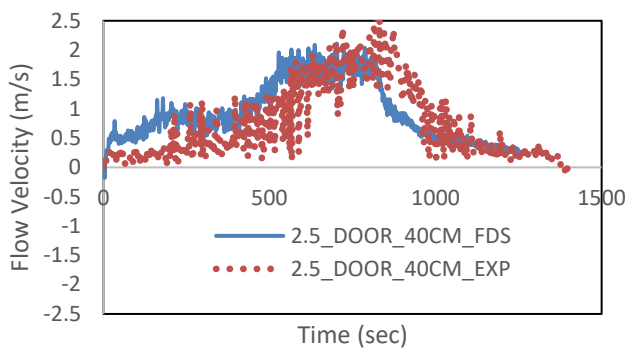


(e) TSC 15 cm from the side wall

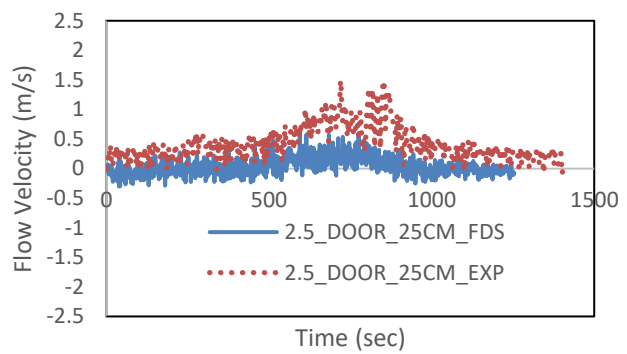
**Figure 26:: Validation of the heat balance for the 2.5\_open case**

### 3.2.2.2 Mass Balance

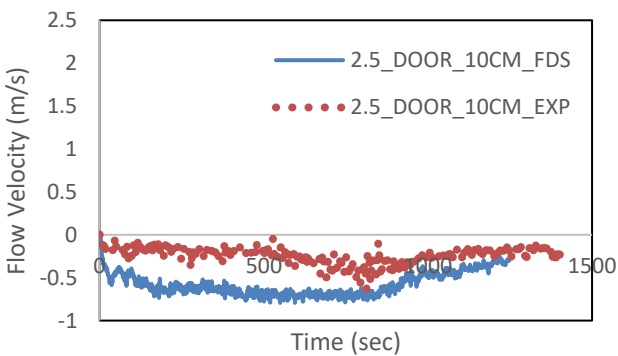
The oscillating flames' frequency increased when the opening size got bigger, and this was clear in the experimental flow probes' data especially with the top and middle flow probe as shown in Figure 27a and 27b. Nevertheless, as FDS could not anticipate these oscillations, less matching would be expected as seen with the flow at the top flow probe. When compared to the middle flow probe. Due to the lower turbulences occurring at 0.25 m from the floor, the middle flow probe matched very well with the experimental data. Finally, the trend of overestimated flow velocities at the lower flow probes was still happening, showing one explicit limitation for FDS even with a finer mesh.



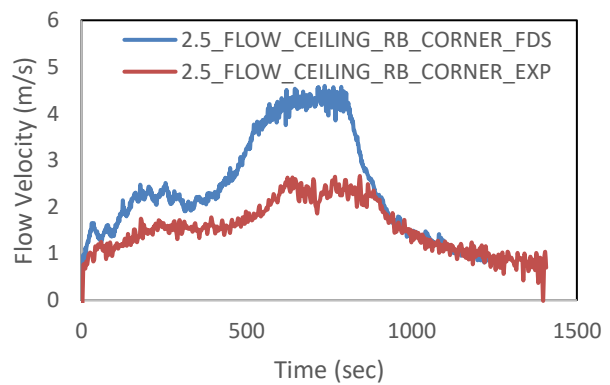
(a) 0.4 m from the floor at the door



(b) 0.25 m from the floor at the door



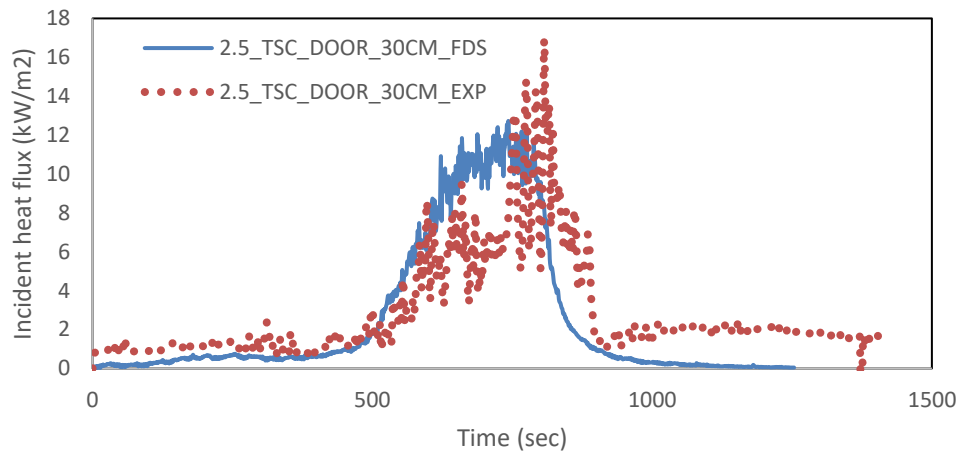
(c) 0.1 m from the floor at the door



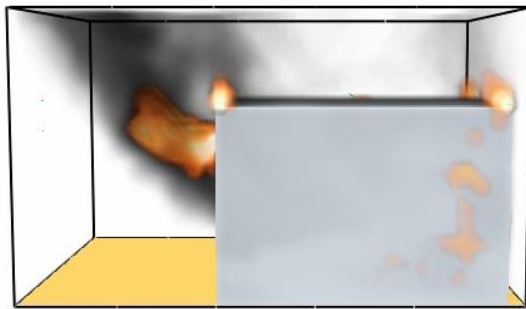
(d) Right back ceiling corner

**Figure 27: Validation of the mass balance for the 2.5\_open case**

### 3.2.2.3 External Flaming



(a) TSC at 0.3 m from the door



(b) SMV Screenshot



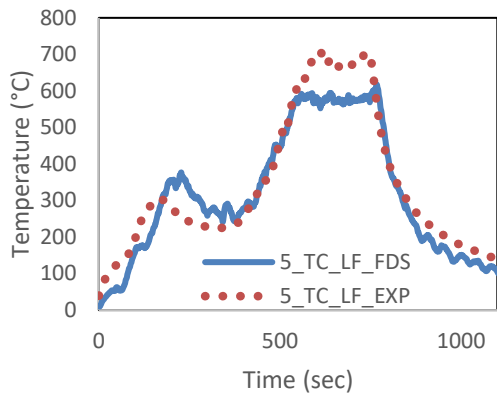
(c) Experiment screenshot

**Figure 28: Validation of the external flaming for the 2.5\_open case**

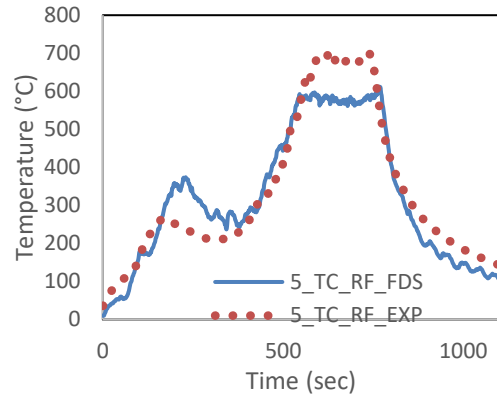
Figure 28a displayed numerical data representing the incident heat flux at 0.3 m from the door is showing an acceptable fit for the experimental radiative heat flux. Even by looking at the radiative energy for both cases, it showed an underestimation of only 11% which would be accepted as a reasonable percentage that would assure the reliability of FDS to mimic the real experiment.

### 3.2.3 0.05x0.05 m square Corner Openings

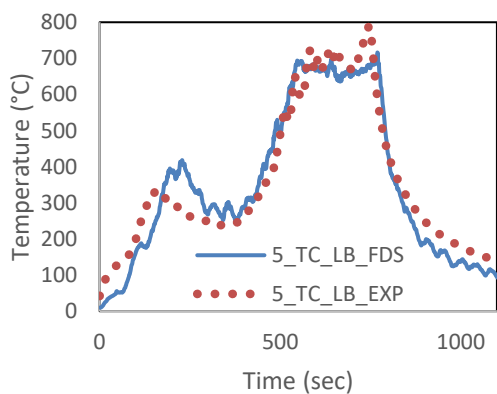
#### 3.2.3.1 Heat Balance



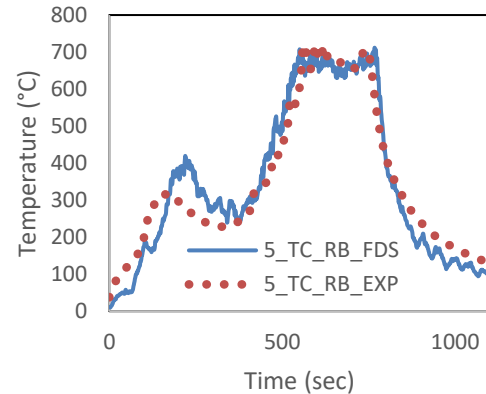
(a) TC Left Front Corner



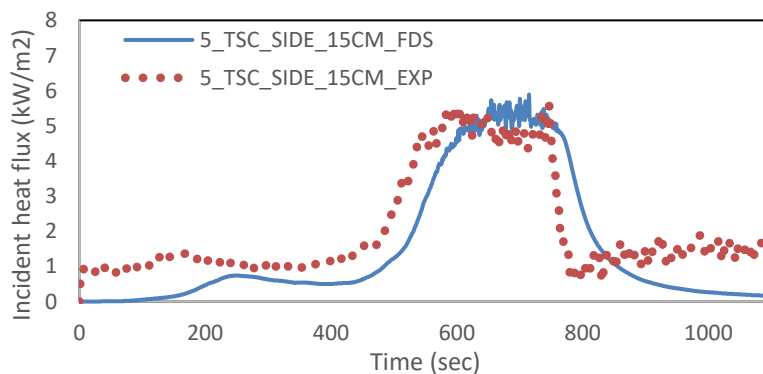
(b) TC Right Front Corner



(c) TC Left Back Corner



(d) TC Right Back Corner



(e) TSC 0.15 m from the side

**Figure 29: Validation of the heat balance of the 5\_open case**

The temperatures at the back corners were well-estimated by FDS, as shown in Figure 29c and 29d, with the curves following the similar pattern accurately. This was a good observation because it meant that FDS well-recognized the corner ceiling openings and was estimating their influence on the

internal temperatures accurately. As illustrated in Figure 29a and 29b, FDS underestimated the gas layer temperature near the door which means that the combined effect of the door and ceiling corner openings may pose some complexities with FDS which seems to require a finer mesh. Another satisfying result was the heat flux at 0.15 m from the side ass seen in Figure 29e, where it was mimicked very accurately by FDS which was a great sign that the combustion inside and outside the compartment was almost similar to the real case. Based on Table 12, the radiative energy generated at 0.15 m from the side was only overestimated by 2% when compared to the experimental data.

Finally, it was concluded that the horizontal openings’ effect, in this case, was accurately simulated and this would that this check was validated

### 3.2.3.2 Mass Balance

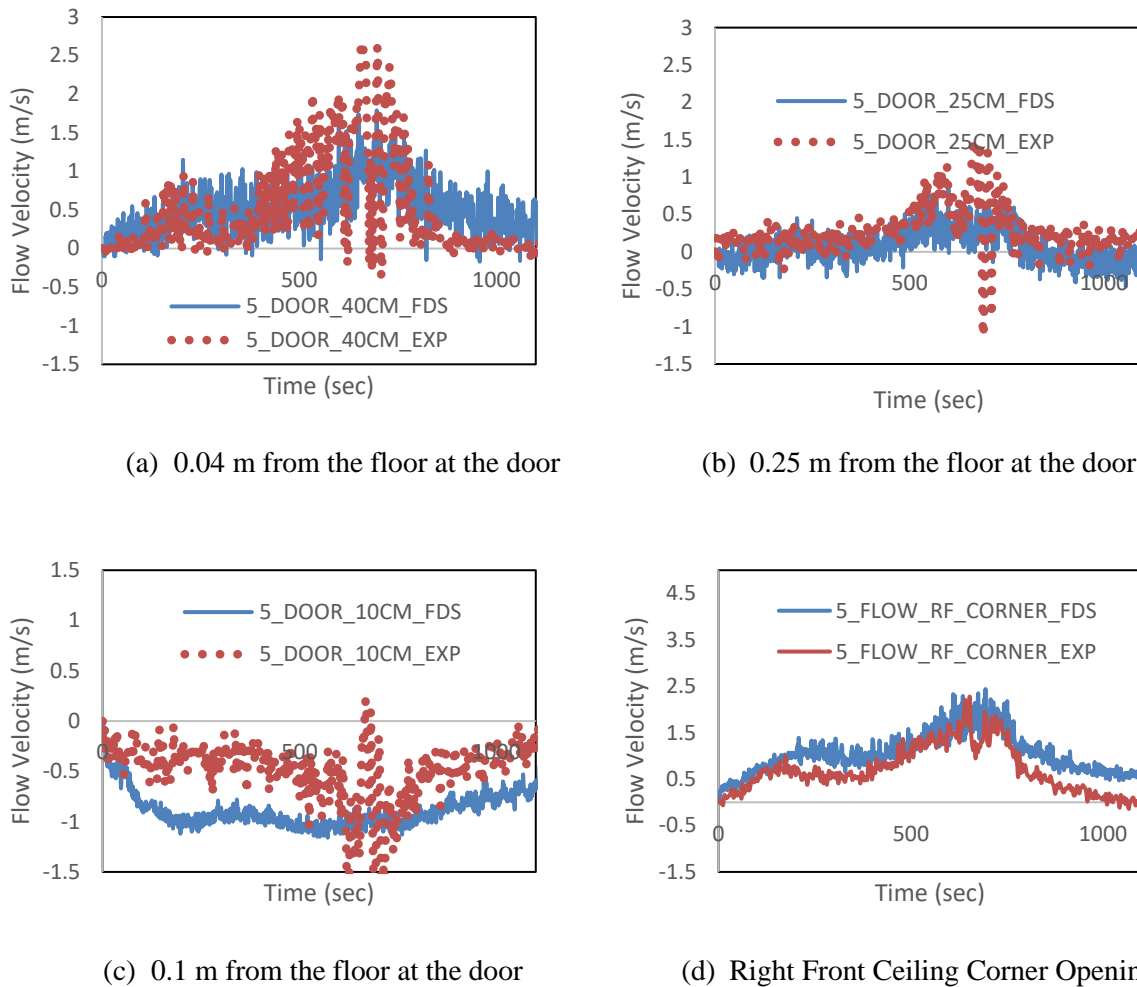


**Figure 30: Validation of the mass balance of the 5\_open case**

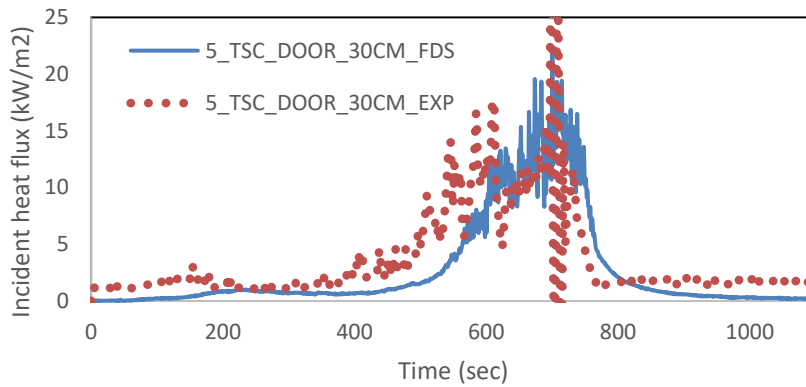
The mass balance verified what was expected before and showed good accuracy between the numerical and experimental data for most of the flow probes either across the door or the horizontal ceiling openings. Having accurate flow velocities would show an overall success of numerically simulate the experiment as it would show that the program could estimate the mass of the pyrolyzed gases and the escaping masses through the horizontal and vertical openings. Of course, the model still would not



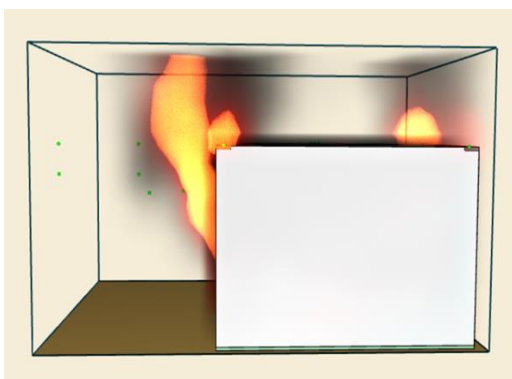
capture the turbulence occurring during the experiment and especially the continuous over-estimation of the lower door flow probe, which was never accurately captured by FDS.

### 3.2.3.3 External Flaming

FDS accurately replicated the external heat flux radiating at 30 cm from the door with a slight underestimation of  $\pm 11\%$  similar to the 2.5\_open and hence the external flaming check for this case was validated with the experimental results. However, it could also be noted that FDS showed external ceiling flames which did not show up in the real experiment, yet this could not consider a problem because almost all the data was well-simulated by FDS. Besides, the presence of external flames in FDS did not mean different fire behaviour was happening, but it could be the way FDS would give this colour when the temperature would reach a specific temperature regardless, or it could be a mesh-related problem but still would not change the validation success.



(a) TSC at 0.3 m from the door



(b) SMV Screenshot



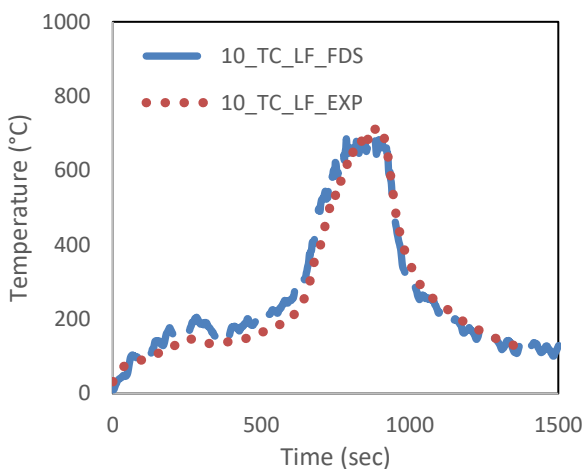
(c) Lab experiment screenshot

**Figure 31: Validation of the external flaming for the 5\_open case**

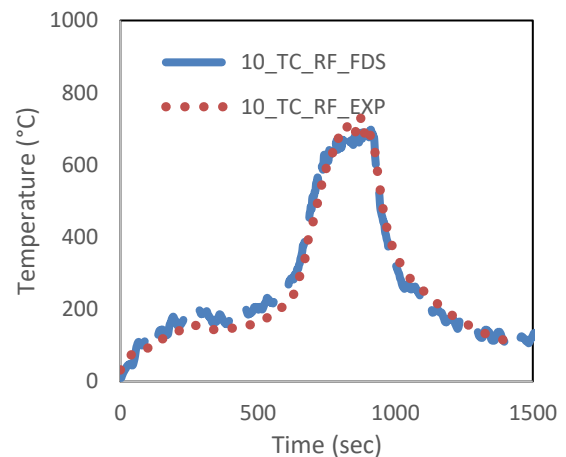
### 3.2.4 0.1x0.1 m square Corner Openings

#### 3.2.4.1 Heat Balance

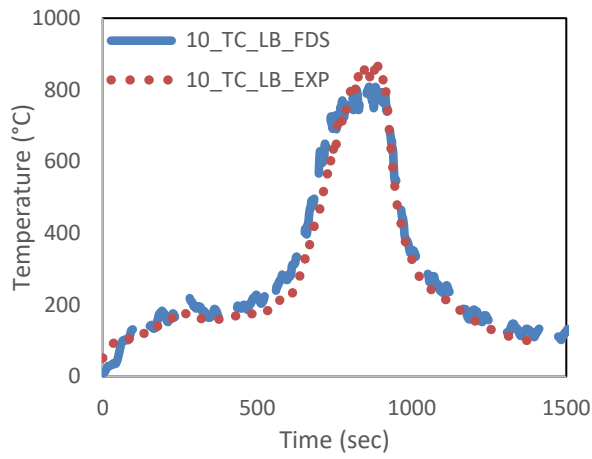
This case was chosen randomly to show the temperature distribution for one complete TC tree to accompany it with the temperatures at the top of the four corners to be a more comprehensive validation for this case. Looking at the temperature graphs above, it was apparent that this case was showing a high level of accuracy when comparing the numerical and experimental data with the curves almost matching for the front side with minimal margins within the backside. Even the left front tree, when compared to the similar one in FDS, showed a high level of accuracy except for some margin of difference (still acceptable) for the bottom TC which still posed a question about FDS simulating the cold air layer and its turbulences in a precise way which there are still some questioning of the FDS ability to do that. Now, jumping to the incident heat flux at 0.15 m from the side which was showing an overestimation of the peak heat flux by about 25% which was similar to the margin of difference for the total radiative energy listed in Table 12. It was believed that  $\pm 25\%$  would still be an acceptable bound, putting in mind the cell size influence in addition to other uncertainties associated with both the experimental set-up and FDS. At the end of this section, it could be said that the heal balance was well-mimicked by FDS and hence considered validated.



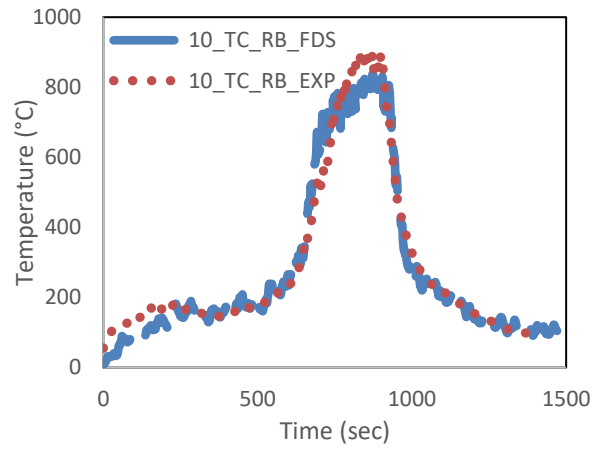
(a) TC Left Front Corner



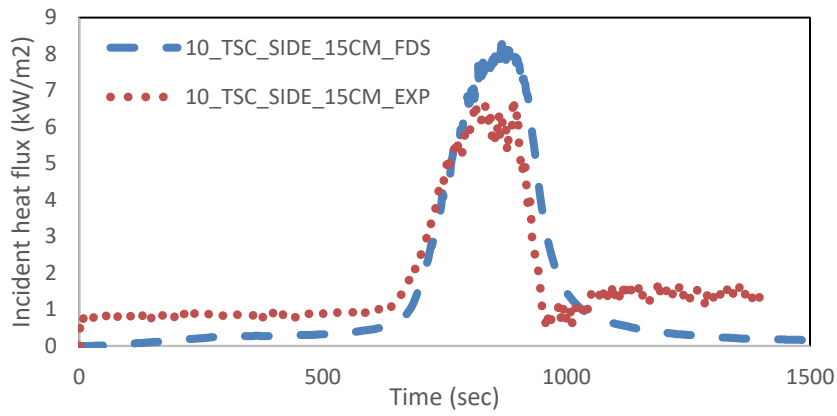
(b) TC Right Front Corner



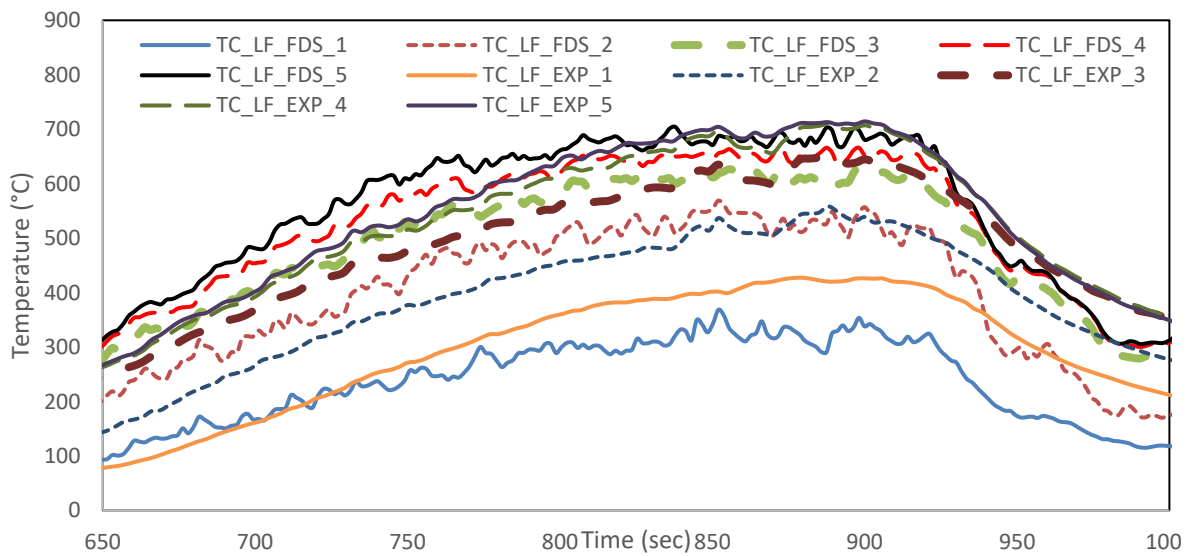
(c) TC Left Back Corner



(d) TC Right Back Corner



(e) TSC 0.15 m from the side wall



(f) TC Left Front Tree

Figure 32: Validation of the heat balance for the 10\_open case

### 3.2.4.2 Mass Balance

Looking at the Figure 33,, it was notable that the numerical output data match the trends of the experimental ones; however, a sudden increase in the outflow of the experiment’s top door flow probe ,as shown in Figure 33a, at about 650 seconds was not captured via FDS. First of all, the overestimation in the flow velocity at the bottom flow measurement device was seen in all of the cases, and therefore it will not be discussed further. Secondly, the middle door probe managed to capture a similar flow to some extent when compared to the experimental results and finally the flow through the right front ceiling opening showed an overestimation by some extent which would raise some doubts on whether this could be validated or not. As a result of the restrictions of running extra models, this point would be left for future work to check the mesh size effect.

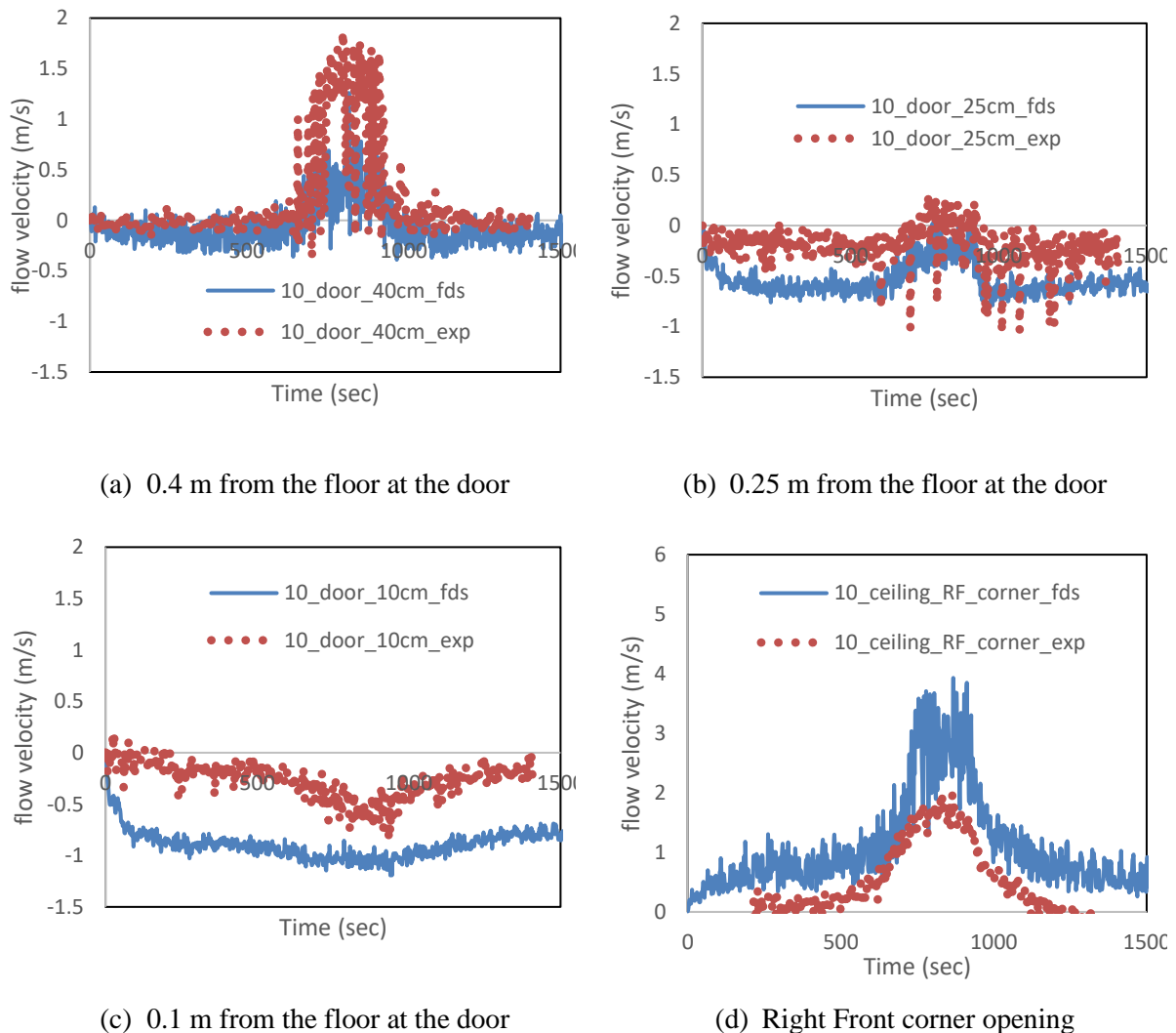
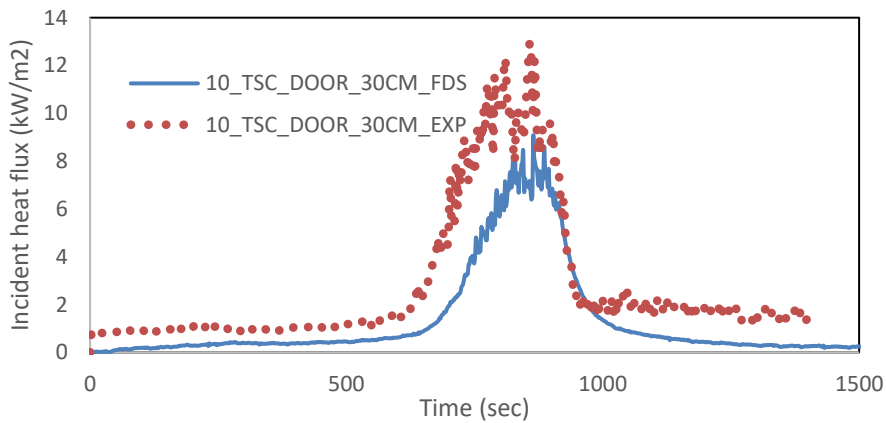


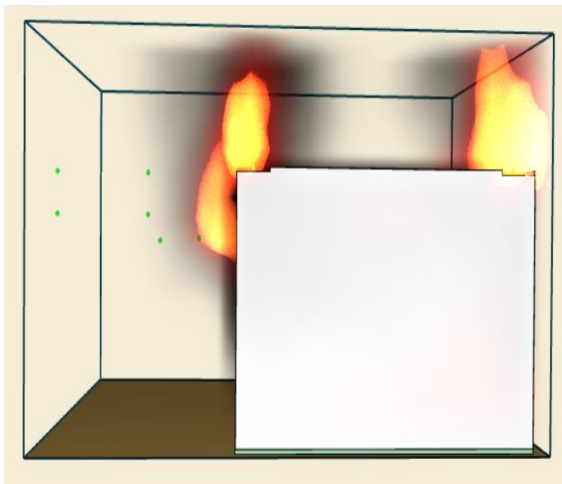
**Figure 33: Validation of mass balance for the 10\_open case**

### 3.2.4.3 External Flaming

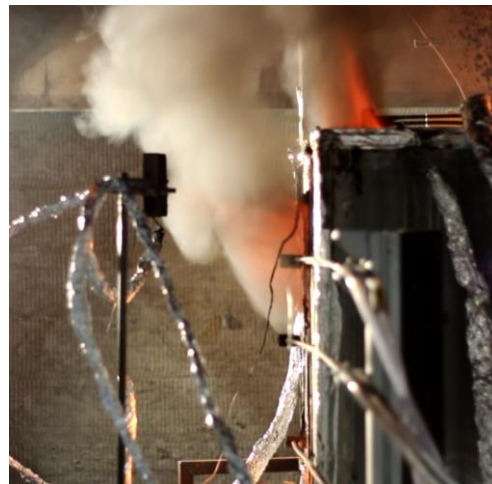
Based on Figure 34a, an overestimation was noticed for the numerical data for the incident heat flux at 0.3 m from the door, however that observation was expected due to the underestimation that was found in the incident heat flux at 0.15 m from the side. This was a pure energy balance within the compartment. The resulting radiative energy from FDS showed an undervaluation of approximately  $\pm 30\%$  when compared against that calculated in the lab experiment. With the 0.05 m cell size, it was expected to have a lower margin of difference if a finer mesh to be used. Owing to that, external flaming would be considered validated.



(a) TSC at 0.3 m from the door



(b) SMV Screenshot



(c) Experiment Screenshot

**Figure 34: Validation of the external flaming of the 10\_open case**

### 3.2.5 0.6x0.07 m Central Opening

#### 3.2.5.1 Combustion Efficiency

Figure 35a and 35b illustrated high level of resemblance between the combustion efficiency in the lab experiment and the FDS one. With the two reaching almost the same peaks with some differences in the steady-state duration. This margin of difference in the steady period would be due to the cell size in FDS being 0.025 m because this size would affect how the opening size was modelled by FDS to accommodate it with the specified cell size. However, in general, it seems that FDS accurately modelled the effect of the ceiling opening on the combustion efficiency and therefore, this check was considered validated..

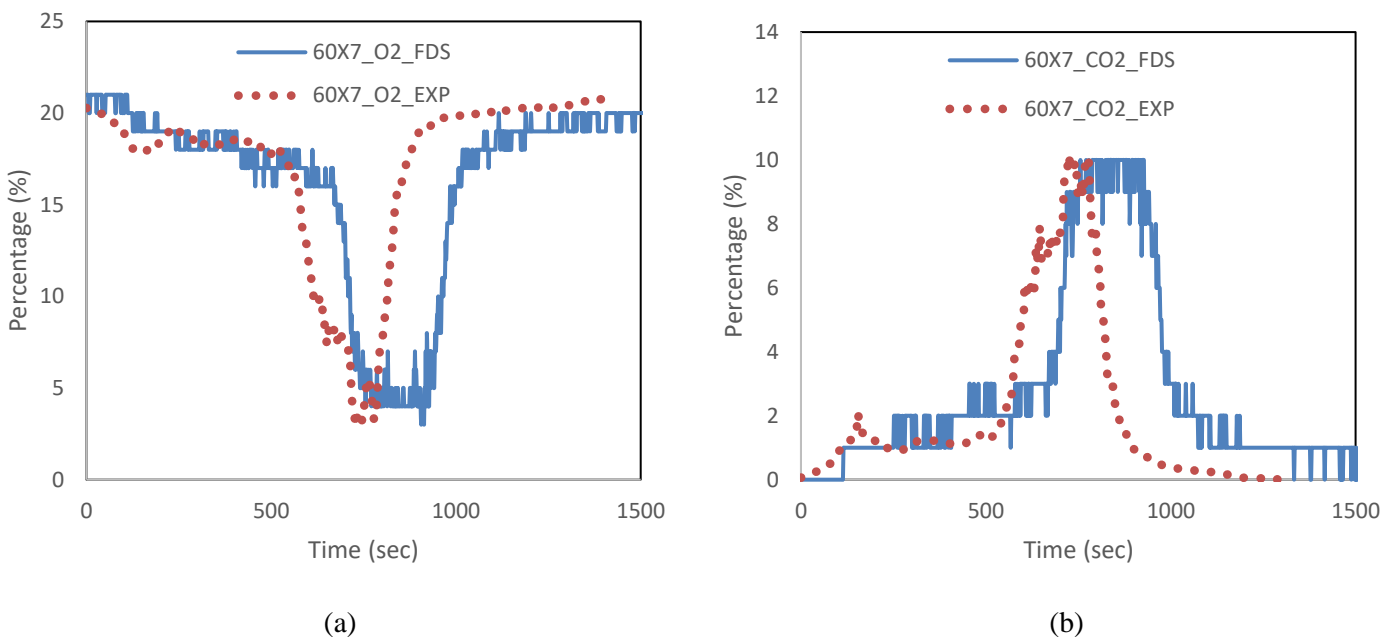
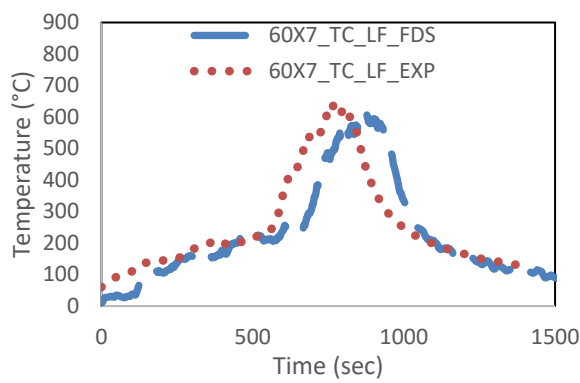


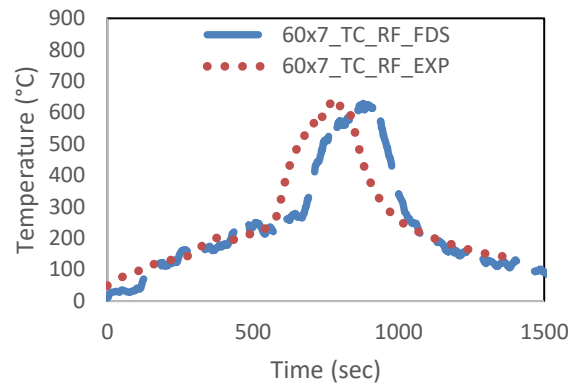
**Figure 35: Validation of the combustion efficiency for the 60x7\_open case for (a) O<sub>2</sub> (b) CO<sub>2</sub>**

#### 3.2.5.2 Heat Balance

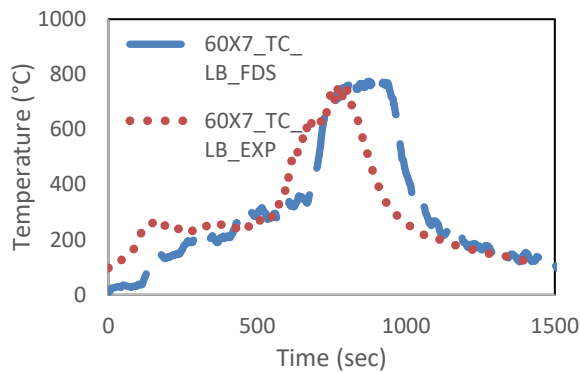
It could be observed that the top TCs were giving a close match, but it was also seen that there was a time delay between the experimental and numerical data and this could be a result of the cell size which would model the opening in FDS with a different size to accommodate for the cell size used. This would cause this delay, but as a curve trend and peak value, it could be considered validated. However, moving to the heat flux from the side, it was surprising to see that significant overestimation of about 60% in FDS compared to the experimental data. The reason for that may not be evident due to the mesh size, and hence a finer mesh should be used to investigate if it was a mesh-related problem or FDS is not able to model such circumstances.



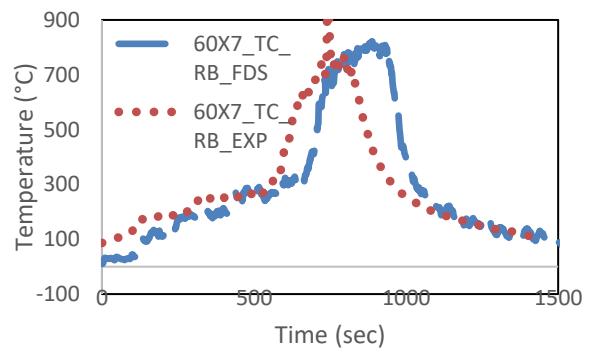
(a) TC Left Front Corner



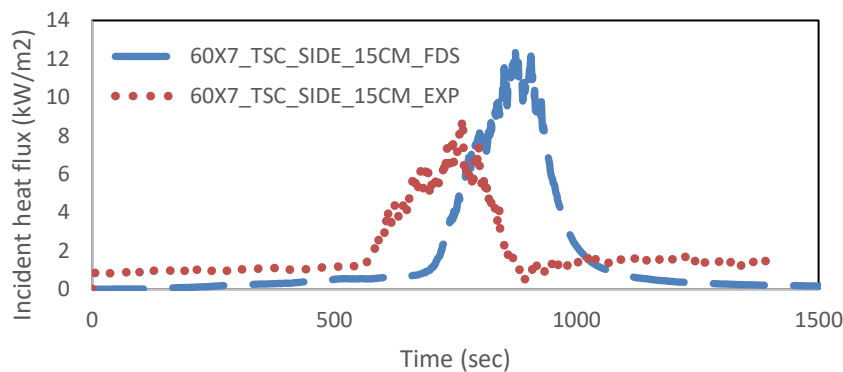
(b) TC Right Front Corner



(c) TC Left Back Corner



(d) TC Right Back Corner



(e) TSC 0.15 m from the side wall

**Figure 36: Validation of the heat balance for the 60x7\_open case**

### 3.2.5.3 Mass Balance

The mass balance indicated some apparent misalignment with the experimental data except for the middle door flow probe, which showed an accurate fit with the experimental data. While the top and bottom flow probes showed opposite trends with underestimation of the numerical data for the outflow

compared to an underestimation of the inflow for the bottom flow probe. Besides, the ceiling opening flow probe showed an overestimation showed a relative overestimation in its flow velocities by 100%, which would explain the significant overestimation in the heat flux from the side. To sum up this check, it was clear that FDS failed to match the mass balance within the compartment.

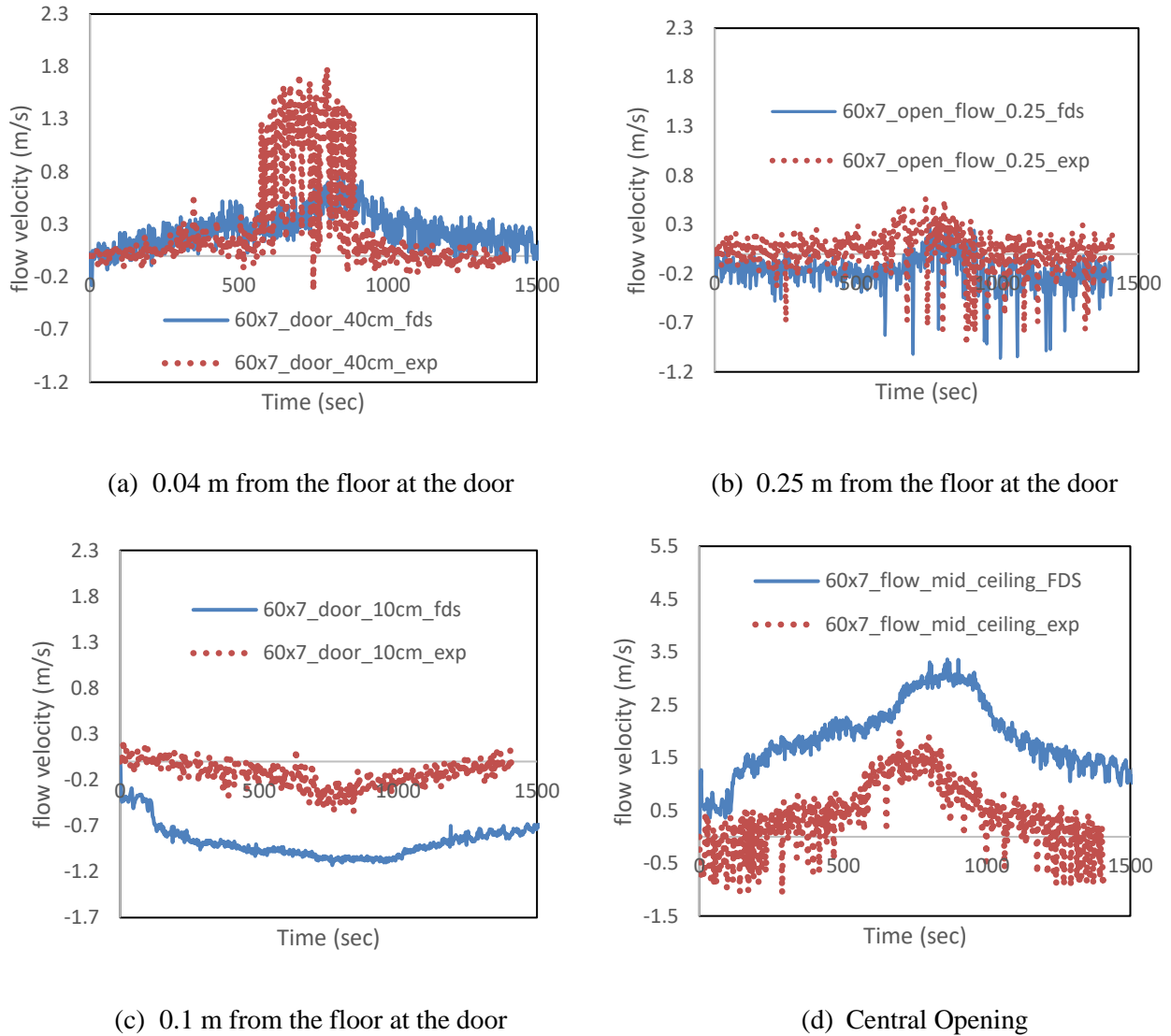
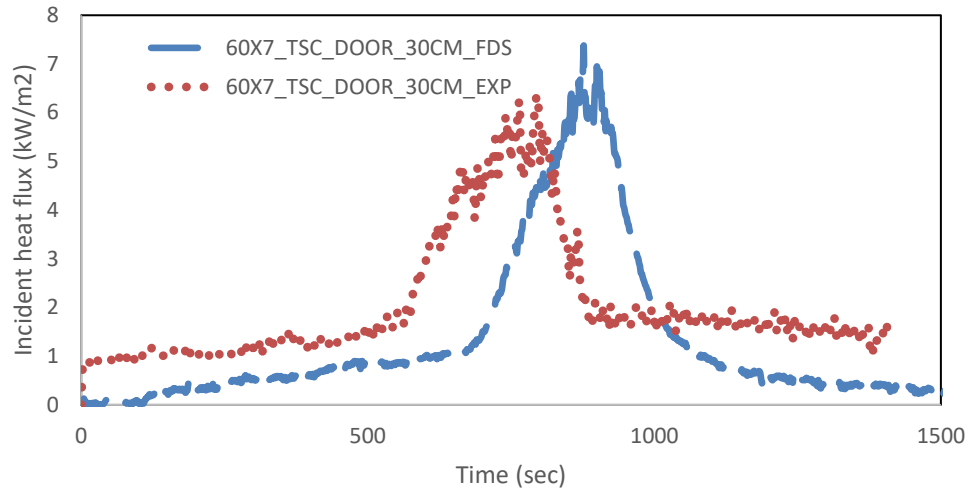


Figure 37: Validation of the mass balance for the 60x7\_open case

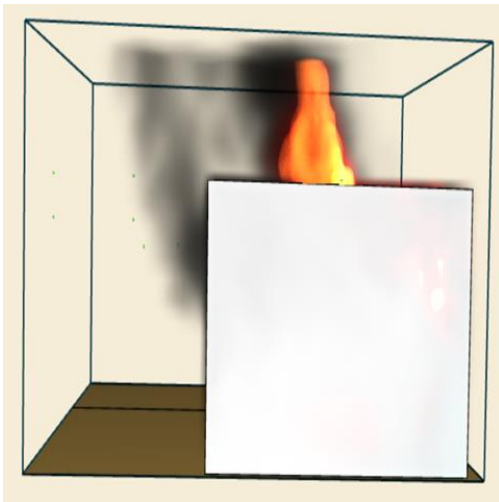
### 3.2.5.4 External Flaming

It was found that FDS overestimated the heat flux radiating at 0.3 m from the door by about 26% in comparison to the experimental data. Also, visually FDS appeared to mimic the fire behavior in this compartment to a reasonable extent which was not indicative of anything, but generally, it could be seen that the external flaming was validated for this case.





(a) TSC 0.3 m from the door



(b) SMV Screenshot



(c) Experiment screenshot

**Figure 38: Validation of the external flaming for the 60x7\_open case**

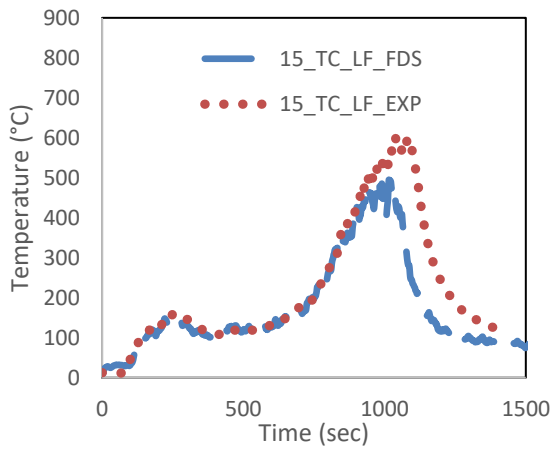
It was found that FDS overestimated the heat flux radiating at 0.3 m from the door by about 26% in comparison to the experimental data. Also, visually FDS appeared to mimic the fire behavior in this compartment to a reasonable extent which was not indicative of anything, but generally, it could be seen that the external flaming was validated for this case.

### 3.2.6 0.15 x0.15 m square Corner Openings

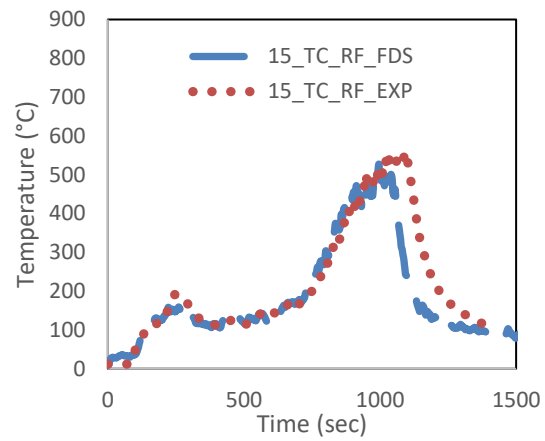
#### 3.2.6.1 Heat Balance

This case would be classified as the first over-ventilated corner opening case; the reason behind this conclusion would be the significantly lower overall temperatures within this case. This meant that now FDS reliability would be tested against over-ventilated cases with a 0.05 m cell size for the FDS domain.

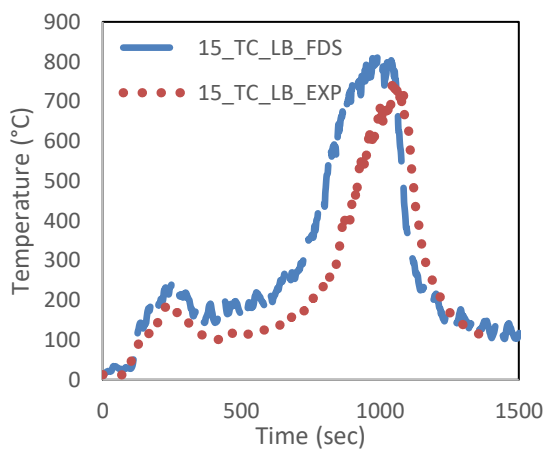
A first look at the top TCs measurements in Figure 39a, 39b, 39c and 39d would show that the accuracy of the numerical data in comparison to the experimental data did not show the same accuracy as the previous cases. However, even though these margins of difference were accepted for previous cases, in this case, there was a distinctive observation concerning the steady-state period for each case. All the top TC had different steady-state period in comparison to the similar experimental ones. This identified a possible weakness of FDS, yet this would be inspected later for compartments with bigger horizontal openings. On the other side, as seen in Figure 39e, the incident heat flux to the side matched to an acceptable level with the experimental data showing a slight underestimation of  $\pm 3\%$  which when combined with the insignificant margins for the temperature would make this heat balance validated. However, it is recommended to furtherly investigate this case by using a finer mesh to investigate its effect on the temperature distribution and their steady-state periods.



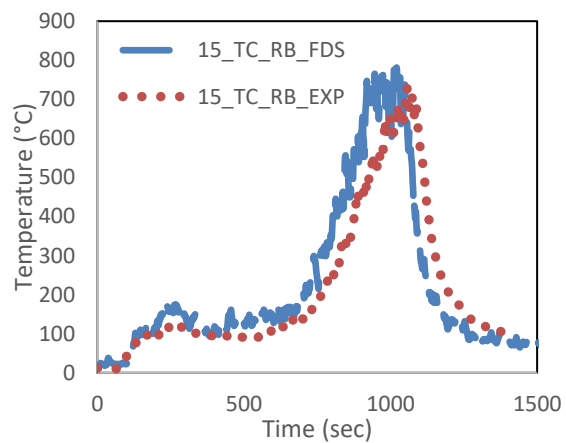
(a) TC Left Front Corner



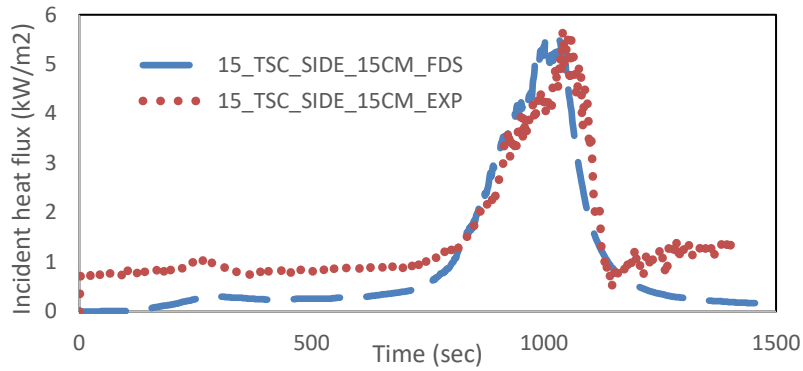
(b) TC Right Front Corner



(c) TC Left Back Corner



(d) TC Right Back Corner

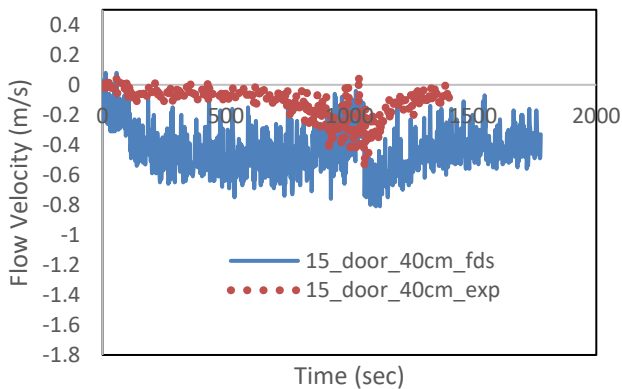


(e) TSC 0.15 m from the side wall

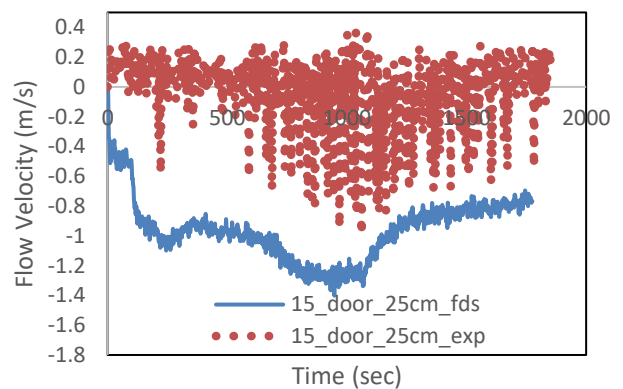
**Figure 39: Validation of the heat balance for the 15\_open case**

### 3.2.6.2 Mass Balance

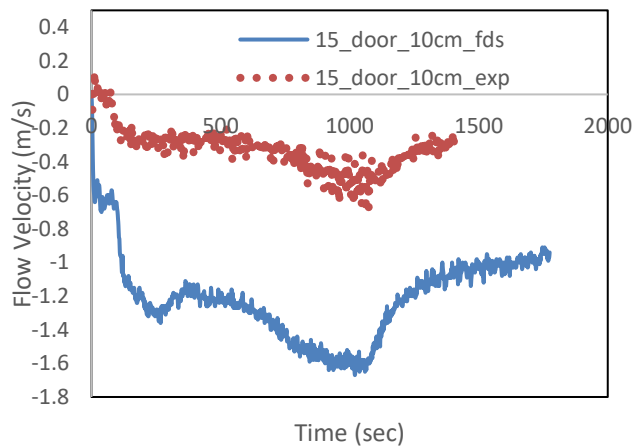
The mass balance looked completely off-point for the 15\_open. Even with some curves appearing to almost match with the experimental data, yet the remaining flow velocities were significantly inaccurate and therefore, it was so evident that this mass balance check was far away from being validated.



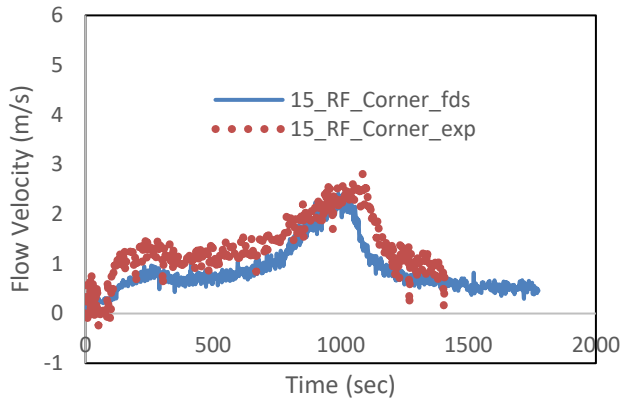
(a) 0.4 m from the floor at the door



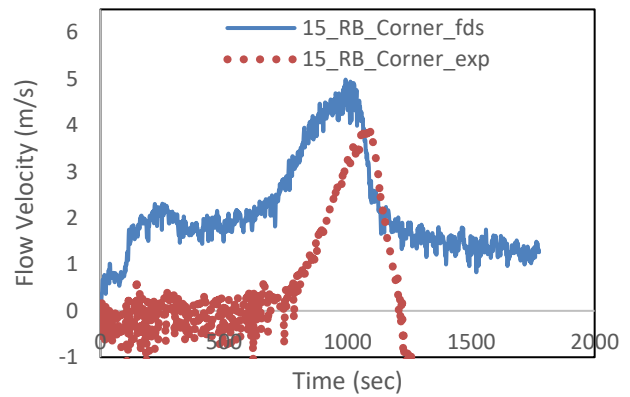
(b) 0.25 m from the floor at the door



(c) 0.1 m from the floor at the door



(d) Right Front corner ceiling opening

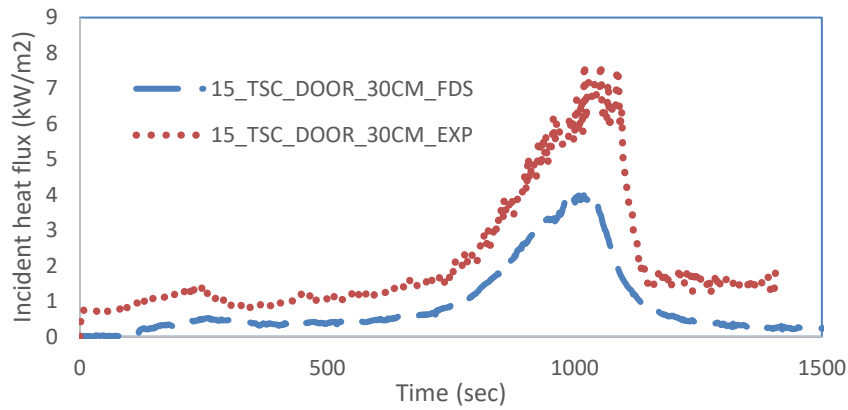


(e) Right Back corner ceiling opening

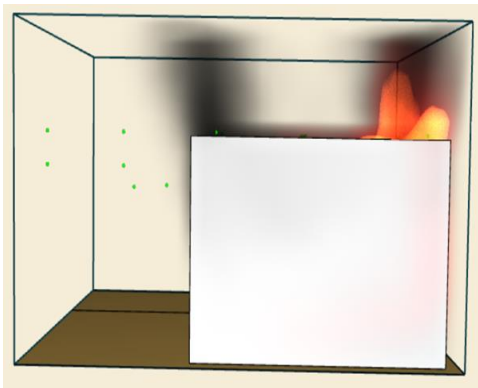
**Figure 40: Validation of the mass balance of the 15\_open case**

### 3.2.6.3 External Flaming

At first, visually, it seemed that FDS was underestimating the external flaming through the door. Despite the absence of sustained consistent flames within the experiment, yet small flames would rarely appear for less than a second throughout the whole experiment, in contrary, there were no flames at all in SMV. So, in order to investigate this point quantitatively. The incident heat flux at 0.3 m from the door was checked based on Figure 41a, and it showed a shred of clear evidence that FDS completely underestimated the external flaming. Looking at the figure above, it showed that numerically the heat flux reached an approximate peak of 4 kW/m<sup>2</sup> compared to an estimated peak of 7 kW/m<sup>2</sup> and which could give an underestimating of about  $\pm 44\%$  which was equivalent to the underestimation of the radiative energy measured at the same position. In brief, it could be concluded that the external flaming was not validated for this case.



(a) TSC 0.3 m from the door



(b) SMV Screenshot



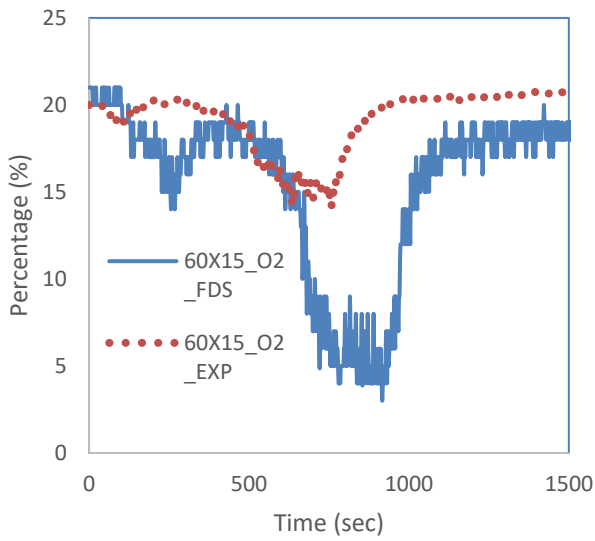
(c) Experiment Screenshot

**Figure 41: Validation of the external flaming 0.3 m from the door for the 15\_open case**

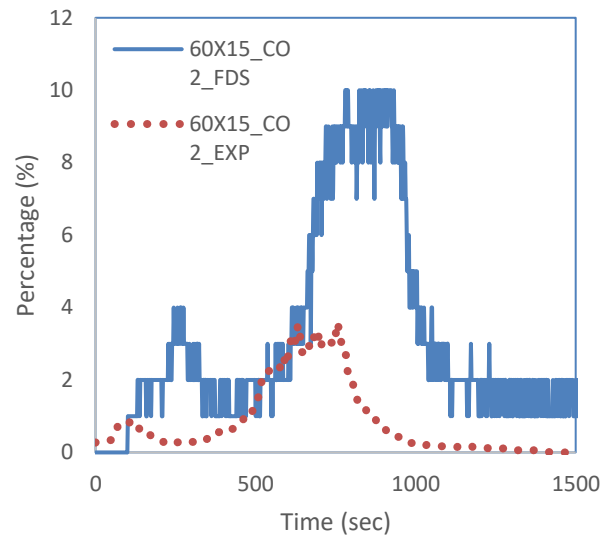
### 3.2.7 0.6x0.15 m Central Opening

#### 3.2.7.1 Combustion Efficiency

FDS failed to model the combustion efficiency accurately, as Figure 42 indicated that FDS saw this case as an under-ventilated case with a tiny percentage of oxygen in the top left corner which would be indicative of the formation of a thick smoke layer which was all contradictive to the experimental results. The experimental data showed that this was an over-ventilated compartment with no visible smoke layer formed as oxygen appeared with a high percentage at the top corner, indicating a mixture of air and hot gases. All of that led to the clear conclusion of the failure of FDS to precisely simulate the combustion efficiency in this case.



(a)

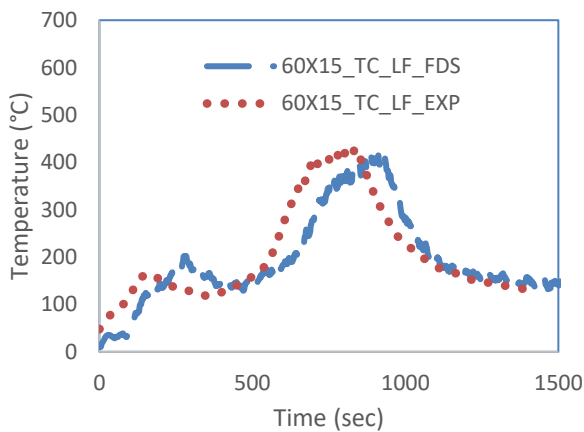


(b)

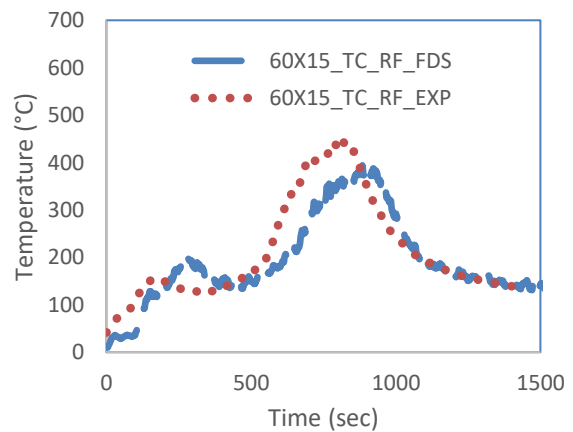
**Figure 42: Validation of the combustion efficiency for the 60x15\_open case for (a) O<sub>2</sub> and (b) CO<sub>2</sub>**

### 3.2.7.2 Heat Balance

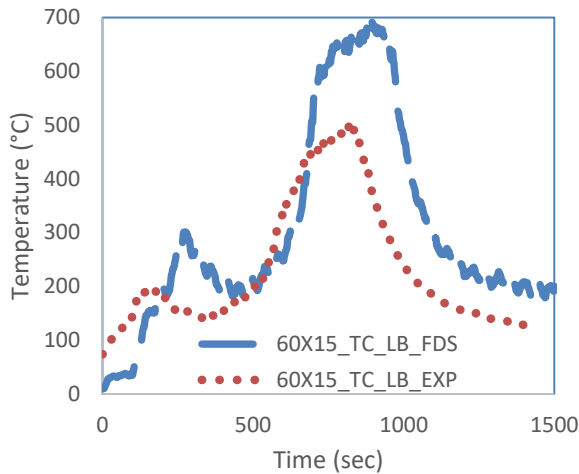
Based on the combustion efficiency, it was anticipated to see significant margins of errors when comparing FDS data with experimental ones who were clearly seen in Figure 43. Despite seeing a small margin of difference in the front top TCs, yet the backside showed notable overestimation by FDS which could be explained regarding the gas analyzer data which indicated more burning happening at the backside and consequently led to higher simulated temperatures. Also, the side TSC showed an increase of it measured incident heat flux by almost 50% and therefore it was concluded that this was far from being validated.



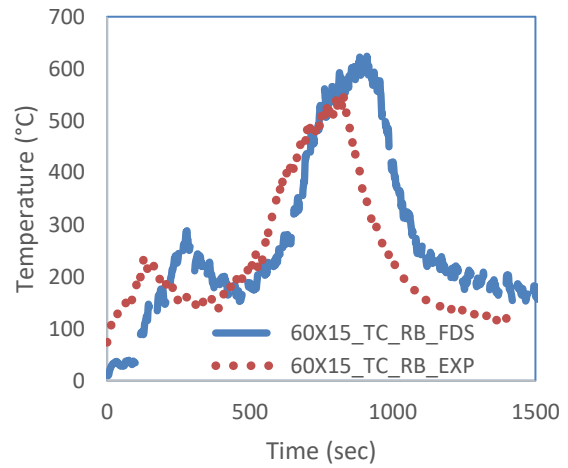
(a) TC Left Front Corner



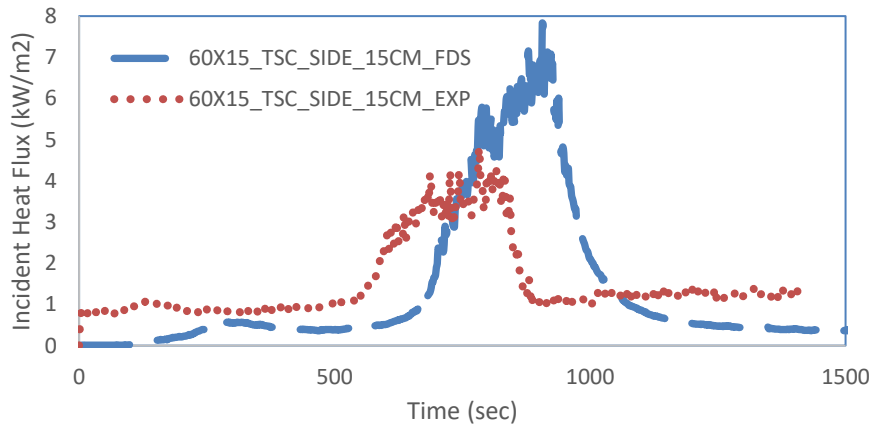
(b) TC Right Front Corner



(c) TC Left Back Corner



(d) TC Right Back Corner

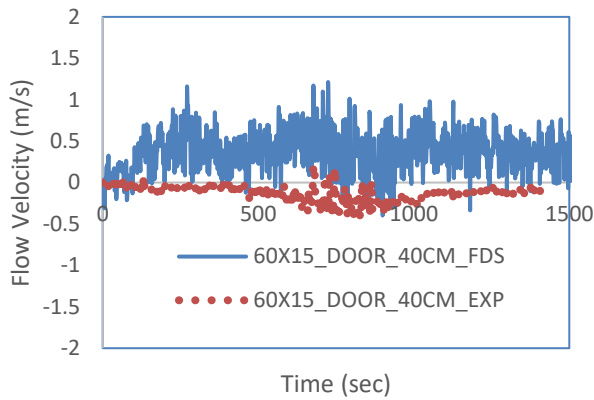


(e) TSC 0.15 m from the side wall

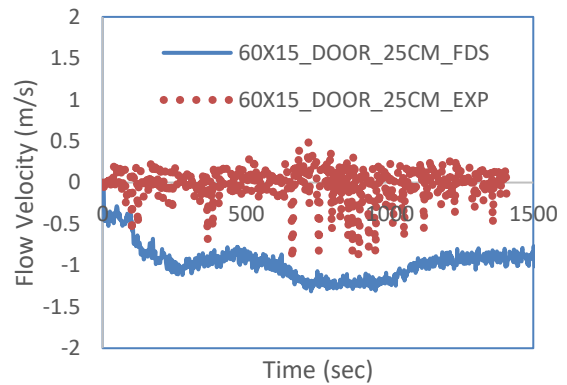
**Figure 43: Validation of the heat balance for the 60x15\_open case**

### 3.2.7.3 Mass Balance

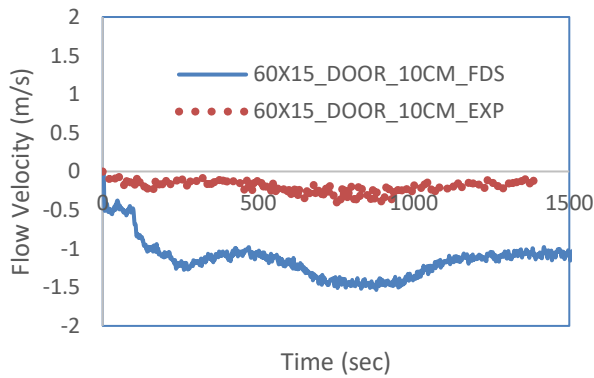
The failure of FDS with the simulation of this case continued with the mass balance, which also was utterly off-point. Firstly, it showed a high outflow and inflow of smoke and cold air from the door and ceiling opening compared to the experimental data which showed almost no outflow of hot smoke from the top of the door. Therefore, this check was not validated similar to the remaining checks.



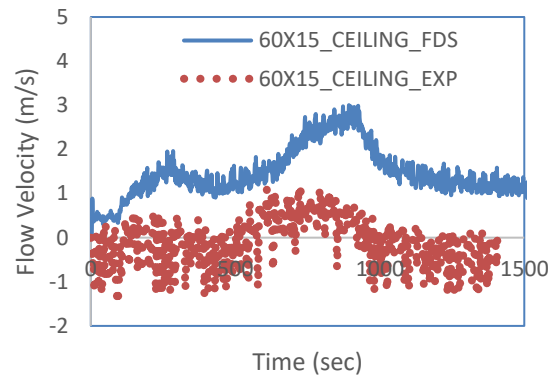
(a) 0.4 m from the floor at the door



(b) 0.25 m from the floor at the door



(c) 0.1 m from the floor at the door



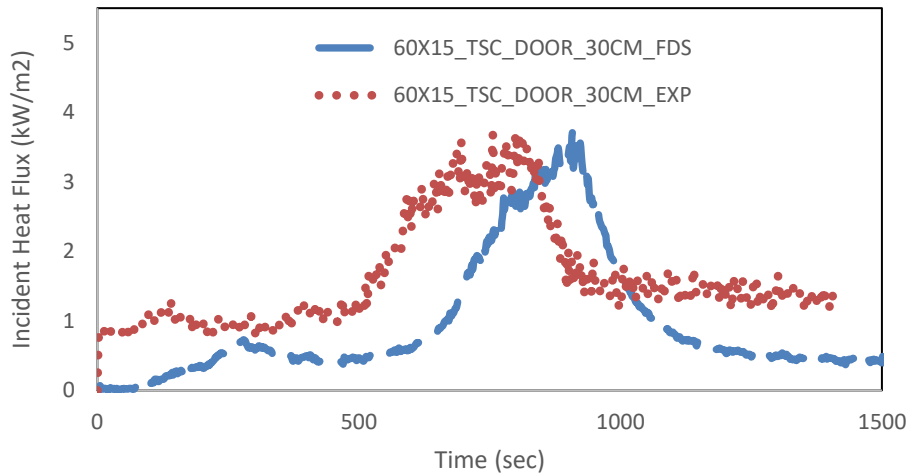
(d) Central Opening

**Figure 44: Validation of the mass balance for the 60x15\_open case**

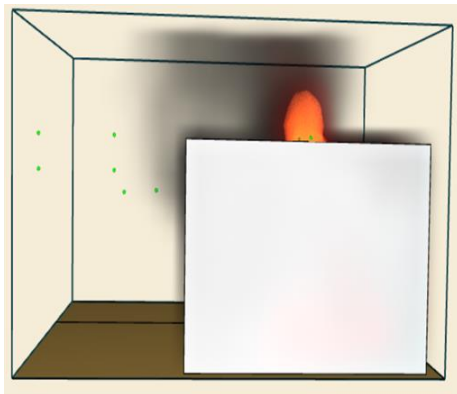
### 3.2.7.4 External Flaming

Despite seeing high resemblance in the heat flux at 0.3 m from the door, it would not make sense to consider it validated with all the remaining checks being off-point. The matching could be a result of the small heat flux radiating from the door for both FDS and experiment, which would not show a significant difference with such small values.





(a) TSC at 0.3 m from the door



(b) SMV Screenshot



(c) Experiment screenshot

Figure 45: Validation of the external flaming for the 60x15\_open case

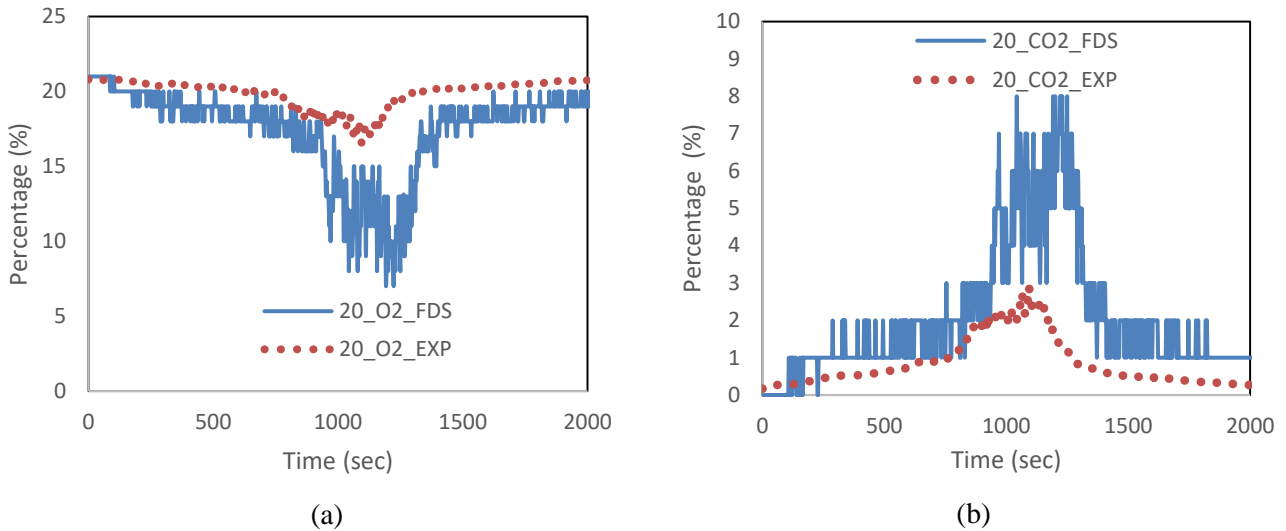
### 3.2.8 0.2x0.2 m square corner openings

#### 3.2.8.1 Combustion Efficiency

It was beneficial to have the gas analyzer data at the top left back corner inside the compartment as it would be the first step of the validation process and it would give the first impression whether the remaining parameters like the temperatures and heat fluxes would match or not.

Based on Figure 46a and 46b, it was undoubtedly clear that combustion efficiency was significantly different between the experimental and numerical data. The FDS data indicated the existence of a thicker smoke layer on the ceiling in addition to a leaner mixture of air-fuel within the compartment which contradicted the experimental data, which showed the presence of excess air. These points were seen in the excess oxygen and the less CO<sub>2</sub> that were present at the smoke leaving the ceiling opening. Now, it was clear that the temperatures would not match with any expected overestimation of temperature

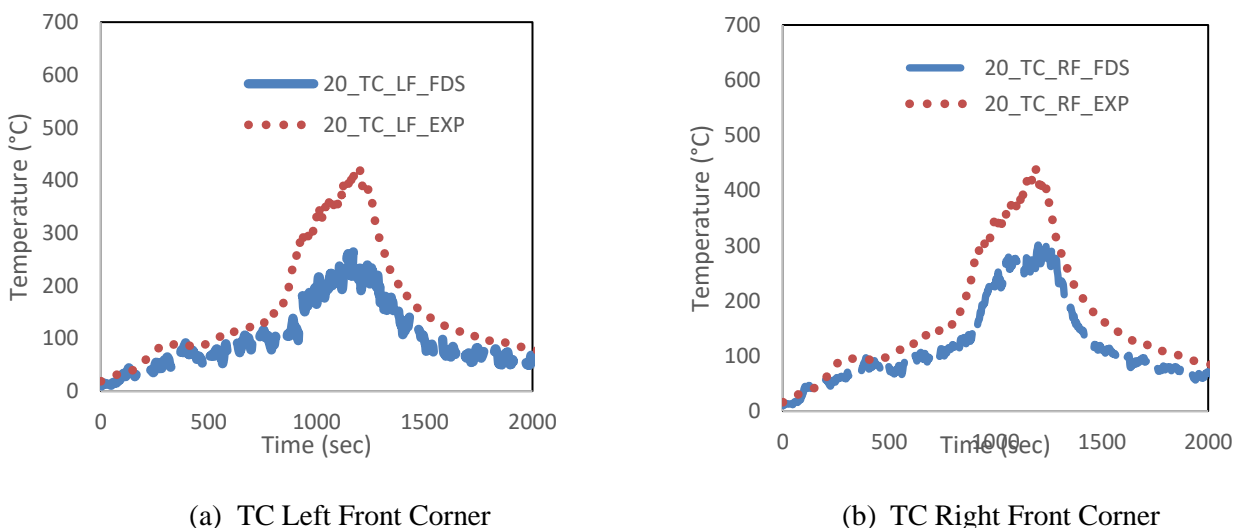
measurements at the backside of the compartment resulting from a less lean mixture within the compartment.

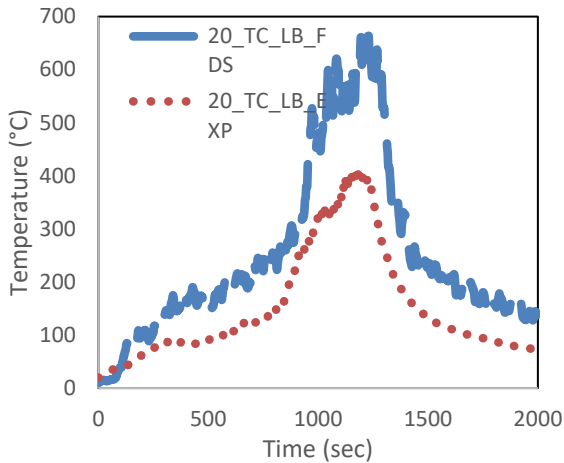


**Figure 46: Validation of the combustion efficiency for the 20\_open\_1 case for (a) O<sub>2</sub> and (b) CO<sub>2</sub>**

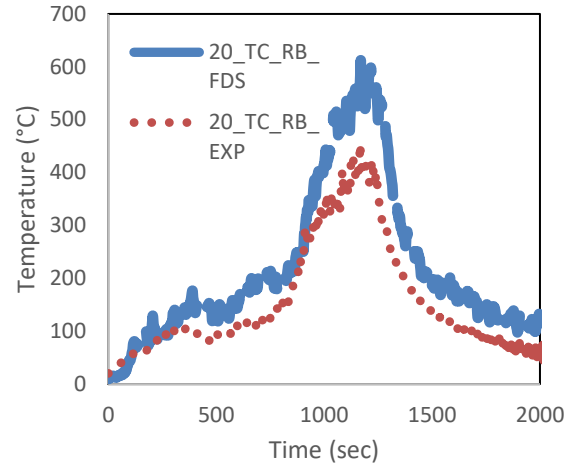
### 3.2.8.2 Heat Balance

As predicted from the previous section, the back and front corner temperatures were overestimated and underestimated by FDS respectively in contrast to the numerical data. This indicated more burning happening at the back than the front side, besides an unbalanced temperature distribution between the front and backside. Then, moving to the heat flux from the side, which surprisingly matched with the experimental data with an overestimation of only  $\pm 4\%$ . This could be justified by looking at the temperatures at the front and back, and from that, it could be seen that the front and back top corner had the same margin of overestimation and underestimation and therefore this made a balance when it came to the side heat flux. However, overall, this check was not validated.

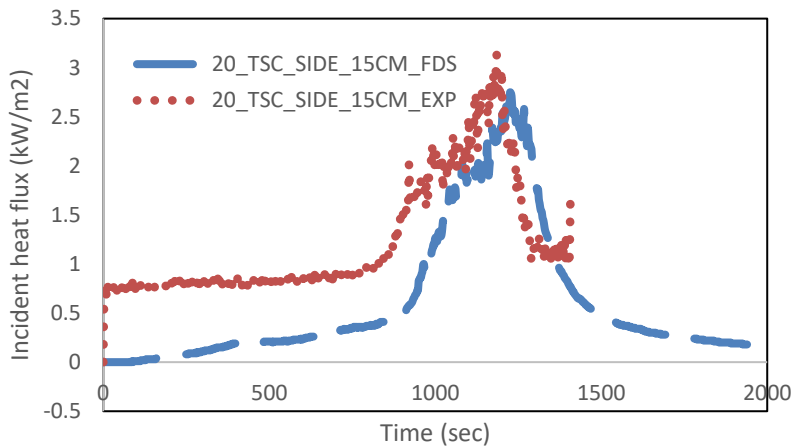




(c) TC Left Back Corner



(d) TC Right Back Corner



(e) TSC 0.15 m from the side wall

Figure 47: Validation of the heat balance for the 20\_open\_1 case

### 3.2.8.3 Mass Balance

It was observed that FDS failed to model the mass balance for this case with a significant overestimation of the flow velocities measured by the flow devices located at the door plane in FDS. Based on that, it was expected that the flow velocity leaving the ceiling opening would be underestimated completely by FDS due to the mass balance, which was evident in Figure 48c. **Error! Reference source not found.** Finally, it was concluded that the mass balance was not validated.

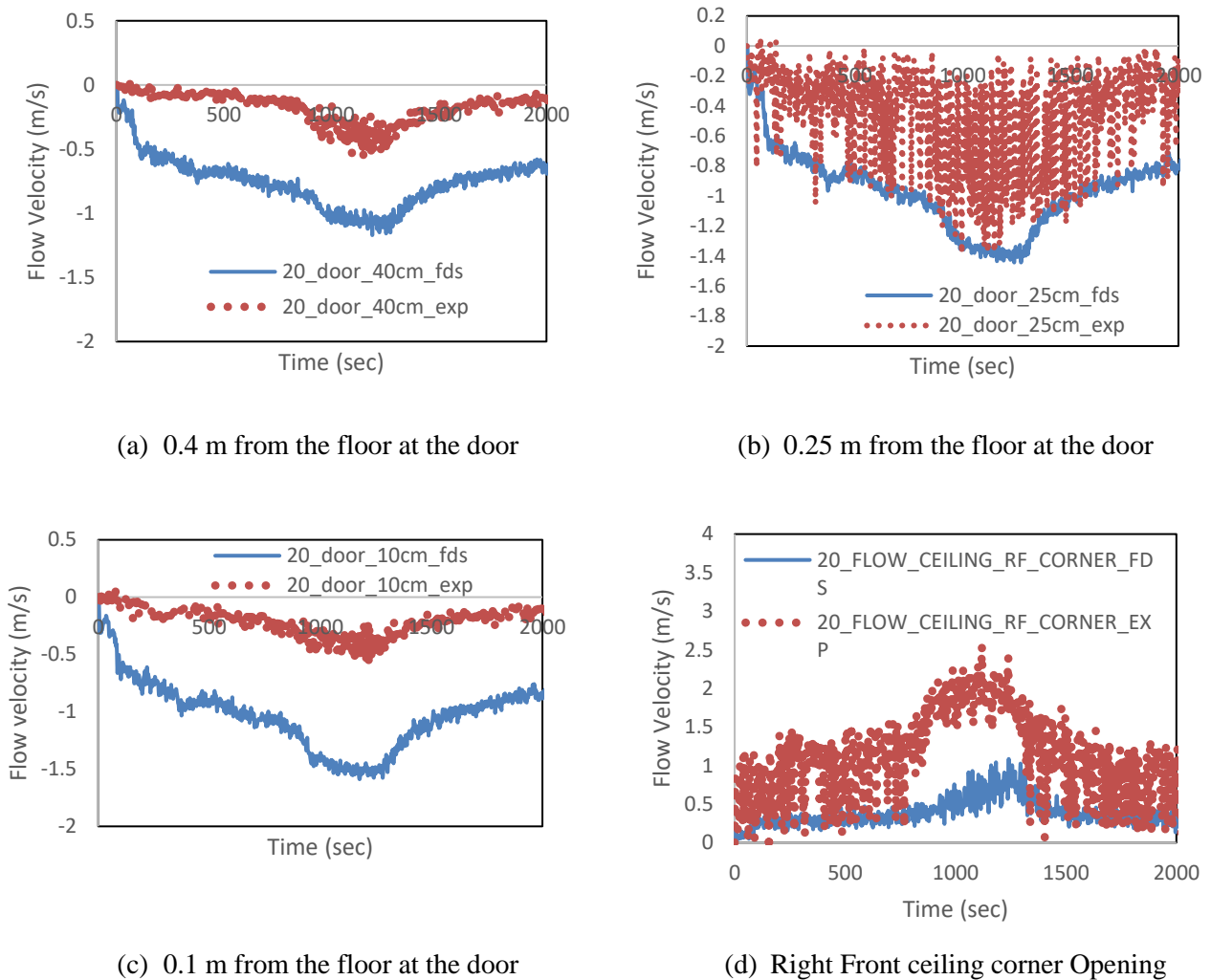
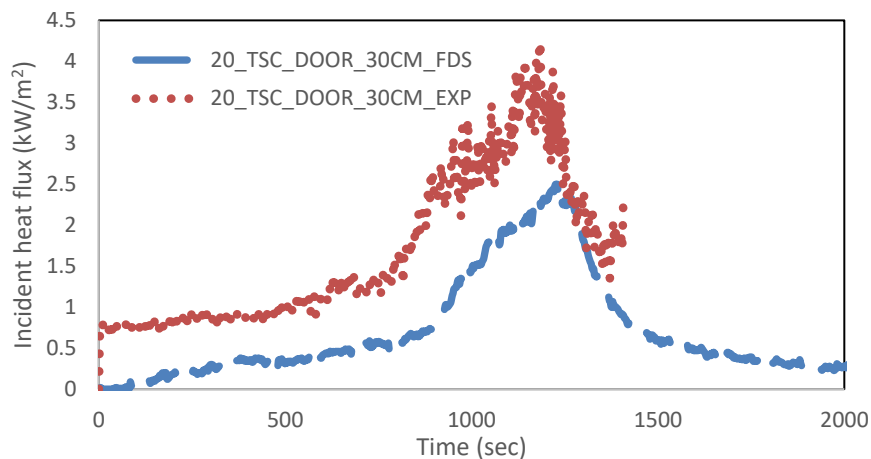


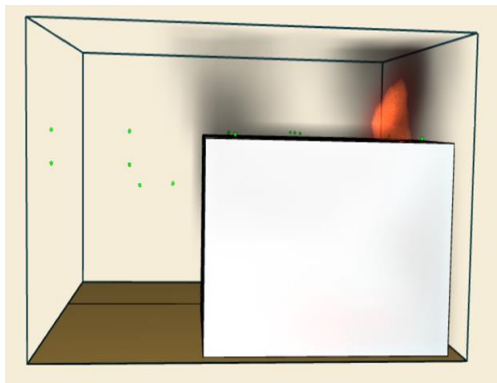
**Figure 48: Validation of the mass balance for the 20\_open\_1 case**

### 3.2.8.4 External Flaming

As usual, this check would start visually; it seemed like FDS did not accurately simulate this case with much less smoke leaving the front ceiling openings compared to the back ones and this was evident in the mass balance, in addition to the complete absence of external flames appearing from the front ceiling openings. It was also concluded that the peak incident heat flux and radiative energy at the door showed a significant underestimation in FDS of about 40%, which was expected based on all the previous inputs. All these observations would conclude that this check was not validated by FDS, and in return, the whole case will not be validated.



(a) TSC at 0.3 m from the door



(b) SMV screenshot



(c) Experiment screenshot

**Figure 49: Validation of the external flaming at 0.3 m from the door for the 20\_open\_1 case**

### 3.2.9 0.6x0.27 m Central Opening

#### 3.2.9.1 Combustion Efficiency

Due to the similarity with the 20\_open\_1 case, the graphs of this case were listed in the appendix. With such big ceiling openings, FDS started recognizing that the compartment was over-ventilated with higher and lower oxygen and carbon dioxide measured in the top left corner respectively. However, the FDS output data was still far from capturing the fire behaviour and dynamics of an over-ventilated compartment.

#### 3.2.9.2 Heat balance

The figures showed an underestimation and overestimation by FDS of temperatures at the back, and front corners respectively similar to that concluded in the 20\_open\_1 case indicating a similar limitation of FDS with such compartment with big horizontal openings.

### 3.2.9.3 Mass balance

A similar overestimation of the inflow of air through the door was seen for this case also similar to the 20\_open\_1 case. However, the only difference was in the outflow velocity of the central opening, as shown in Figure 50, which showed a contradicting overestimation pattern in the numerical data which was the opposite of the trend in the corner opening flow velocity and this was shown in Figure 50. Nevertheless, regardless of that, the mass balance was inaccurate.

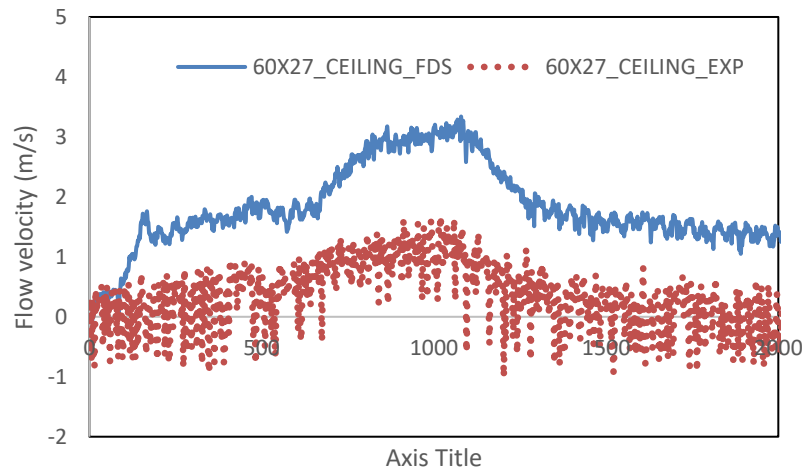


Figure 50: Validation of flow velocity leaving the ceiling opening for 60x27\_open\_1 case

### 3.2.9.4 External flaming

As mentioned before, it would not be practical to ignore all the differences in all the previous checks and just look at the small margin of difference in the heat flux from the door as a close match. This close match would be misleading and would not prove anything in this case, and therefore it would not be considered validated.

## 4. Uncertainty and impact of the shutdown

In such research studies, one of the crucial points is identifying the uncertainties within the whole study. Uncertainties in the fire research arise from various parameters. Having a small-scale lab experiment brings along many uncertainties starting from the testing set-up itself, for example, the measurement instrumentations are already equipped with their errors and uncertainties like the big hood (OC Method), TCs, TSCs and flow probes. Nevertheless, it should be noted that the presence of the fire itself brings numerous ambiguities as its behaviour is always unexpected especially when a parameter surrounding the fire changes like the addition of horizontal openings without forgetting the human error which can include installing errors and judgement errors which can have its impact. Therefore, each of these uncertainties will be discussed briefly in the following section.

### 4.1 Experimental Setup

Starting with the errors associated with the application of Janssens correlation for the calculation of the HRR in the hood. There were certain assumptions used by Janssens that would propose uncertainty within the results, like for example: taking a constant value for of the energy released for a complete combustion per unit mass of burned oxygen, all gases entering the hood were assumed to behave ideally, besides water vapour would be extracted from the sample as calorimeters would have some complexities with wet mixtures. Finally, if the experiment went smoothly and the combustion was complete with no soot or carbon monoxide, an error of about  $\pm 10\%$  would be expected. On the other hand, having soot and CO in the gas products would lead to a larger error. In other words, with the closed ceiling in addition to the small ceiling openings cases, there would be a higher error in the HRR calculation due to the incomplete combustion due to the under-ventilated compartment and the rich mixture, whereas the remaining cases where the compartment was over-ventilated the reaction would be treated as complete combustion and any small amount of CO would be neglected. [22][28]

The second component with the most uncertainties associated with it would be the bi-directional flow probe. Flow probes measure velocities using a differential pressure transducer (DPT). So, when measuring the velocity, the inaccuracy of the DPTs in addition to the lower resolution of the probe would pose many uncertainties when analyzing the flow through the compartment door. The probe might not be able to sense any sharp, sudden velocities occurring in the gases leaving the enclosure besides, any changes in the heat positioning would result in inaccurate measurements that could give misleading conclusions. It would also be hard to quantify the convective heat losses accurately at any compartment opening due to the limitations associated with the measuring device. These limitations appeared in our study where the neutral axis was estimated using a linear flow gradient, which would pose some errors due to the tendency of the neutral axis to be lower due to the significant differences between the measured high outer velocity compared to the much lower inner velocity. So, it would be concluded for this point that the neutral axis location was underestimated by this simple estimation method. Another

relevant issue appeared especially with cases with low velocities ranging from 0.3-3 m/s and how it was hard to capture the differential pressure across the opening with a DPT that could have an error embedded in it that would exceed this small differential pressure for inflow and outflow. The second part of the flow probes uncertainties would arise from the equations and calculation methods adopted based on McCaffrey and Heskestad[29] as shown in the equation below

$$V \text{ (Flow velocity)} = C \sqrt{\frac{2 \cdot \Delta P \cdot K}{\rho_{\text{gas}}}} \quad (4)$$

It was understood that the flow probe measures the flow velocity using the differential pressure across the two sides of the probe head, which is similar to the same concept of a pitot tube. Therefore, the constant K was used, which also brings its uncertainty as an estimated average value of this constant was used in the calibration of this probe. Another very significant factor was the probe constant C which was associated with removing the errors related to the head of the probe. This constant is a function of Reynolds number and the gas density, which required the addition of a TC to measure the gas temperature at each flow probe. Based on the assumption that the velocities were very low, which meant a very low Reynolds number and hence a correction factor of 0.6 would be chosen to account for the uncertainties in the flow probes. This was still a big assumption, yet a conservative one based on the measured data.

Moving to the TSCs which also had its uncertainties and errors incorporated within its calculation equations. As explained before that the incident heat flux was measured by conducting an energy balance on a controlled volume represented by the metallic disc. So, the source of uncertainty arises from the different terms used to quantify the energy losses in this balance. As these detailed calculations are not within the scope of this study, the only point of uncertainty mentioned would be the TC measurements of the air temperature on the side of the TSC's insulating core. Besides the errors with the TC measurements itself, any slip of the TC could give wrong measurements and in return would affect the convective losses that should be measured in the energy balance. Finally, it was observed during some experiments that at the door the flame would be impinging the TSC and this was not within the calibration capabilities of the TSC as it may affect the heat transfer characteristics of the disc and cause other errors. That is why this case was excluded from the validation process for the closed ceiling case due to the TSC covered with external flames.[30]

## 4.2 FDS

There were some uncertainties within the numerical study associated with the assumptions incorporated in FDS plus the inputs to the model. There is still some question unanswered even after conducting this study, these questions relate to the understanding whether the failure of FDS to model some cases (over-ventilated case) was due to the mesh size not being very fine or even with a very fine mesh FDS will still struggle to simulate it. This point would require further analysis as no mesh sensitivity analysis was conducted in this study due to the restriction of the shutdown. The remaining model input like ambient



temperature would incorporate some small error within it due to this temperature being different from each ambient temperature during each experiment. Therefore, an ambient temperature of 10°C was chosen for all the cases.

## 5. Conclusion

This study presented a small-scale experimental study for the sake of investigating the influence of adding horizontal ceiling openings (horizontal ventilation) to an informal settlement dwelling with the thermally-thin wall material. The main objective of adding ceiling ventilation was to try and develop a novel scientific solution to decrease the radiative energy generated from the original fire dwelling towards the adjacent ones. The incident heat flux data were compared against the burning characteristics of materials used in informal settlements. These numerical data were analyzed by looking at temperatures from four TC trees with each located at one corner, incident heat flux measured by TSC located outside the compartment, flow velocities measured by a set of flow probes located at the door plane and above ceiling openings and finally the concentrations of the gas products (O<sub>2</sub>, CO<sub>2</sub> and CO) resulting from the fuel burning.

Following the analysis of the experimental data, numerical models were developed to test FDS's ability to model informal settlement fires especially with the addition of ceiling ventilation, which tested the reliability of FDS with both over-ventilated and under-ventilated. These numerical data were later compared to the experimental data to check whether it could be validated based on four aspects, naming: combustion efficiency, heat balance, mass balance and external flaming.

After completing the whole study by investigating and analyzing both experimental and numerical data, it was found that with the addition of horizontal openings to an ISD, these points were concluded:

- The repeatability of the experiment with more than one ceiling opening would lead to some differences in the peaks and delay times which was seen when the ceiling opening was distributed into 4 square openings. On the other hand, one equivalent central opening indicated a very close fit when replicated.
- The temperature of the hot gas layer increased by a maximum estimated value of about 20% when the area of the ceiling openings became 0.04 m<sup>2</sup>, then following this threshold layer's temperature decreased by approximately 40% when the horizontal ventilation area reached 0.16 m<sup>2</sup>.
- The incident heat flux to the surroundings decreased with the addition of ceiling openings. The heat flux from the door and side by about 58% and 62% respectively for the 0.16 m<sup>2</sup> ceiling opening area compared to the closed ceiling case. Also, the radiative energy from the backside decreased by about 50% for the 0.16 m<sup>2</sup> case, but it was observed to increase for the 10\_open and 15\_open by about 30% before decreasing significantly to almost 50%.

- The central openings illustrated more reduction in its radiative energy to the surrounding compared to the corner openings, even the backside radiation intensity decreased through all experiments.
- The incident heat flux at 0.3 m from the door when compared to the critical heat fluxes some of the materials in ISD, showed some concerns of spontaneously starting ignition for some materials, while the side heat flux showed much less concern for fire spread.
- The height of the neutral axis from the floor seemed to increase with the addition of bigger ceiling openings. For the closed\_1, 2.5\_open, 5\_open, 60x2\_open cases the neutral axis location slightly increased from 0.12 m to 0.15 m. On the other side, when the horizontal ventilation area reached 0.04 m<sup>2</sup> (10\_open and 60x7\_open), the neutral axis height increased significantly reaching 0.25 m, the moment this value of the area was exceeded, there was no neutral axis present on the door plane.
- The flow probes output data plus the visual observations of the lab experiments indicated the occurrence of the ‘ghosting or oscillating flames’ for the case where the compartment was under-ventilated. When the ceiling openings area reached 0.04 m<sup>2</sup>, this phenomenon disappeared. These oscillating flames showed significant fluctuations in the flow probes output signals. This point needs further analysis as the combination of a door, and different shapes of ceiling openings were not studied before with the intent of locating the neutral axis as far as the literature indicated.
- The gas analyzers indicated a lower combustion efficiency indicating incomplete combustion until the area of the opening reached 0.01 m<sup>2</sup> when this value was surpassed almost no CO existed indicating the change of the compartment from being under-ventilated to over-ventilated.
- The time to flashover reached a maximum reduction of about 30% for the 0.01 m<sup>2</sup> ceiling openings, then started increasing again when the ceiling opening area increased.
- When the sizes of the opening exceeded 0.04 m<sup>2</sup>, the compartment failed to reach the flashover criteria specified by the MQH method (525°C for all top corners).
- FDS was able to simulate the fire behaviour for under-ventilated compartments, there were some mismatches with some flow probes, but in general, FDS managed to capture the turbulences and fire dynamics within these cases.
- FDS failed to simulate fires in ISDs with considerably big ceiling openings, it did not only fail at one of the four checks, but it also failed all of them with no close matching in any of them. Therefore, the failure of modelling over-ventilated compartment would need more analysis with finer meshes to investigate what could be the problem. Are the combustion and turbulence

models in FDS too simple to capture more complex phenomena in the compartment or it is a mesh-related problem?

These points listed above were the clear conclusions that were observed within this study. However, due to the complexities of such a study, more future work is required, and this future vision is mentioned below.

## **5.1 Future Work**

As a result of the limited space and time of a master thesis besides the impact of the shutdown, the following points were not discussed within this report and will be investigated later on following the submission of this report. Some of these points were already conducted but listed in the appendix while the remaining points will be conducted as future work:

- Eleven polycarbonate covered horizontal openings experiments were not discussed within the scope of this report as they were not validated by FDS due to time restrictions. These eleven experiments were divided into six corner openings and five central opening experiments with one repeated test for each type of horizontal openings.
- Numerical models were not developed for the polycarbonate-covered corner/central openings and hence no further analysis and validation for these cases. These models would indicate the effectiveness of using polycarbonate in ISD ceilings and how it would react during a fire.
- A parametric study will be established to furtherly analyze and understand the sensitivity of changing some parameters on the output data. For example. Fire size and location would be studied in-depth to understand their impact on smoke production, smoke movement, flashover time, external flaming, gas layer temperature, and flow velocities exiting from the door and ceiling openings.
- Using all the data in this report and the extra data generated from further research will be used to develop an empirical correlation for the ventilation factor of horizontal openings.

The findings of this research project will be presented in a scientific paper after all the data is gathered and are shown to be broadly in line with the original plan.

## 6. References

- [1] W. R. Avis, “Urban governance (Topic Guide).,” *Gsdrc*, 2016.
- [2] UN-Habitat, “Urbanization and Climate Change in Small Island Developing States,” p. 52, 2015.
- [3] “About the IRIS-Fire Project - 99designs-5963385309897.” [Online]. Available: <https://www.iris-fire.com/about-1/>. [Accessed: 30-Jan-2020].
- [4] “Informal settlements - GSDRC.” [Online]. Available: <https://gsdrc.org/topic-guides/urban-governance/key-policy-challenges/informal-settlements/>. [Accessed: 10-Apr-2020].
- [5] “Right of Response: Cape Town spends hundreds of million...” [Online]. Available: <https://www.dailymaverick.co.za/article/2015-06-01-right-of-response-cape-town-spends-hundreds-of-millions-of-rand-on-informal-settlement-sanitation/>. [Accessed: 28-Apr-2020].
- [6] “WHO | Burns.” [Online]. Available: [https://www.who.int/violence\\_injury\\_prevention/other\\_injury/burns/en/](https://www.who.int/violence_injury_prevention/other_injury/burns/en/). [Accessed: 30-Jan-2020].
- [7] R. Walls, G. Olivier, and R. Eksteen, “Informal settlement fires in South Africa: Fire engineering overview and full-scale tests on ‘shacks,’” *Fire Saf. J.*, vol. 91, no. February, pp. 997–1006, 2017, doi: 10.1016/j.firesaf.2017.03.061.
- [8] D. Rush *et al.*, “Fire risk reduction on the margins of an urbanizing world,” *Glob. Assess. Rep. 2019*, pp. 1–25, 2018.
- [9] “In photos: Fire destroys numerous homes in Hout Bay | GroundUp.” [Online]. Available: <https://www.groundup.org.za/article/photos-fire-destroys-numerous-homes-hout-bay/>. [Accessed: 29-Apr-2020].
- [10] A. Cicione, R. S. Walls, and C. Kahanji, “Experimental study of fire spread between multiple full scale informal settlement dwellings,” *Fire Saf. J.*, vol. 105, no. February, pp. 19–27, 2019, doi: 10.1016/j.firesaf.2019.02.001.
- [11] D. Drysdale, *An introduction to fire dynamics*. Wiley, 2011.
- [12] L. Poon, “Predicting Time of Flashover,” *Int. Assoc. Fire Saf. Sci.*, 1988.
- [13] V. Babrauskas, “Estimating room flashover potential,” *Fire Technol.*, vol. 16, no. 2, pp.

- 94–103, May 1980, doi: 10.1007/bf02481843.
- [14] T. E. Waterman, “Room flashover-Criteria and synthesis,” *Fire Technol.*, vol. 4, no. 1, pp. 25–31, Feb. 1968, doi: 10.1007/BF02588603.
- [15] “An Experimental Study of the Radiation from Wood Flames - Bengt Hägglund, Lars-Evert Persson - Google Books.” [Online]. Available: [https://books.google.co.uk/books/about/An\\_Experimental\\_Study\\_of\\_the\\_Radiation\\_f.html?id=LthWtAEACAAJ&redir\\_esc=y](https://books.google.co.uk/books/about/An_Experimental_Study_of_the_Radiation_f.html?id=LthWtAEACAAJ&redir_esc=y). [Accessed: 06-Apr-2020].
- [16] B. J. McCaffrey, J. G. Quintiere, and M. F. Harkleroad, “Estimating room temperatures and the likelihood of flashover using fire test data correlations,” *Fire Technol.*, vol. 17, no. 2, pp. 98–119, May 1981, doi: 10.1007/BF02479583.
- [17] Y. Wang, L. Gibson, M. Beshir, and D. Rush, “Preliminary Investigation of Critical Separation Distance Between Shacks in Informal Settlements Fire,” in *The Proceedings of 11th Asia-Oceania Symposium on Fire Science and Technology*, Springer Singapore, 2020, pp. 379–389.
- [18] M. Beshir, Y. Wang, F. Centeno, R. Hadden, S. Welch, and D. Rush, “Semi-empirical model for estimating the Heat Release Rate required for flashover in compartments with thermally-thin boundaries and ultra-fast fires,” in *IAFSS*, 2020, p. 12.
- [19] “ISO 9705:1993 Fire tests — Full-scale room test for surface products.”
- [20] M. Beshir, Y. Wang, L. Gibson, S. Welch, and D. Rush, “A Computational Study on the Effect of Horizontal Openings on Fire Dynamics within Informal Dwellings,” *Proc. Ninth Int. Semin. Fire Explos. Hazards (ISFEH9)*, no. March, pp. 512–523, 2019, doi: 10.18720/spbpu/2/k19-122.
- [21] Q. Li, J. Zhang, and S. Lu, “Influence of roof opening on gas temperature rise in an enclosure,” *Procedia Eng.*, vol. 62, pp. 194–201, 2013, doi: 10.1016/j.proeng.2013.08.055.
- [22] M. L. Janssens, “Measuring rate of heat release by oxygen consumption,” *Fire Technol.*, vol. 27, no. 3, pp. 234–249, 1991, doi: 10.1007/BF01038449.
- [23] B. Karlsson and J. G. Quintiere, *Enclosure fire dynamics*. CRC Press, 2000.
- [24] Y. Wang, C. Bertrand, M. Beshir, C. Kahanji, R. Walls, and D. Rush, “Developing an experimental database of burning characteristics of combustible informal dwelling materials based on South African informal settlement investigation,” *Fire Saf. J.*, vol.

- 111, no. November 2019, p. 102938, 2020, doi: 10.1016/j.firesaf.2019.102938.
- [25] O. Aljumaiah, H. N. Phylaktou, G. E. Andrews, I. M. L. Heath, and J. S. P. Ledger, “Ghosting flames in a low ventilation compartment with kerosene pool fires,” *Int. Congr. "Combustion Fire Dyn. CFD2010"*, 2010.
- [26] K. McGrattan, S. Hostikka, R. McDermott, J. Floyd, C. Weinschenk, and K. Overhold, “Sixth Edition Fire Dynamics Simulator User ’s Guide (FDS),” *NIST Spec. Publ. 1019*, vol. Sixth Edit, 2016, doi: 10.6028/NIST.SP.1019.
- [27] “SFPE Handbook of Fire Protection Engineering | Morgan J. Hurley | Springer.” [Online]. Available: <https://www.springer.com/gp/book/9781493925643>. [Accessed: 14-Apr-2020].
- [28] H. Biteau *et al.*, “Calculation methods for the heat release rate of materials of unknown composition,” *Fire Saf. Sci.*, pp. 1165–1176, 2008, doi: 10.3801/IAFSS.FSS.9-1165.
- [29] B. J. McCaffrey and G. Heskestad, “A robust bidirectional low-velocity probe for flame and fire application,” *Combust. Flame*, vol. 26, no. C, pp. 125–127, 1976, doi: 10.1016/0010-2180(76)90062-6.
- [30] J. P. Hidalgo, C. Maluk, A. Cowlard, C. Abecassis-Empis, M. Krajcovic, and J. L. Torero, “A Thin Skin Calorimeter (TSC) for quantifying irradiation during large-scale fire testing,” *Int. J. Therm. Sci.*, vol. 112, pp. 383–394, 2017, doi: 10.1016/j.ijthermalsci.2016.10.013.

## Appendix

### A. SMALL SCALE MODEL

#### A.1.1 Peak HRR Values for all the cases

Table 13: Peak HRR Values for all experiments

Case Name	Peak HRR (KW)	% Difference with respect to the closed ceiling test
<b>Closed Ceiling Cases</b>		
Closed_2	113.66	100%
<b>Corner Openings</b>		
2.5_open	124.04	9.1%
5_open	153.21	34.8%
10_open	180.626	58.9%
15_open	160.52	41.2%
20_open_1	111.29	-2%
<b>Central Openings with Polycarbonate</b>		
60x2_poly	173.09	52.2%
60x7_poly	165.54	45.6%
60x15_poly	130.64	14.9%
60x27_poly_1	104.63	-7.9%
<b>Central Openings without Polycarbonate</b>		
60x2_open	159.16	40%
60x7_open	165.34	45.4%
60x15_open	122.17	7.4%
60x27_open	97.64	-14%

### A.1.2 HRR Data

#### A.1.2.1 Corner Openings

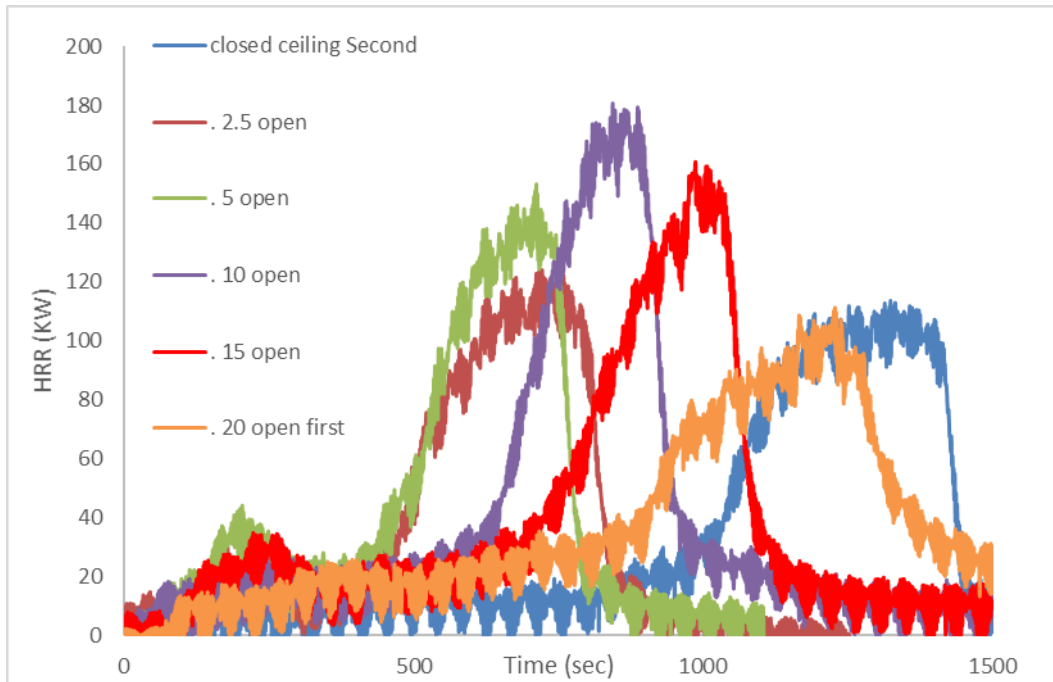


Figure 51: HRR For Corner Openings Without Polycarbonate

#### A.1.2.2 Central Slot Opening

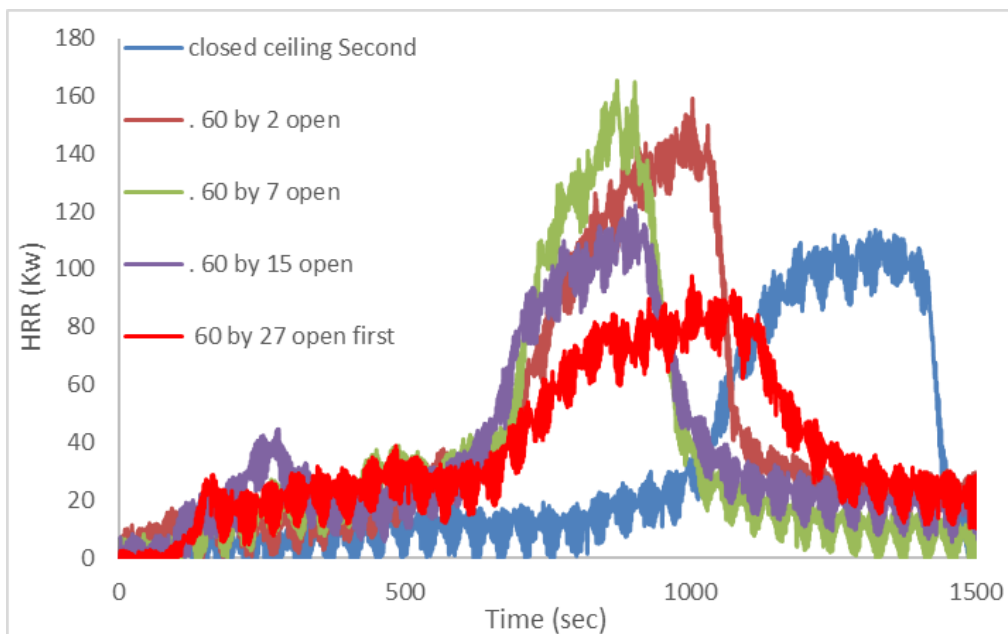


Figure 52: HRR For Central Openings without Polycarbonate



## A.2. TC Trees Results

### A.2.1 Closed Ceiling Repeated Tests

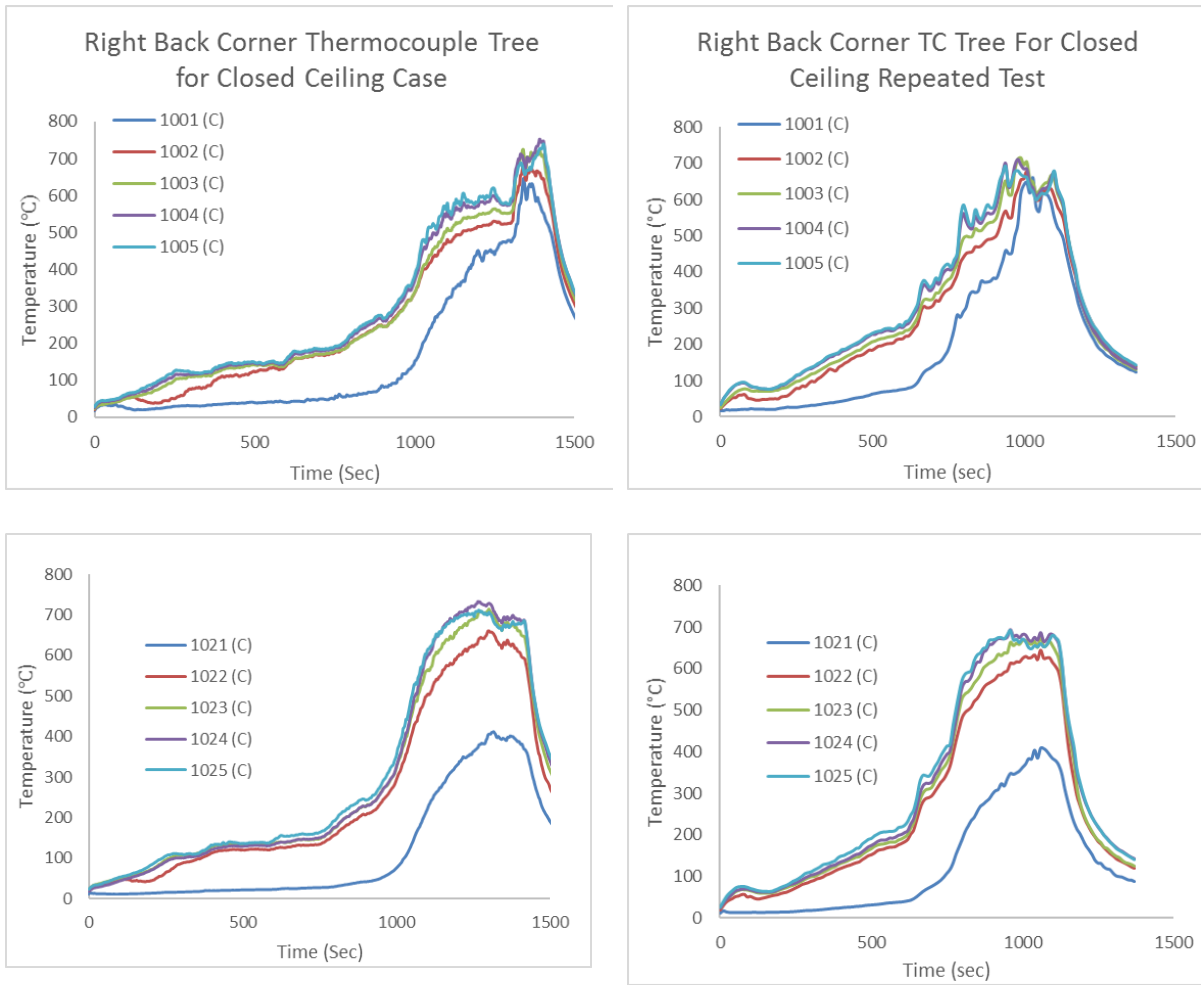


Figure 53: TC Comparison between The First (Left) and Second (Right) Closed Ceiling Test

### A.2.2 Central Slot Opening Covered with Polycarbonate

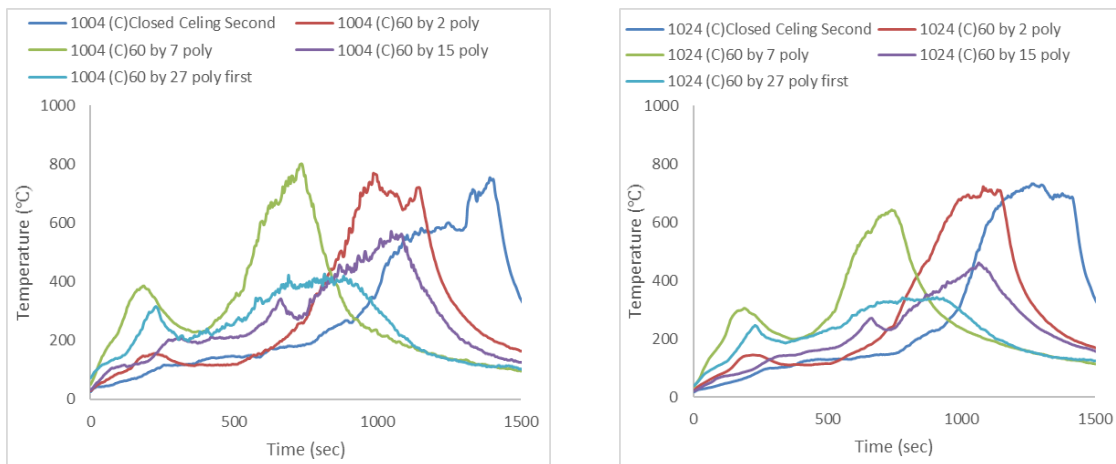


Figure 54: Top TC in Right Back (Left) and front (Right) Central with Polycarbonate

### A.3. Heat Flux Gauges

#### A.3.1 Corner Openings

##### A.3.1.1 60 cm from The Door

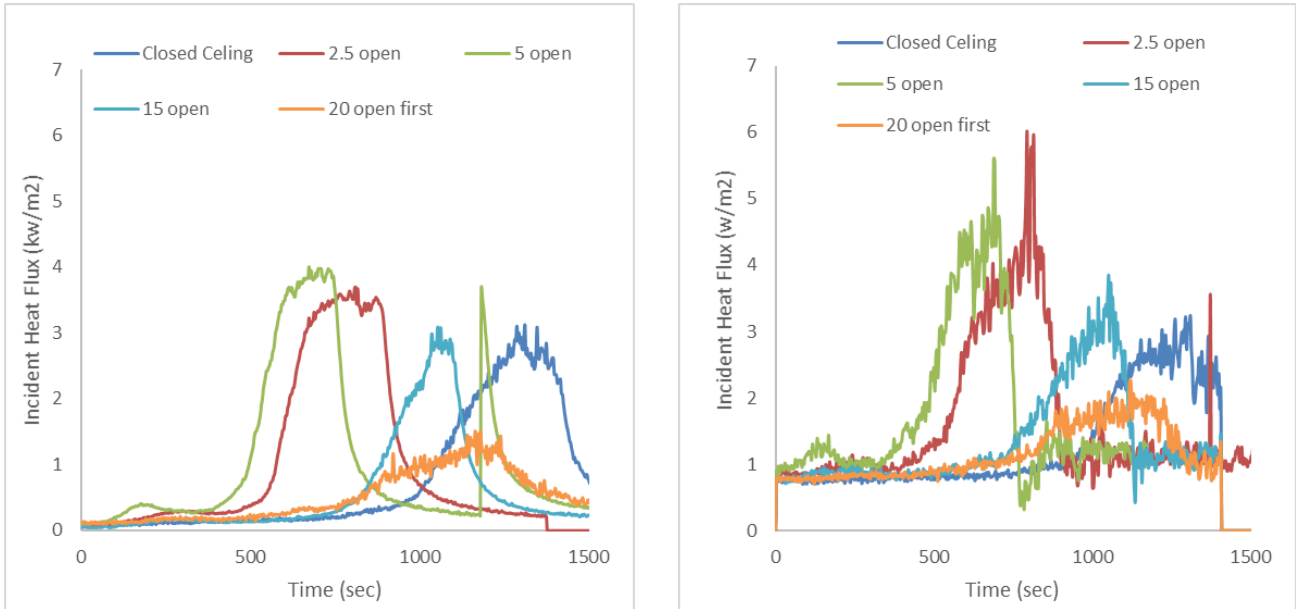


Figure 55: Heat Flux Sensor (Left) vs. TSC (Right) at 60 cm from door for Corner Openings without Polycarbonate

##### A.3.1.2 15 cm from the side wall

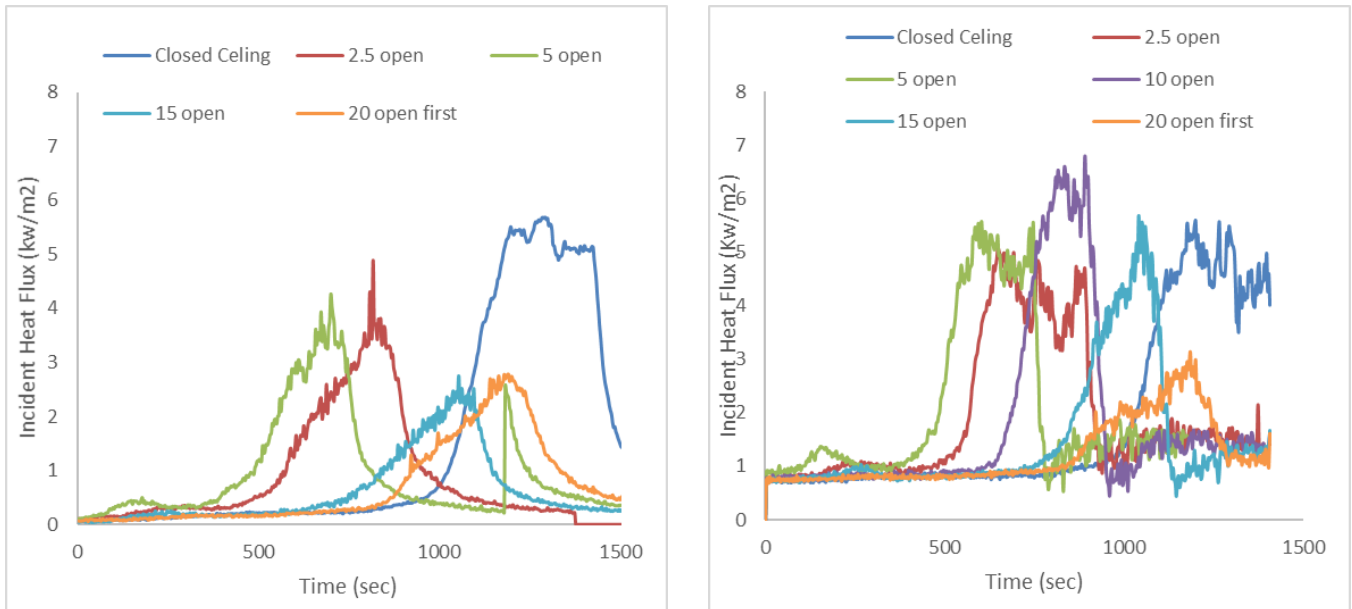
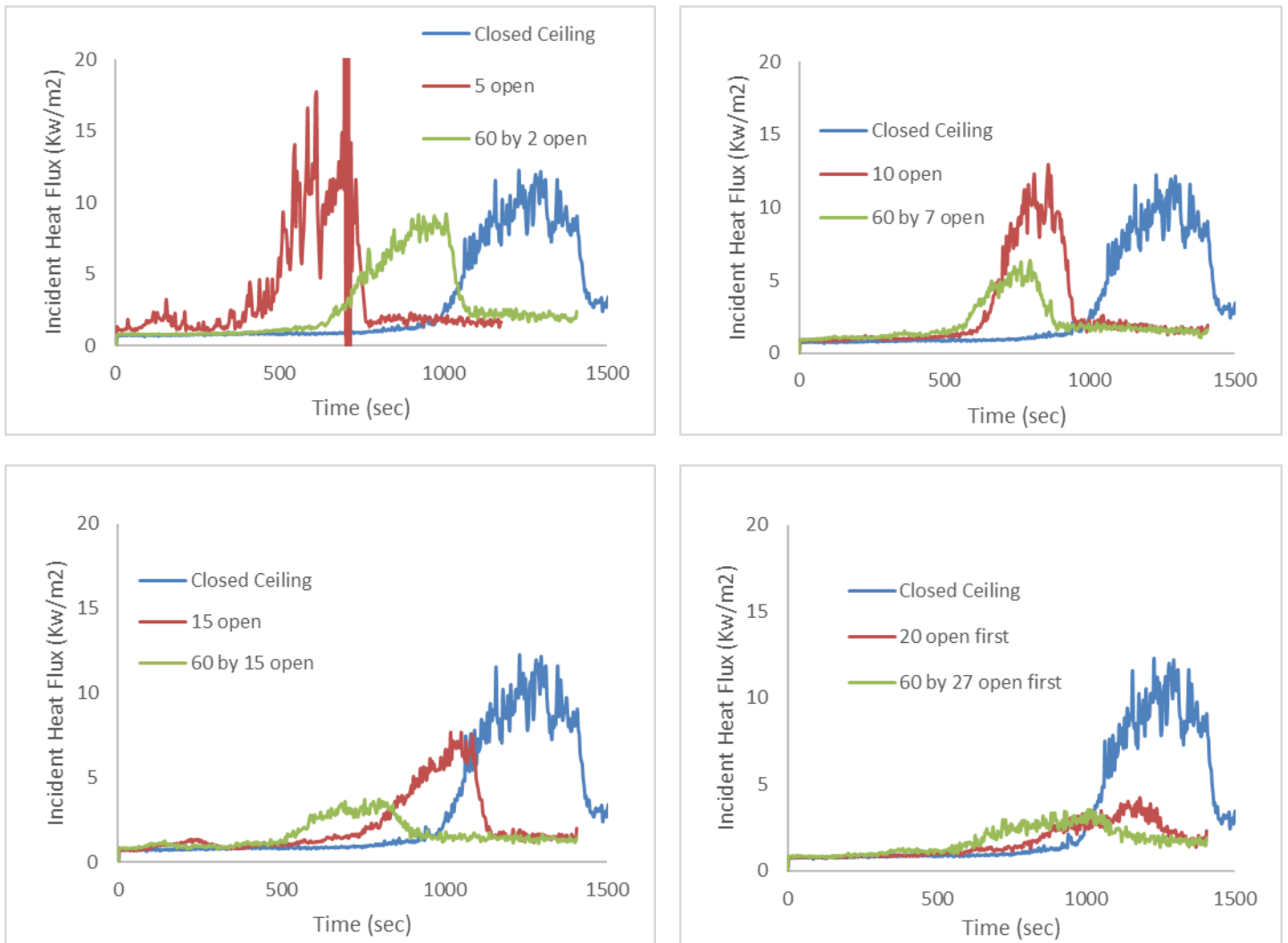


Figure 56: Heat Flux Sensor (Left) vs. TSC (Right) 15 cm from side wall for Corner Openings without Polycarbonate

**A.3.2 Openings without Polycarbonate 30 cm from the door**



**Figure 57: Closed Ceiling Vs. Open Corner Openings Vs. Open Central Opening (Heat Flux 30 cm from the door))**

**A.3.3 Openings without Polycarbonate 15 cm from the side**

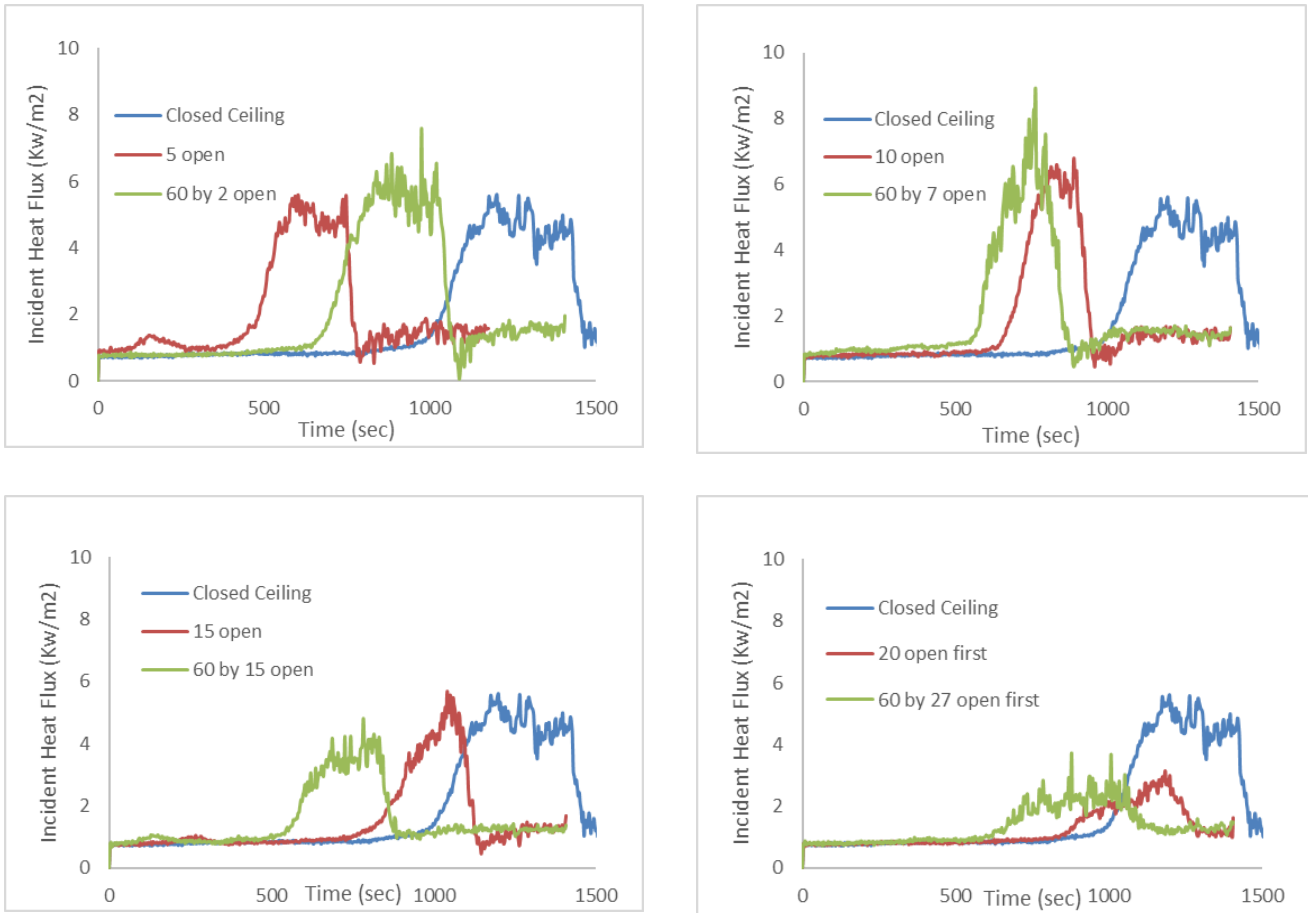


**Figure 58: Closed Ceiling Vs. Open Corner Openings Vs. Open Central Opening (Heat Flux 15 cm from the side)**

## B. VALIDATION

### B.1. 60 cm by 27 cm Central Opening Without Polycarbonate Cover

#### B.1.1 Combustion Efficiency

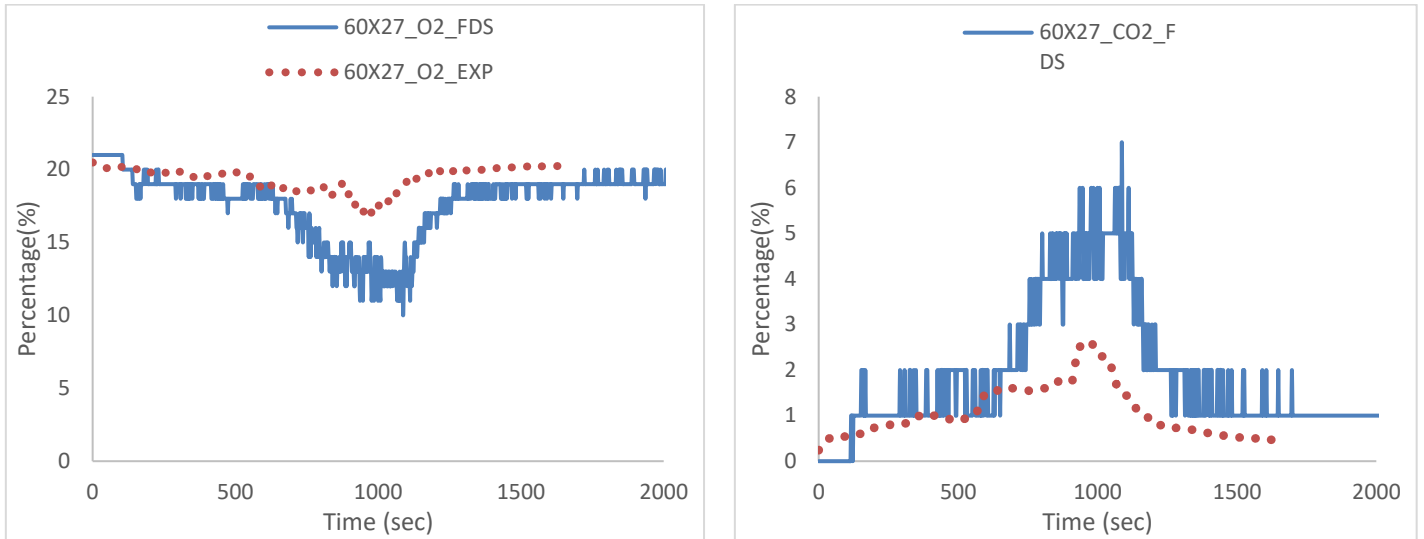
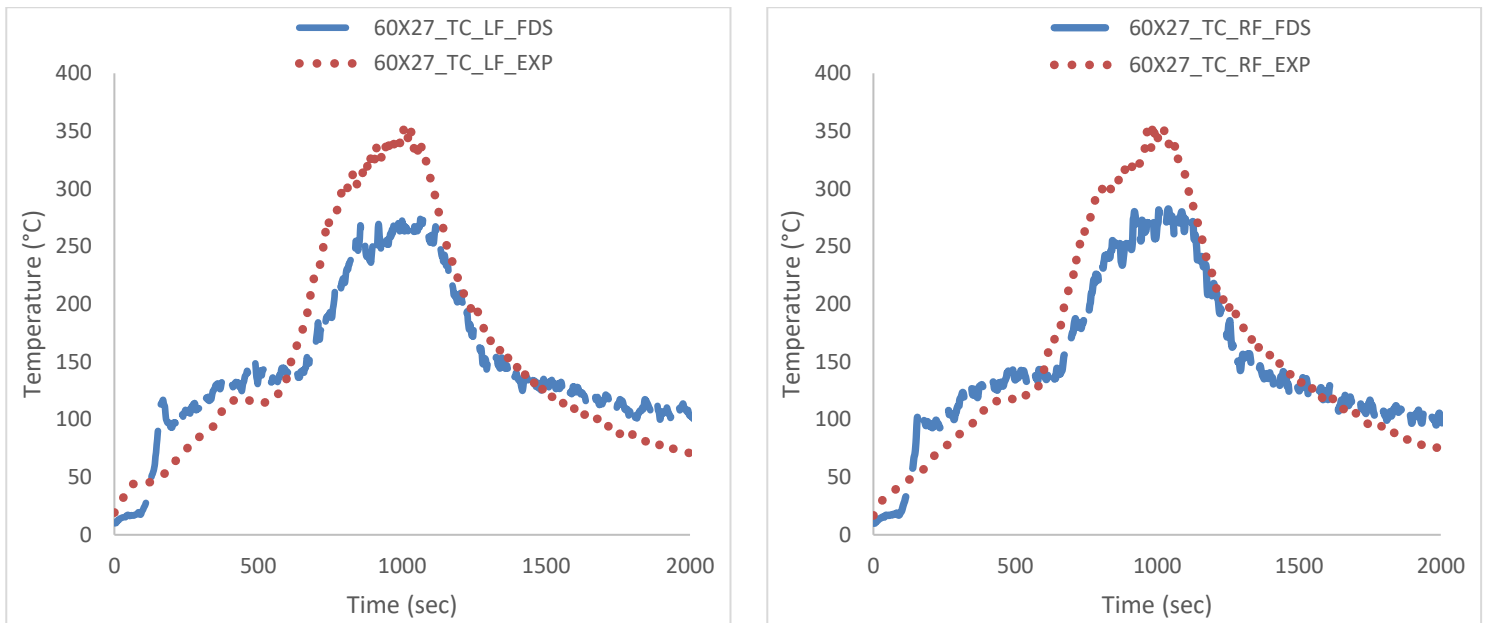


Figure 59: Validation of the combustion efficiency for the 60x27\_open\_1 case

#### B.1.2 Heat Balance



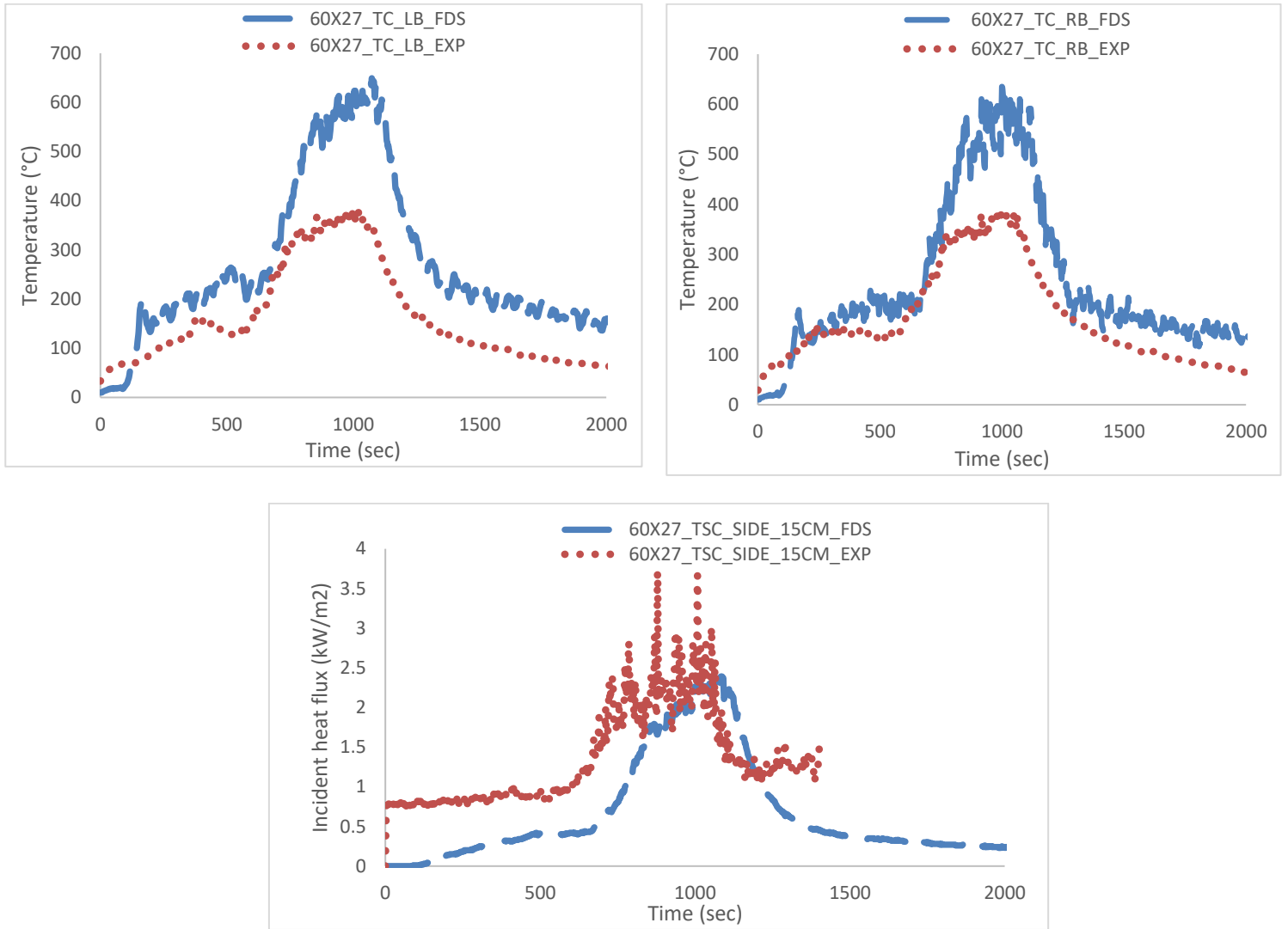
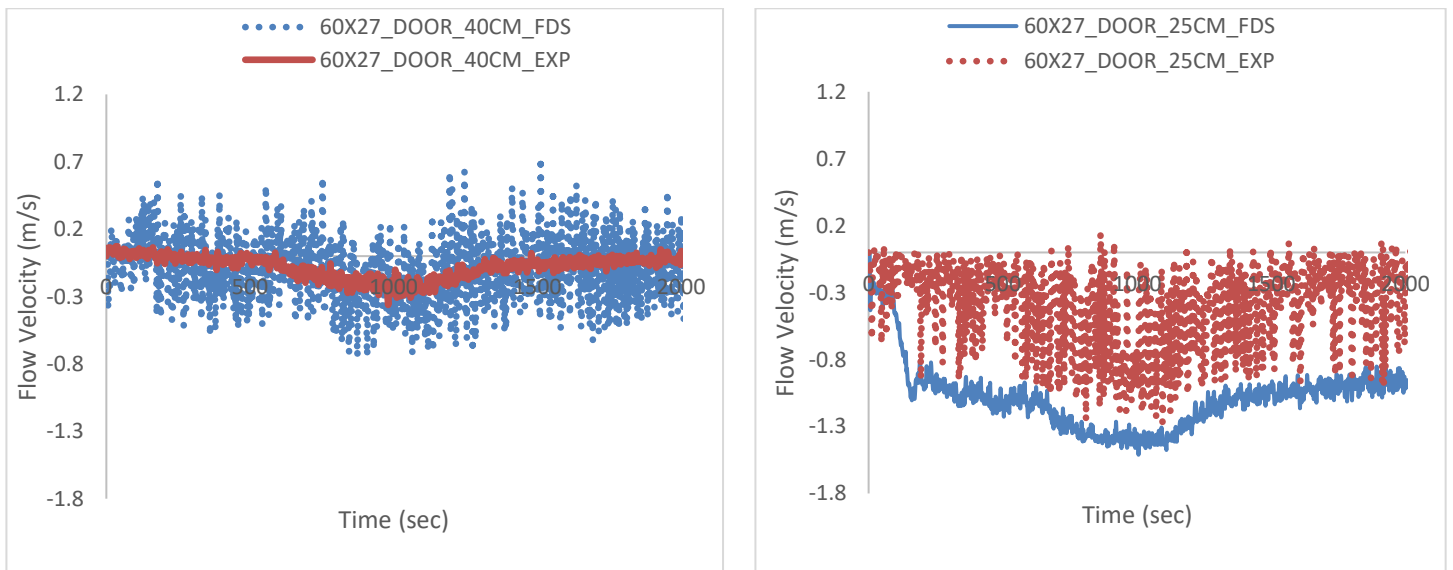


Figure 60: Validation of the heat balance for the 60x27\_open\_1 case

**B.1.3 Mass Balance**



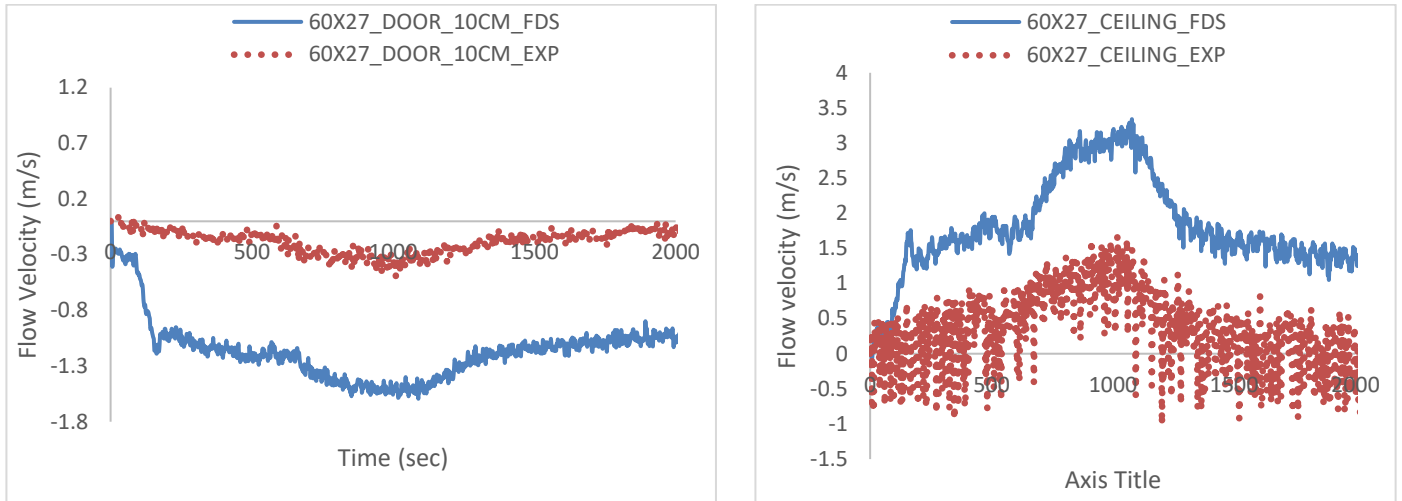


Figure 61: Validation of the mass balance for the 60x27\_open\_1 case

**B.1.4 External Flaming**

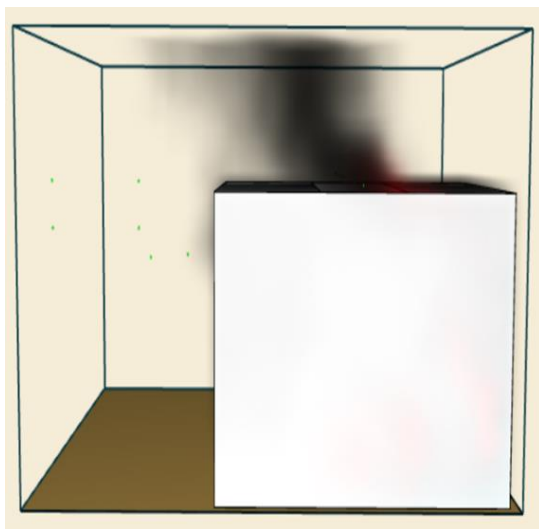
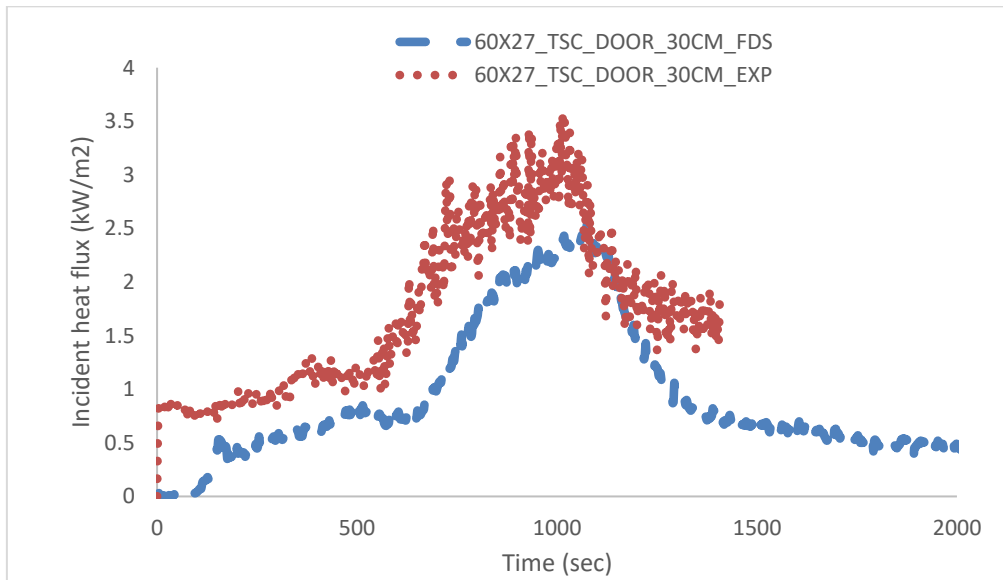


Figure 62: Validation of the external flaming for the 27\_open\_1 case

## B.2. FDS Code

2.5 cm Corner exposed.fds

Generated by PyroSim - Version 2019.3.1204

Apr 21, 2020 4:13:08 PM

```
&HEAD CHID='2_5_cm_Corner_exposed'/
```

```
&TIME T_END=1255.0/
```

```
&DUMP COLUMN_DUMP_LIMIT=.TRUE., DT_RESTART=300.0, DT_SL3D=0.25/
```

```
&MISC TMPA=10.0/
```

```
&MESH ID='Mesh01-a-b', IJK=16,12,36, XB=-0.486387,-0.088165,-0.610248,-0.3,-0.01,0.89/
```

```
&MESH ID='Mesh01-a-a', IJK=16,12,36, XB=-0.486387,-0.088165,-0.3,0.0,-0.01,0.89/
```

```
&MESH ID='Mesh01-a-b01', IJK=16,12,36, XB=-0.486387,-0.088165,0.0,0.3,-0.01,0.89/
```

```
&MESH ID='Mesh01-a-b02', IJK=16,12,36, XB=-0.486387,-0.088165,0.3,0.6,-0.01,0.89/
```

```
&MESH ID='Mesh01-a-b03', IJK=16,14,36, XB=-0.486387,-0.088165,0.6,0.939752,-0.01,0.89/
```

```
&MESH ID='Mesh 1-b_03', IJK=29,12,36, XB=-0.088165,0.633613,-0.610248,-0.3,-0.01,0.89/
```

```
&MESH ID='Mesh 1-b_2', IJK=29,12,36, XB=-0.088165,0.633613,-0.3,0.0,-0.01,0.89/
```

```
&MESH ID='Mesh 1-b_01', IJK=29,12,36, XB=-0.088165,0.633613,0.0,0.3,-0.01,0.89/
```

```
&MESH ID='Mesh 1-b_02', IJK=29,12,36, XB=-0.088165,0.633613,0.3,0.6,-0.01,0.89/
```

```
&MESH ID='Mesh01-b01', IJK=29,14,36, XB=-0.088165,0.633613,0.6,0.939752,-0.01,0.89/
```

```
&REAC ID='Reaction1',
```

```
  FUEL='REAC_FUEL',
```

```
  FORMULA='C3H6',
```

```
  SOOT_H_FRACTION=0.0,
```

```
  CO_YIELD=0.024,
```

```
  SOOT_YIELD=0.058,
```

```
  HEAT_OF_COMBUSTION=4.3E4,
```

```
  RADIATIVE_FRACTION=0.37/
```

```
&PROP ID='THC_LB_5 props', BEAD_DIAMETER=1.5E-3/
```

```
&PROP ID='THC_LB_1 props', BEAD_DIAMETER=1.5E-3/
```

```
&PROP ID='THC_LB_2 props', BEAD_DIAMETER=1.5E-3/
```

```
&PROP ID='THC_LB_3 props', BEAD_DIAMETER=1.5E-3/
```

```
&PROP ID='THC_LB_4 props', BEAD_DIAMETER=1.5E-3/
```

```
&DEVC ID='TC_L_F_1', QUANTITY='TEMPERATURE', XYZ=0.05,0.05,0.1/
```



&DEVC ID='TC\_L\_F\_2', QUANTITY='TEMPERATURE', XYZ=0.05,0.05,0.2/  
&DEVC ID='TC\_L\_F\_3', QUANTITY='TEMPERATURE', XYZ=0.05,0.05,0.3/  
&DEVC ID='TC\_L\_F\_4', QUANTITY='TEMPERATURE', XYZ=0.05,0.05,0.4/  
&DEVC ID='TC\_L\_F\_5', QUANTITY='TEMPERATURE', XYZ=0.05,0.05,0.5/  
&DEVC ID='THC\_LF\_1', QUANTITY='THERMOCOUPLE', XYZ=0.05,0.05,0.1/  
&DEVC ID='THC\_LF\_2', QUANTITY='THERMOCOUPLE', XYZ=0.05,0.05,0.2/  
&DEVC ID='THC\_LF\_3', QUANTITY='THERMOCOUPLE', XYZ=0.05,0.05,0.3/  
&DEVC ID='THC\_LF\_4', QUANTITY='THERMOCOUPLE', XYZ=0.05,0.05,0.4/  
&DEVC ID='THC\_LF\_5', QUANTITY='THERMOCOUPLE', XYZ=0.05,0.05,0.5/  
&DEVC ID='TC\_R\_F\_1', QUANTITY='TEMPERATURE', XYZ=0.55,0.05,0.1/  
&DEVC ID='TC\_R\_F\_2', QUANTITY='TEMPERATURE', XYZ=0.55,0.05,0.2/  
&DEVC ID='TC\_R\_F\_3', QUANTITY='TEMPERATURE', XYZ=0.55,0.05,0.3/  
&DEVC ID='TC\_R\_F\_4', QUANTITY='TEMPERATURE', XYZ=0.55,0.05,0.4/  
&DEVC ID='TC\_R\_F\_5', QUANTITY='TEMPERATURE', XYZ=0.55,0.05,0.5/  
&DEVC ID='THC\_RF\_5', QUANTITY='THERMOCOUPLE', XYZ=0.55,0.05,0.5/  
&DEVC ID='THC\_RF\_4', QUANTITY='THERMOCOUPLE', XYZ=0.55,0.05,0.4/  
&DEVC ID='THC\_RF\_3', QUANTITY='THERMOCOUPLE', XYZ=0.55,0.05,0.3/  
&DEVC ID='THC\_RF\_2', QUANTITY='THERMOCOUPLE', XYZ=0.55,0.05,0.2/  
&DEVC ID='THC\_RF\_1', QUANTITY='THERMOCOUPLE', XYZ=0.55,0.05,0.1/  
&DEVC ID='Door\_TC\_0.40', QUANTITY='TEMPERATURE', XYZ=0.3,0.0,0.4/  
&DEVC ID='Door\_TC\_0.25', QUANTITY='TEMPERATURE', XYZ=0.3,0.0,0.25/  
&DEVC ID='Door\_TC\_0.1', QUANTITY='TEMPERATURE', XYZ=0.3,0.0,0.1/  
&DEVC ID='Velocity\_0.40', QUANTITY='V-VELOCITY', XYZ=0.3,0.0,0.4,  
ORIENTATION=0.0,1.0,0.0/  
&DEVC ID='Velocity\_0.25', QUANTITY='V-VELOCITY', XYZ=0.3,0.0,0.25,  
ORIENTATION=0.0,1.0,0.0/  
&DEVC ID='Velocity\_0.1', QUANTITY='V-VELOCITY', XYZ=0.3,0.0,0.1,  
ORIENTATION=0.0,1.0,0.0/  
&DEVC ID='THC\_Prop\_0.10', QUANTITY='THERMOCOUPLE', XYZ=0.3,0.0,0.1/  
&DEVC ID='THC\_Prop\_0.25', QUANTITY='THERMOCOUPLE', XYZ=0.3,0.0,0.25/  
&DEVC ID='THC\_Prop\_0.4', QUANTITY='THERMOCOUPLE', XYZ=0.3,0.0,0.4/  
&DEVC ID='TC\_L\_B\_1', QUANTITY='TEMPERATURE', XYZ=0.05,0.85,0.1/  
&DEVC ID='TC\_L\_B\_2', QUANTITY='TEMPERATURE', XYZ=0.05,0.85,0.2/  
&DEVC ID='TC\_L\_B\_3', QUANTITY='TEMPERATURE', XYZ=0.05,0.85,0.3/  
&DEVC ID='TC\_L\_B\_4', QUANTITY='TEMPERATURE', XYZ=0.05,0.85,0.4/  
&DEVC ID='TC\_L\_B\_5', QUANTITY='TEMPERATURE', XYZ=0.05,0.85,0.5/  
&DEVC ID='THC\_LB\_5', PROP\_ID='THC\_LB\_5 props', QUANTITY='THERMOCOUPLE',  
XYZ=0.05,0.85,0.5/  
&DEVC ID='THC\_LB\_1', PROP\_ID='THC\_LB\_1 props', QUANTITY='THERMOCOUPLE',  
XYZ=0.05,0.85,0.1/

&DEVC ID='THC\_LB\_2', PROP\_ID='THC\_LB\_2 props', QUANTITY='THERMOCOUPLE', XYZ=0.05,0.85,0.2/  
&DEVC ID='THC\_LB\_3', PROP\_ID='THC\_LB\_3 props', QUANTITY='THERMOCOUPLE', XYZ=0.05,0.85,0.3/  
&DEVC ID='THC\_LB\_4', PROP\_ID='THC\_LB\_4 props', QUANTITY='THERMOCOUPLE', XYZ=0.05,0.85,0.4/  
&DEVC ID='TC\_R\_B\_1', QUANTITY='TEMPERATURE', XYZ=0.55,0.85,0.1/  
&DEVC ID='TC\_R\_B\_2', QUANTITY='TEMPERATURE', XYZ=0.55,0.85,0.2/  
&DEVC ID='TC\_R\_B\_3', QUANTITY='TEMPERATURE', XYZ=0.55,0.85,0.3/  
&DEVC ID='TC\_R\_B\_4', QUANTITY='TEMPERATURE', XYZ=0.55,0.85,0.4/  
&DEVC ID='TC\_R\_B\_5', QUANTITY='TEMPERATURE', XYZ=0.55,0.85,0.5/  
&DEVC ID='TCH\_RB\_1', QUANTITY='THERMOCOUPLE', XYZ=0.55,0.85,0.1/  
&DEVC ID='TCH\_RB\_2', QUANTITY='THERMOCOUPLE', XYZ=0.55,0.85,0.2/  
&DEVC ID='TCH\_RB\_3', QUANTITY='THERMOCOUPLE', XYZ=0.55,0.85,0.3/  
&DEVC ID='TCH\_RB\_4', QUANTITY='THERMOCOUPLE', XYZ=0.55,0.85,0.4/  
&DEVC ID='TCH\_RB\_5', QUANTITY='THERMOCOUPLE', XYZ=0.55,0.85,0.5/  
&DEVC ID='TCH\_TSC\_0.5', QUANTITY='THERMOCOUPLE', XYZ=0.3,-0.6,0.5/  
&DEVC ID='TSC\_Door\_Top\_Ceiling\_0.6\_Door', QUANTITY='RADIATIVE HEAT FLUX GAS', XYZ=0.3,-0.6,0.6, ORIENTATION=0.0,1.0,0.0/  
&DEVC ID='TCH\_TSC\_0.6\_Door', QUANTITY='THERMOCOUPLE', XYZ=0.3,-0.6,0.6/  
&DEVC ID='TSC\_Door\_Top\_Ceiling\_0.5', QUANTITY='RADIATIVE HEAT FLUX GAS', XYZ=0.3,-0.6,0.5, ORIENTATION=0.0,1.0,0.0/  
&DEVC ID='TSC\_Wall\_1', QUANTITY='RADIATIVE HEAT FLUX GAS', XYZ=-0.15,0.45,0.6, ORIENTATION=1.0,0.0,0.0/  
&DEVC ID='TSC\_Wall\_2', QUANTITY='RADIATIVE HEAT FLUX GAS', XYZ=-0.3,0.45,0.6, ORIENTATION=1.0,0.0,0.0/  
&DEVC ID='TSC\_Wall\_3', QUANTITY='RADIATIVE HEAT FLUX GAS', XYZ=-0.45,0.45,0.6, ORIENTATION=1.0,0.0,0.0/  
&DEVC ID='THC\_Wall\_3', QUANTITY='THERMOCOUPLE', XYZ=-0.45,0.45,0.6/  
&DEVC ID='THC\_Wall\_2', QUANTITY='THERMOCOUPLE', XYZ=-0.3,0.45,0.6/  
&DEVC ID='THC\_Wall\_1', QUANTITY='THERMOCOUPLE', XYZ=-0.15,0.45,0.6/  
&DEVC ID='MASS FLOW DOOR', QUANTITY='MASS FLOW', XB=0.2,0.4,0.0,0.0,0.0,0.5/  
&DEVC ID='VOLUME FLOW DOOR', QUANTITY='VOLUME FLOW', XB=0.2,0.4,0.0,0.0,0.0,0.5/  
&DEVC ID='HRR', QUANTITY='HRR', XB=2.775558E-17,0.6,-0.260248,-2.081668E-17,0.0,0.89/  
&DEVC ID='GAS Analyzer Back CO2', QUANTITY='VOLUME FRACTION', SPEC\_ID='CARBON DIOXIDE', XYZ=0.05,0.85,0.5/  
&DEVC ID='GAS Analyzer Back CO', QUANTITY='VOLUME FRACTION', SPEC\_ID='CARBON MONOXIDE', XYZ=0.05,0.85,0.5/  
&DEVC ID='GAS Analyzer Back O2', QUANTITY='VOLUME FRACTION', SPEC\_ID='OXYGEN', XYZ=0.05,0.85,0.5/

&DEVC ID='TSC\_Door\_Top\_Ceiling\_0.3\_Door', QUANTITY='RADIATIVE HEAT FLUX GAS', XYZ=0.3,-0.3,0.6, ORIENTATION=0.0,1.0,0.0/  
&DEVC ID='TCH\_TSC\_0.3\_Door', QUANTITY='THERMOCOUPLE', XYZ=0.3,-0.6,0.6/  
&DEVC ID='TCH\_TSC\_0.3 Top\_Door', QUANTITY='THERMOCOUPLE', XYZ=0.3,-0.3,0.5/  
&DEVC ID='TSC\_Door\_Top\_door\_0.3', QUANTITY='RADIATIVE HEAT FLUX GAS', XYZ=0.3,-0.3,0.5, ORIENTATION=0.0,1.0,0.0/  
&DEVC ID='GAS Analyzer front CO2', QUANTITY='VOLUME FRACTION', SPEC\_ID='CARBON DIOXIDE', XYZ=0.290892,0.0,0.438106/  
&DEVC ID='GAS Analyzer Front CO', QUANTITY='VOLUME FRACTION', SPEC\_ID='CARBON MONOXIDE', XYZ=0.290892,0.0,0.438106/  
&DEVC ID='GAS Analyzer front O2', QUANTITY='VOLUME FRACTION', SPEC\_ID='OXYGEN', XYZ=0.290892,0.0,0.438106/  
&DEVC ID='VOLUME FLOW Corner Opening Front Left', QUANTITY='VOLUME FLOW', XB=0.0,0.025,0.0,0.025,0.6005,0.6005/  
&DEVC ID='MASS FLOW Corner Opening Front Left', QUANTITY='MASS FLOW', XB=0.0,0.025,0.0,0.025,0.6005,0.6005/  
&DEVC ID='VOLUME FLOW Corner Opening Front Right', QUANTITY='VOLUME FLOW', XB=0.575,0.6,0.0,0.025,0.6005,0.6005/  
&DEVC ID='MASS FLOW Corner Opening Front Right', QUANTITY='MASS FLOW', XB=0.575,0.6,0.0,0.025,0.6005,0.6005/  
&DEVC ID='VOLUME FLOW Corner Opening Back Right', QUANTITY='VOLUME FLOW', XB=0.575,0.6,0.875,0.9,0.6005,0.6005/  
&DEVC ID='MASS FLOW Corner Opening Back Right', QUANTITY='MASS FLOW', XB=0.575,0.6,0.875,0.9,0.6005,0.6005/  
&DEVC ID='VOLUME FLOW Corner Opening Back Left', QUANTITY='VOLUME FLOW', XB=0.0,0.025,0.875,0.9,0.6005,0.6005/  
&DEVC ID='MASS FLOW Corner Opening Back Left', QUANTITY='MASS FLOW', XB=0.0,0.025,0.875,0.9,0.6005,0.6005/  
&DEVC ID='Velocity\_Front Left Corner Opening', QUANTITY='VELOCITY', XYZ=0.0125,0.0125,0.6005, ORIENTATION=0.0,0.0,1.0/  
&DEVC ID='Velocity\_Front Right Corner Opening', QUANTITY='VELOCITY', XYZ=0.5875,0.0125,0.6005, ORIENTATION=0.0,0.0,1.0/  
&DEVC ID='Velocity\_Back Right Corner Opening', QUANTITY='VELOCITY', XYZ=0.5875,0.8875,0.6005, ORIENTATION=0.0,0.0,1.0/  
&DEVC ID='Velocity\_Back Left Corner Opening', QUANTITY='VELOCITY', XYZ=0.0125,0.8875,0.6005, ORIENTATION=0.0,0.0,1.0/  
  
&MATL ID='STEEL',  
FYI='Drysdale, Intro to Fire Dynamics - ATF NIST Multi-Floor Validation',  
SPECIFIC\_HEAT\_RAMP='STEEL\_SPECIFIC\_HEAT\_RAMP',  
CONDUCTIVITY\_RAMP='STEEL\_CONDUCTIVITY\_RAMP',  
DENSITY=7850.0,  
EMISSIVITY=0.6/

```

&RAMP ID='STEEL_SPECIFIC_HEAT_RAMP', T=20.0, F=0.45/
&RAMP ID='STEEL_SPECIFIC_HEAT_RAMP', T=377.0, F=0.6/
&RAMP ID='STEEL_SPECIFIC_HEAT_RAMP', T=677.0, F=0.85/
&RAMP ID='STEEL_CONDUCTIVITY_RAMP', T=20.0, F=48.0/
&RAMP ID='STEEL_CONDUCTIVITY_RAMP', T=677.0, F=30.0/
&MATL ID='INSULATION',
  FYI='Isolatek BLAZE-SHIELD DC/F - WTC FDS5 Validation',
  SPECIFIC_HEAT_RAMP='INSULATION_SPECIFIC_HEAT_RAMP',
  CONDUCTIVITY_RAMP='INSULATION_CONDUCTIVITY_RAMP',
  DENSITY=208.0/
&RAMP ID='INSULATION_CONDUCTIVITY_RAMP', T=20.0, F=0.05/
&RAMP ID='INSULATION_CONDUCTIVITY_RAMP', T=377.0, F=0.1/
&RAMP ID='INSULATION_CONDUCTIVITY_RAMP', T=677.0, F=0.2/
&RAMP ID='INSULATION_SPECIFIC_HEAT_RAMP', T=20.0, F=0.8/
&RAMP ID='INSULATION_SPECIFIC_HEAT_RAMP', T=677.0, F=2.0/

&SURF ID='Wall',
  RGB=220,229,236,
  BACKING='EXPOSED',
  MATL_ID(1,1)='STEEL',
  MATL_MASS_FRACTION(1,1)=1.0,
  THICKNESS(1)=5.0E-4/
&SURF ID='Pan_Steel',
  COLOR='BLACK',
  MATL_ID(1,1)='STEEL',
  MATL_MASS_FRACTION(1,1)=1.0,
  THICKNESS(1)=5.0E-3/
&SURF ID='Pool',
  COLOR='RED',
  HRRPUA=775.279594,
  RAMP_Q='Pool_RAMP_Q'/
&RAMP ID='Pool_RAMP_Q', T=0.0, F=0.077687/
.
.
&.RAMP ID='Pool_RAMP_Q', T=1254.0, F=-0.018505/
&SURF ID='Floor',
  RGB=146,202,166,
  BACKING='VOID',

```

```
MATL_ID(1,1)='INSULATION',  
MATL_MASS_FRACTION(1,1)=1.0,  
THICKNESS(1)=0.01/
```

```
&OBST ID='Front_Wall', XB=0.0,0.6,0.0,5.0E-4,0.0,0.6, SURF_ID='Wall'/  
&OBST ID='Left_Wall', XB=-5.0E-4,0.0,0.0,0.9,0.0,0.6, SURF_ID='Wall'/  
&OBST ID='Back_Wall', XB=0.0,0.6,0.9,0.9005,0.0,0.6, SURF_ID='Wall'/  
&OBST ID='Right_Wall', XB=0.5995,0.6,0.0,0.9,0.0,0.6, SURF_ID='Wall'/  
&OBST ID='Burner', XB=0.1,0.5,0.25,0.65,0.0,0.05,  
SURF_IDS='Pool','Pan_Steel','Pan_Steel'/  
&OBST ID='Floor', XB=0.0,0.6,0.0,0.9,-0.01,0.0, SURF_ID='Floor'/  
&OBST ID='Cieling', XB=0.0,0.6,0.0,0.9,0.6,0.6005, SURF_ID='Wall'/
```

```
&HOLE ID='Door', XB=0.2,0.4,-0.022285,0.014418,-0.015,0.5/  
&HOLE ID='2.5 cm corner opening', XB=0.0,0.025,-2.5E-3,0.025,0.59,0.61/  
&HOLE ID='2.5 cm corner opening', XB=0.575,0.6,0.875,0.9,0.59,0.61/  
&HOLE ID='2.5 cm corner opening', XB=0.0,0.025,0.875,0.9,0.59,0.61/  
&HOLE ID='2.5 cm corner opening', XB=0.575,0.6,-2.5E-3,0.025,0.59,0.61/
```

```
&VENT ID='Mesh Vent: Mesh01 [XMAX]', SURF_ID='OPEN', XB=0.633613,0.633613,-  
0.610248,0.939752,-0.01,0.89/  
&VENT ID='Mesh Vent: Mesh01 [XMIN]', SURF_ID='OPEN', XB=-0.486387,-0.486387,-  
0.610248,0.939752,-0.01,0.89/  
&VENT ID='Mesh Vent: Mesh01 [YMAX]', SURF_ID='OPEN', XB=-  
0.486387,0.633613,0.939752,0.939752,-0.01,0.89/  
&VENT ID='Mesh Vent: Mesh01 [YMIN]', SURF_ID='OPEN', XB=-0.486387,0.633613,-  
0.610248,-0.610248,-0.01,0.89/  
&VENT ID='Mesh Vent: Mesh01 [ZMAX]', SURF_ID='OPEN', XB=-0.486387,0.633613,-  
0.610248,0.939752,0.89,0.89/
```

```
&SLCF QUANTITY='HRRPUV', VECTOR=.TRUE., PBX=0.3/  
&SLCF QUANTITY='TEMPERATURE', VECTOR=.TRUE., PBX=0.3/  
&SLCF QUANTITY='VELOCITY', VECTOR=.TRUE., PBX=0.3/  
&SLCF QUANTITY='PRESSURE', VECTOR=.TRUE., PBX=0.3/
```

```
&TAIL /
```